TPO-E00-G-CDR-X-000101
AAA-TPO-ADTF-01-0032
LA-UR-01-2496
Revision 0
May 2001

Advanced Accelerator Applications
Project Technical Note
Target/Blanket and Materials ED&D Program

Accelerator-Driven Test Facility: Preconceptual Design

Accelerator-Driven Test Facility: Preconceptual Design

Document Number:
TPO-E00-G-CDR-X-000101
AAA-TPO-ADTF-01-0032
LA-UR-01-2496

Abstract:

This report describes the status of the Accelerator-Driven Test Facility (ADTF) preconceptual design. The design includes the modular target-multiplier concept, the vessel target-multiplier concept, the accelerator, and the balance of facility. To meet the design requirements of flux and power level, a 600-MeV, 13.3-mA linear accelerator delivers a proton beam to the target-multiplier. The spallation neutron source (target) produces a strong source of neutrons that diffuse into the multiplier producing up to 100 megawatts of fission power. Two concepts have been considered for the multiplier system: a modular design that allows for horizontal movement of target and multiplier components and a sodium-cooled vessel system similar in configuration to fast-reactor facilities. Based on the development of these concepts and the subsequent reviews, it is recommended that the modular target-multiplier concept design be revised as a dedicated target and materials testing station. The sodium-vessel concept should continue development of the subcritical multiplier with a power level up to 100 megawatts.

Approval:

ADTF Project Leader	***Signature on file 5/30/01***
AAA-TPO	Michael W. Cappiello

Distribution List

Ahlfeld, Charles	C341
APT-TPO files	H816
Arthur, Ed	H816
Baxter, Alan	C341
Bennett, Deborah	H816
Boore, Brent	WSRC
Cappiello, Michael	H816
Chuebon, Ray	C341
Cohen, Howard	C341
Crawford, Doug	ANL-W
Edwards, Jack	H816
Finck, Phillip	ANL
Gambhir, Arun (RMDC)	C341
Gohar, Yousry	ANL
Goldner, Frank	DOE
Guffee, Ray	H821
Herceg, Joe	ANL
Herczeg, John	DOE
Hill, david	ANL
Koploy, Maria	GA (San Diego)
Laidler, James	ANL
Marquez, Rich	C341
McConnell, Steve	H816
McGill, John	H816
Metzler, Jack	DOE
Newman, Frank	DOE HQ
Parme, Larry	C341

Pasamehmetoglu, Kemal	H816
Pederson, Dean	ANL
Pitcher, Eric	H805
Quintana, Lawrence (QA)	H816
Rodriguez, Carmelo	C341
Roglans, Jordi	ANL
Russell, Alan	GA (San Diego)
Schneider, Dave	H816
Scott, Michelle	DOE HQ
Sheffield, Rich	H816
Tooker, Joe	H816
Van Tuyle, Greg	H816
Williams, Mark	DOE HQ
Zimmer, Alan	GA (San Diego)

Table of Contents

List of Figures

Chapter 1

Chapter 2

Chapter 3

Chapter 4

List of Tables

Chapter 1

Chapter 2

Chapter 3

List of Acronyms

AAA	Advanced Accelerator Applications
AC	Alternating current
ADTF	Accelerator-Driven Test Facility
AFU	Air-filter units
AHU	Air-handling units
ALARA	As Low As Reasonably Achievable
ANL	Argonne National Laboratory
ANL-W	Argonne National Laboratory-West
ANS	American Nuclear Society
APT	Accelerator Production of Tritium
ASME	American Society of Mechanical Engineers
ATW	Accelerator Transmutation of Waste
BOEC	Beginning of the equilibrium cycle
BOF	Balance of Facility
BOL	Beginning of life
BPM	Beam position monitor
CCDTL	Coupled-cavity drift tube linac
CCL	Coupled-cavity linac
CPS	Cathodic Protection System
DBA	Design basis accident
DC	Direct current
DOE	Department of Energy
DTL	Drift-tube-linac
EBR-II	Experimental Breeder Reactor
ED&D	Engineering development and demonstration
EFAN	Exhaust/purge fan
EOEC	End of the equilibrium cycle
ESS	European Spallation Source

FAS	Fire Alarm System
FDS	Fire Detection System
FFTF	Fast Flux Test Facility
FODO	Focus-drift-defocus-drift
FPS	Non-Sodium Fire Protection System
FSV	Fort Saint Vrain
GLPS	Grounding and Lightning Protection System
GS	General Services
HE	High energy
HEBT	High-energy beam transport
HEPA	High-efficiency Particulate Air
HP&EMS	Health Protection & Environmental Monitoring System
HTS	Heat Trace System
HVACS	Heating, ventilation, air-conditioning system
ICS	Integrated Control System
ID	Inside/inner diameter
ISIS	United Kingdom neutron-scattering facility
LANSCE	Los Alamos Neutron Science Center
LBE	Lead-bismuth eutectic
LBP	Lumped burnable poison
LE	Low energy
LEBT	Low-energy beam transport
LEDA	Low-Energy Demonstration Accelerator
LOCA	Loss-of-coolant accident
LWR TRU	Light-water reactor transuranic, transuranium
MCCs	Motor Control Centers
MCR	Main Control Room
MPSS	MainPower supply System
MTBF	Mean time between failures
MVACS	Multiplier vessel air-cooling system

NFPA	National Fire Protection Association
NPH	Natural phenomena hazard
PABX	Private Automatic Branch Exchange
PCS	Plant Communication System
PLS	Plant Lighting System
PPA	Property Protection Area
RCCS	Resonance Control Cooling System
REPS	Radiation Exposure Protection System
RF	Radio frequency
RFQ	Radio-frequency quadrupole
RGIPM	Residual gas ionization proportional monitor
RH	Remotely handled
RIA	Rare Isotope Accelerator
RMPS	Radiation Monitoring and Protection System
RWTS	Radioactive Waste Treatment System
SC	Safety class
SCRF	Superconducting radiofrequency
SNS	Spallation Neutron Source
SS	Safety significant
TBD	To be determined
TBS	Target Beam Shut-down
TMT	Target & Materials Test
UPS	Uninterruptible power supplies

Executive Summary

This report documents the status of the Accelerator-Driven Test Facility (ADTF) preconceptual design. The design includes the modular target-multiplier concept, the vessel target-multiplier concept, the accelerator, and the balance of facility. To meet the flux and power level design requirements, a 600-MeV, 13.3-mA linear accelerator delivers a proton beam to the target-multiplier. The spallation neutron source (target) produces a strong source of neutrons that diffuse into the multiplier, producing up to 100 megawatts of fission power. Two concepts have been considered for the multiplier system: a modular design that allows for horizontal movement of target, multiplier components, and a sodium-cooled vessel system similar in configuration to fast-reactor facilities. Based on the development of these concepts and the subsequent reviews, it is recommended that the modular target-multiplier concept design be revised as a dedicated target and materials-testing station. The sodium-vessel concept should continue development of the subcritical multiplier with a power level up to 100 megawatts.

Introduction

To meet the objectives of the Advanced Accelerator Applications (AAA) program, the ADTF provides a world-class accelerator-driven test facility to

1. provide the capability to assess technology options for the transmutation of spent nuclear fuel and waste through a proof-of-performance;
2. provide a user facility that allows testing of advanced nuclear technologies and applications, material science and research, experimental physics, and conventional nuclear engineering science applications;
3. provide the capability, through upgrades or additions to the ADTF accelerator, to produce tritium for defense purposes, if required; and
4. provide the capability, through upgrades or additions, to produce radioisotopes for medical and commercial purposes.

These missions are diverse and demand a facility of tremendous flexibility. In particular, this facility must provide the capability to

1. irradiate proposed Accelerator-driven Transmutation of Waste (ATW) fuels and materials at prototypic flux, temperature, and coolant conditions;
2. provide significant throughput of irradiated fuel for separations testing at adequate scale;
3. perform transient testing;
4. test both liquid (lead-bismuth) and solid spallation targets with either water, sodium, or helium coolant;
5. test and demonstrate the safe coupling and operation of an accelerator-driven subcritical multiplier;
6. test generation-IV fuels for advanced nuclear systems (requires high-intensity thermal flux);
7. irradiate fission-product transmutation targets;
8. test advanced fuel and coolant combinations, including helium, water, sodium, and lead-bismuth;
9. irradiate tritium production targets;
10. produce isotopes for commercial and medical applications; and
11. perform neutron physics experiments.

To provide these capabilities, two target-multiplier concepts were investigated, and the design and analyses of each are presented in Chapters 1 and 2 of this report. Both designs attempt to provide a single system that could meet all of the requirements. The modular system presented in Chapter 1 is a configuration similar to that used in spallation neutron-source facilities primarily built for performing neutron-scattering experiments. With this design, there is a tremendous amount of flexibility in testing different fuels and coolants, but it is difficult to demonstrate high k_{eff} systems and high fission-power levels. It is recognized that the modular concept is, therefore, a strong option for a dedicated target-material testing station, whereas the sodium-vessel concept is capable of demonstrating the safe

coupling of the spallation source to the multiplier, can operate at high k_{eff} levels, and can provide the necessary throughput of fuel.

Based on the subsequent review of the designs presented in this report, it has been recommended that the ADTF project proceed with the initial construction of two target stations, the Target & Materials Test (TMT) and the Subcritical Multiplier Test Station that is 100-megawatts capable (SCM-100). The two test stations share common hot-cell facilities for post-irradiation examination. The TMT provides the test environment for materials and fuel experiments, coolant and target technology experiments, and demonstration of tritium production, as well as the potential for isotope production. The basis for the TMT is the modular design provided in Chapter 1 of this report. The SCM-100 provides the test environment for demonstration of accelerator-multiplier coupling, irradiation of significant quantities of fuel and the eventual transition to an actinide core. The basis for the SCM-100 is the sodium-vessel concept provided in Chapter 2 of this report. A third target station for an as-yet-to-be-determined purpose would be constructed at a later date.

1 Modular Target and Multiplier System

1.1 Executive Summary

The Accelerator-Driven Test Facility (ADTF) modular design concept is a target-multiplier configuration that provides optimum operation and testing flexibility. This system provides a versatile irradiation environment that allows both demonstration of transmutation technologies and testing of advanced nuclear systems. The modular concept consists of a centrally located irradiation chamber that contains a spallation neutron source (target) and a subcritical multiplier. The proton beam, target, and multiplier segments are all brought horizontally into the cell. This provides for a simple, straightforward beam-transport system from the accelerator to the irradiation chamber. The mechanisms for implementing a horizontal target and multiplier insertion configuration also are a demonstrated technology based on existing and planned facilities. At the completion of an irradiation cycle, target and multiplier components are moved into and out of the irradiation chamber from adjoining hot-cells. All primary heat-removal equipment resides in the hot-cells, providing for safe operation and maintenance. The base-case fast-spectrum design employs a driver-fuel design that has a predictable performance based on a previously established database. Upgrading to higher power levels can be facilitated by using more fuel and an expandable heat-removal system. In addition to fast spectrum systems, a thermal-spectrum multiplier can also be accommodated by replacement of the multiplier components; for example, a graphite-moderated, helium-cooled system based on high temperature gas-cooled technology can be tested using the same configuration.

Analyses show that by using this design configuration one can produce neutrons with a spectrum prototypical of the current base-case Accelerator-driven Transmutation of Waste (ATW) system, which is envisioned to employ a sodium-cooled multiplier and a lead-bismuth eutectic (LBE) target. The environment is achieved with an LBE target and sodium-cooled multiplier with a k_{eff} between 0.8 and 0.97. Calculations show a fast-spectrum flux level on the order of 1×10^{15} n/cm^2-s is achievable by using metal fuel. The total multiplier power level is approximately 20 MW-thermal at this flux level. The multiplier power level can be increased up to approximately 100 MW-thermal to achieve higher flux levels. Because the beam is delivered horizontally to the target and multiplier, neutron-source distribution can be tailored to provide a uniform flux over the length of the fuel.

Scoping calculations indicate that thermal-hydraulic limits can easily be met by the current concept. Extending the database developed for the APT Project, a structural design criterion will be developed to address the high-energy portion of the neutron spectrum near the spallation target. Based on materials irradiation data and structural design criteria, component-lifetime limits will be developed and implemented with an adequate safety margin. Although the design is tailored to accommodate the need to frequently replace the components, engineering development and demonstration efforts will be aimed at maximizing the design lifetime of the components to maximize the facility availability.

The modular concept simplifies the operational aspects of the facility while providing adequate safety levels. Using a safety-by-design approach, the target-multiplier and beam shut-down systems are designed with the maximum reliance on passive safety features.

Natural circulation of coolants for both the target and multiplier segments and diverse cooling mechanisms provide adequate protection in the event of accidents. In the event of a leak or break in either the target or multiplier pressure boundary inside the irradiation chamber, the loss of vacuum will passively shut down the beam. This shut-down mechanism provides a back-up to a highly reliable active shut-down system.

As discussed in the introduction, the modular concept is also a strong option for a dedicated target-material testing station. With the separate station approach, the multiplier vessels discussed in this report would be downsized to contain fuel with a fission power on the order of a few megawatts and a low multiplication factor. Various high-power target options can be tested. Inserts can also be provided for testing material samples.

1.2 Introduction

The preconceptual design of the target-multiplier that contains the spallation target and a subcritical multiplier is presented in this report. The ADTF is envisioned as a major nuclear research facility that will provide multiple testing and production capabilities. Through operation of the ADTF, a number of needs of considerable national and technological importance will be addressed.

In developing the modular design concepts, the primary emphasis is on attributes that provide a maximum possible flexibility for testing different technologies and design options. Primarily, the modular design is motivated by the following testing needs, derived from the ADTF missions:

1. The capability to assess technology options for the transmutation of spent nuclear fuel and waste through proof-of-performance demonstrations, which are aimed at demonstrating the combined performance of a spallation target with a subcritical multiplier under a variety of operating conditions.
2. A user facility that allows testing of advanced nuclear technologies and applications, material science and research, experimental physics, and conventional nuclear engineering science applications.
3. The capability to produce radioisotopes for medical and commercial purposes.

A fourth mission for the facility is the capability to produce tritium if the need arises. This mission is met by designing and building the accelerator in such a way that it does not preclude the future upgrade in energy and current required for tritium production. Space at the site will also be made available to build a separate target station for this purpose; thus, the ADTF target-multiplier does not have a specific tritium production mission, although some testing of tritium-production technology is possible.

A general description of the facility is presented in Section 1.3 of this document. The emphasis in the preconceptual design is on the target, multiplier, and systems directly supporting their operations. Using scoping calculations, the specific design features and performance characteristics in the areas of neutronics, thermal-hydraulics, materials and structures, operations and safety are discussed in Section 1.4 through Section 1.8, respectively. In Section 1.9, the issues that must be addressed through an engineering

design and development (ED&D) program are summarized. Finally, Section 1.10 provides a summary and conclusion.

1.3 Facility Description

The concept is depicted in Figure 1-1 through Figure 1-4, which show the facility isometric, plan view, primary shield isometric, and one possible arrangement for the irradiation chamber detail, respectively. The beam enters the irradiation chamber horizontally and impacts directly on the spallation neutron source, which is also inserted and removed horizontally in the opposite direction. Two multiplier segments are also inserted and removed horizontally, perpendicular to the beam-target axis (Figure 1-3 and Figure 1-4) using technology developed in the APT Program. A steel-and-concrete shield surrounds the irradiation chamber, providing unrestricted access to surrounding support equipment. The inside surface of the cell is cooled to maintain the structure at a reasonable operating temperature. The hot-cells are designed so remote operations may be performed while the beam is on. The physical interface between the target and multiplier segments allows for removal and insertion of a new target without moving the multiplier segments. As is discussed in the following sections, an alternative configuration would move the multiplier into position from one side only. In this case, removal of the target would be necessary before movement of the multiplier.

The three hot-cells adjacent and connected to the shield provide service to the target and to the multiplier segments, respectively (Figure 1-1 and Figure 1-2). The hot-cells contain the primary heat-removal equipment, and all necessary remote-handling equipment for replacement and movement of components. Piping runs through the shield and connects the heat-removal equipment to the target and multiplier segments. For the multiplier segments, the hot-cells contain sufficient space for storage of fresh and spent fuel, and space for disassembly and packaging of fuel and material test elements. Similarly for the target hot-cell, adequate space is provided for spent target materials, disposal containers, and material test coupon analysis.

Configurations of this type have been demonstrated successfully at the ISIS (UK) neutron-scattering facility and are planned for use in the SNS (US) facility under construction at Oak Ridge, Tennessee. The layouts used in ISIS and SNS are shown in Figure 1-5 and Figure 1-6 for comparison. These systems offer superior operational flexibility because they allow for quick replacement of the target, which is necessary to maintain overall facility availability. In the SNS facility, for example, change-out of the liquid mercury target container is planned to take place in five days.

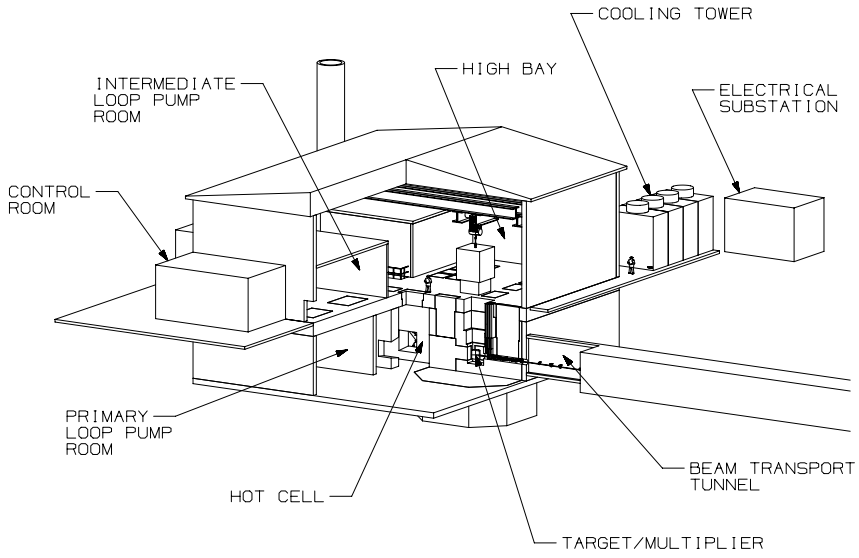

Figure 1-1. Target-multiplier building isometric.

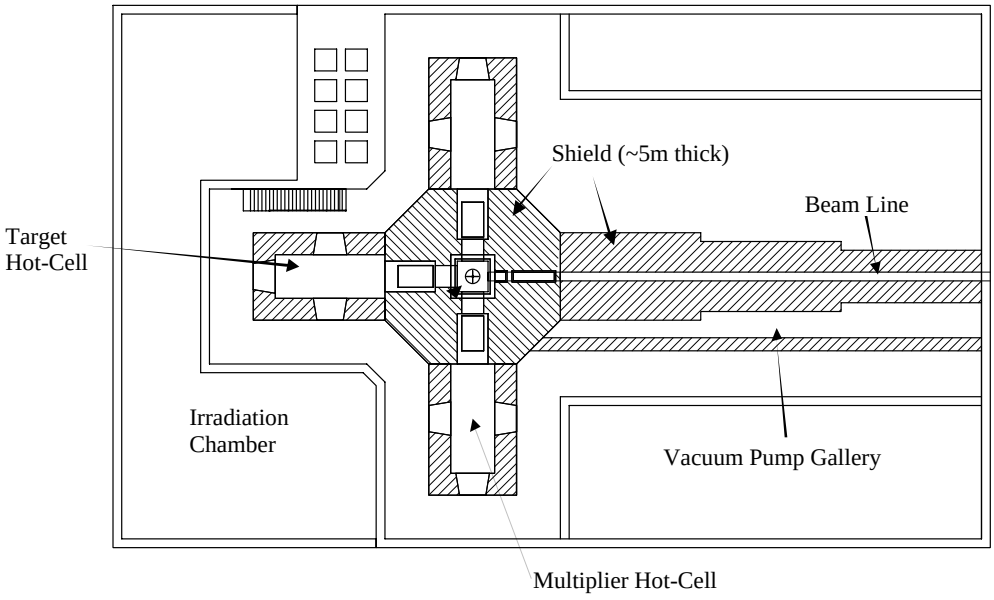

Figure 1-2. Target-multiplier building plan view.

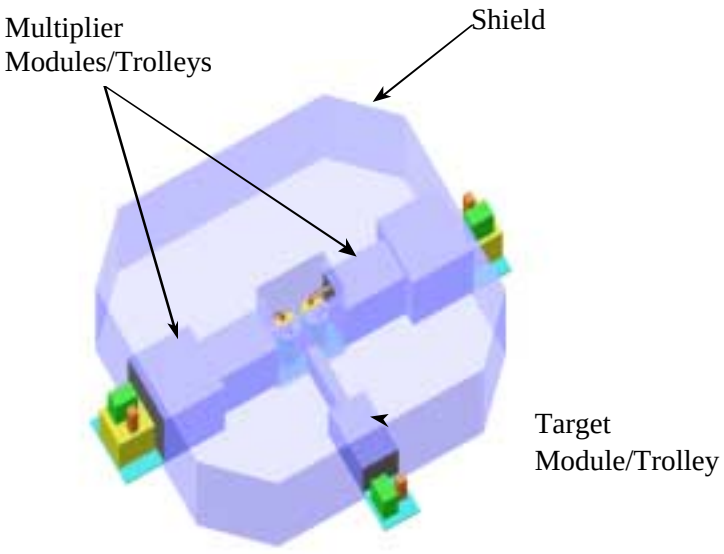

Figure 1-3. Shield isometric.

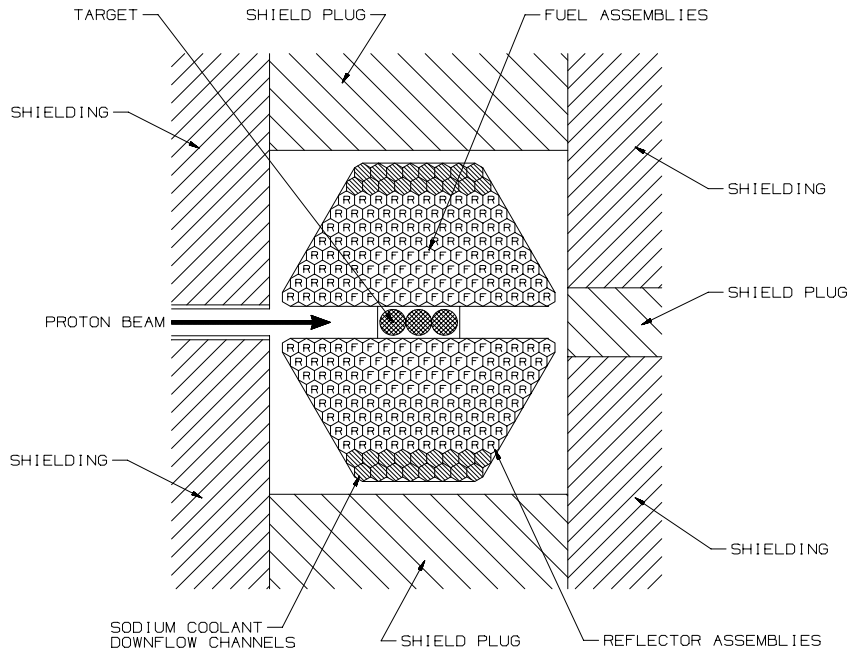

Figure 1-4. Irradiation chamber detail for a target-multiplier example.

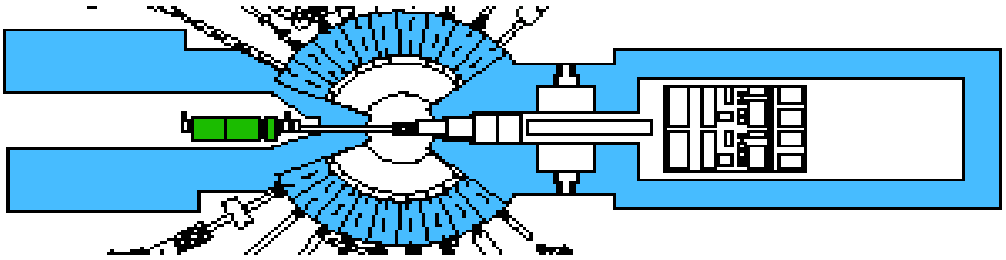

Figure 1-5. The ISIS Facility at Rutherford Appleton Laboratory.

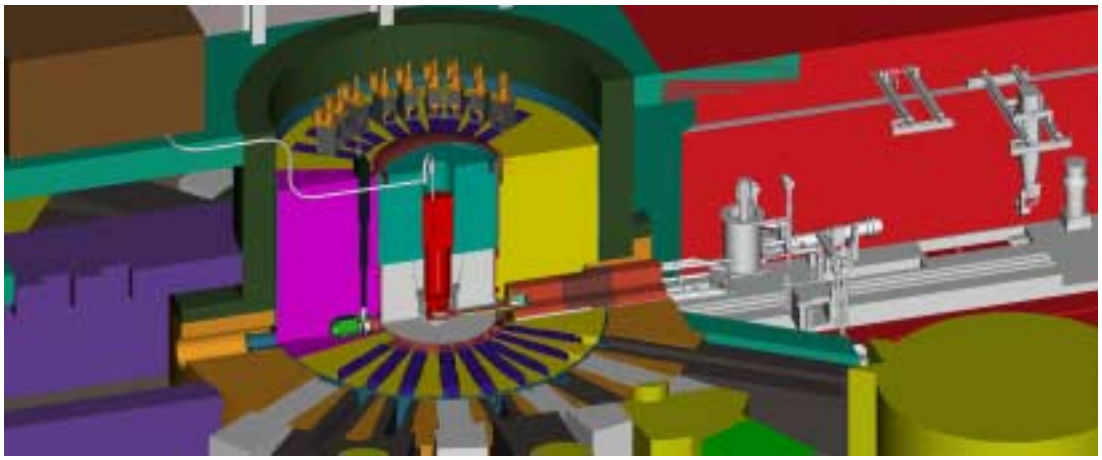

Figure 1-6. The Spallation Neutron Source target-shield and hot-cell configuration.

1.3.1 Spallation Target

The modular configuration can support the testing of either solid or liquid targets, including LBE, lead, sodium-cooled tungsten, helium-cooled tungsten, or water-cooled tungsten. A qualitative assessment of the target options is provided in Table 1-1. A series of sensitivity studies conducted to estimate the beam spot size for various options is also given in Table 1-2. In the calculations, a beam-energy of 600 MeV and a beam-current of 13.3 mA are used for a total of 8 MW of beam power. For the sodium-, helium-, or water-cooled targets, a concentric cylinder arrangement was assumed for the tungsten, where the coolant flows in 1-mm gaps among the concentric cylinders. For the tungsten target, Alloy 718 is used as the structural material and clad, and the peak temperature limit is set to 600°C. For the water-cooled system, the thermal-hydraulic limit is set as half of the thermal excursion heat flux. For the LBE target, the maximum wall temperature is set to 550°C because of the corrosion concerns. As is shown in the tables, the use of LBE results in an efficient neutron

source and the most compact target. If the sodium-flow velocity is increased, targets as small as LBE target sizes can be achieved using sodium-cooled tungsten technology. Helium- or water-cooled systems yield a much larger beam spot size on the target. To reduce the target sizes in these systems, the system pressure must be increased considerably.

Table 1-1. Results of Qualitative Assessment of Target Options

	Nuclear	Thermal	Structural	Chemistry/Waste
LBE	Most favorable neutronics with a compact target.	Favorable heat transfer, direct energy deposition in LBE.	Very corrosive and requires oxygen control and/or special alloys	LBE recycling after retargeting. Potential for exothermic reaction with sodium.
Sodium-cooled tungsten	Neutronics less favorable than LBE.	Highest heat transfer (energy deposited mostly in tungsten.)	Liquid metal embrittlement and proton-flux effects on corrosion. Fabrication demonstrated by APT.	Tungsten waste. Highly reactive with water and air and potentially with LBE
Lead	Favorable neutronics but larger target.	High melting point results in larger target.	Very corrosive and requires oxygen control and/or special alloys	Lead recycling after retargeting. Reaction with sodium is less serious.
Helium-cooled tungsten	Favorable neutronics with larger target.	Low heat transfer.	Requires high pressure for cooling. Fabrication demonstrated by APT.	Tungsten waste.
Water-cooled tungsten	Least favorable neutronics.	Medium heat transfer.	Corrosive and medium pressure for cooling.	Tungsten waste. Coolant is highly reactive with sodium.

Table 1-2. Results of Beam Spot Size Sensitivity Studies

Coolant	Proton Flux (mA/cm^2)	Target Inlet Pressure (MPa)	Coolant Velocity (m/s)	Target Area (cm^2)
Heavy Water	48.1	1.15	10	277
Heavy Water	58.8	2.11	10	226
Helium	65.6	6.89	500	203
Helium	45.9	6.89	300	290
Helium	28.8	4.14	300	462
Sodium	100.9	0.62	12.7	132
Sodium	67.9	0.48	8.2	196
LBE	75.8	0.69	2	175
LBE	104.7	0.69	3	127

Based on this initial assessment, we concluded that the liquid LBE target provides good thermal and neutronic efficiency, and it is chosen as the primary target option. As a back-up, sodium-cooled and helium-cooled tungsten target technologies are also being considered.

In one LBE target concept, four steel pipes are positioned between the two multiplier segments, as is shown in Figure 1-7. The pipes are positioned vertically, in line with the beam axis, and connected at the bottom and top by inlet and outlet plena, respectively. The plena are connected to piping that runs through the removable shield and are connected to a heat exchanger and pump in the hot-cell. The LBE flows continually through the pipes, forming the neutron spallation target when impacted by the proton beam. Because the target material and coolant are the same, the amount of structural material and other low-atomic-number materials that the protons impact is minimized. This, combined with the fact that LBE has very low neutron absorption, makes this spallation target very efficient neutronically. The amount of LBE in the beam is sufficient to completely stop and range out all protons.

The proton beam delivered to the target will be at approximately 600 MeV, with up to 13.3 mA of current (total beam power of 8 MW). The beam enters the irradiation chamber through a beam pipe in the shield and passes unobstructed to the front face of the first pipe of the target. At this power level the beam is expanded or rastered into a beam spot approximately 38 cm high $\times$ 6 cm wide to reduce the power density to acceptable levels. This beam-spot distribution and size can be changed (depending on the needs of the experimenter), as long as thermal, hydraulic, and structural limits are not exceeded in the target. Thermocouples on the front face of the target and upstream sensors provide the necessary information for the operators to center the beam. This is a common practice at existing spallation neutron sources. The 38 cm $\times$ 6 cm beam spot is chosen as a base case because it produces a reasonable power density in the LBE and keeps the pipe wall at a

reasonable temperature, even at 13.3 mA of current. If lower beam currents are used, narrower beam spots are possible.

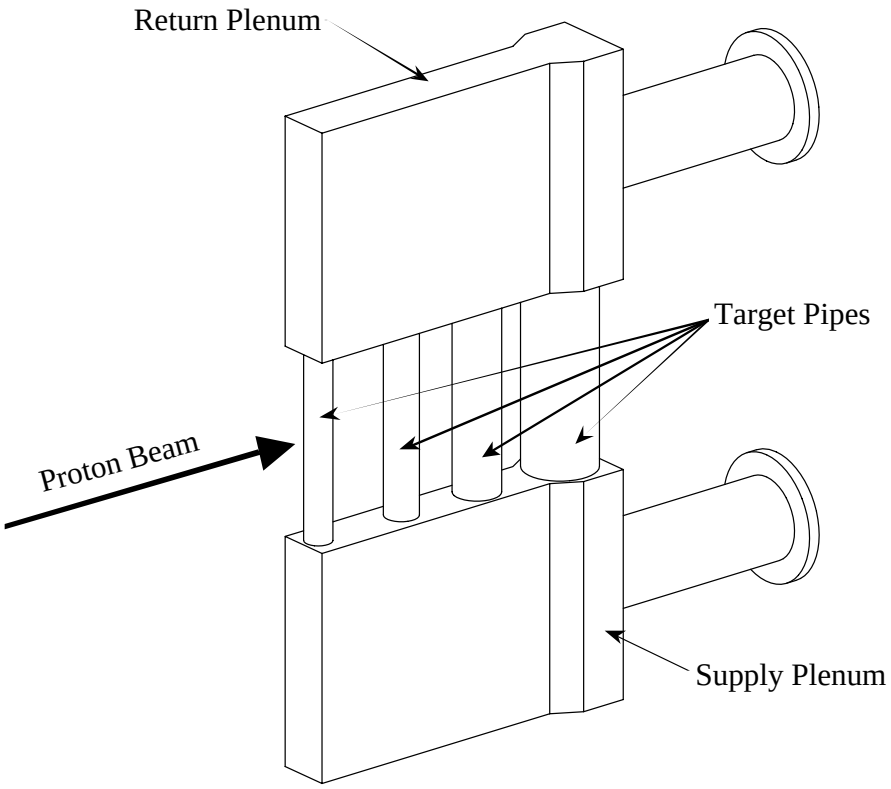

Figure 1-7. LBE target layout.

To provide for material coupon irradiation in the LBE environment, smaller-diameter pipes would be inserted in parallel with the three target pipes. These can be positioned in between, behind, or in front of the target pipes, depending on the needs of the experimenter.

The steel pipes, which contain the LBE, are damaged by proton and neutron irradiation and must be replaced on a regular basis. Depending on the utilized beam current and spot size, replacement of the container may be required every three to 12 months, which is consistent with the expected multiplier irradiation cycle [e.g., both the Fast Flux Test Facility (FFTF) and Experimental Breeder Reactor (EBR-II) operated on a 100-day cycle]. To change out the container, the beam is shut down and the liquid is drained into a storage vessel that resides in the adjacent hot-cell. The target insert, which includes the target, piping, heat-removal equipment, and a section of shielding, is moved horizontally back into the hot-cell on rails (see Section 1.3.5 for details). Remote manipulators are used to disconnect the target container at the piping-to-plena interface and to replace it with the new

one. The system is then leak-checked and refilled with the same fluid as before. Some clean-up may be needed (e.g., removal of spallation products) before the LBE is recycled. The entire assembly is then reinserted into the target cell. From a waste-generation standpoint, the liquid target offers a substantial advantage over the solid target because only the target container (steel) needs to be replaced on a regular basis. Once radioactive, however, the LBE becomes a mixed waste and must be handled appropriately at the end of facility life.

Corrosion is an issue in a LBE target. An effective way of reducing the corrosion rate is to maintain a protective oxide layer on the pipe surface. For a short-lived target, it may be sufficient to control the initial oxygen content in the system. If necessary, an active oxygen control system can be easily implemented. In an active system, oxygen levels are continuously monitored. When needed, small amounts of oxygen are added to the LBE stream. Excess oxygen can be reduced by small additions of hydrogen.

If the use of a LBE target with a sodium-cooled multiplier is not desirable, an alternative target configuration would be a solid tungsten target with either sodium or helium coolant. This may be necessary for safety reasons because of a potentially exothermic chemical reaction between sodium and LBE when they are mixed together. Conceptually such a target would be similar to that shown in Figure 1-7, where tungsten tubes would be nested inside the vertical target pipes. Sodium or helium would flow upwards through the gaps between the tungsten tubes to provide cooling. A tremendous amount of fabrication experience was gained in the APT Program for the solid tungsten option, and would be directly applicable to this application. Figure 1-8 shows the picture of a clad-tungsten cylinder fabricated in the APT prototyping program. This very robust design has demonstrated excellent performance in accommodating thermal cycling, which is expected to be encountered because of beam interrupts.

To replace a solid target, the cooling fluid would continue to flow on the tungsten until decay heat was sufficiently low for the fluid to be safely drained (or, in the case of helium, removed). Then the target would be disconnected, removed, and replaced with the new one. To maintain adequate availability and provide flexibility in operation, adequate space exists in the hot-cell so a spare target assembly may be readied for operation while the other assembly is in use.

Figure 1-8. Clad-tungsten tube.

1.3.2 Multiplier

In the modular configuration the multiplier is separated into two segments that are brought in from the side (Figure 1-3). The segments can be identical or different, depending on the needs of the experimenter. Each segment has an attendant hot-cell similar to the target, which allows for safe replacement of components. For the preconceptual design, a fast-spectrum, sodium-cooled multiplier is being investigated as the base case. As an option, a helium-cooled thermal-spectrum system is also discussed as it can be implemented using the same irradiation chamber but different multiplier components. This demonstrates the flexibility of the configuration for testing a wide range of nuclear systems and, therefore, supports both the transmutation and advanced nuclear-technology missions. For instance, even though it is not discussed in this report, the modular concept also provides an ideal setting for a controlled testing if LBE is pursued as a nuclear coolant for ATW or advanced fast-reactor applications.

1.3.2.1 Fast-Spectrum System

As an example for the fast-spectrum system, the fuel and reflector bundles are contained in a small vessel cooled with liquid sodium. A number of different vessel geometries are being considered (see Figure 1-9). A trapezoidal vessel shown in Figure 1-9(a) is the best option neutronically as it provides a tight coupling with the target. A large circular vessel shown in Figure 1-9(b) has the advantage of being simpler to construct. Further enhancing the simplicity is the option of twin-circular vessels shown in Figure 1-9(c). Because of the neutron leakage, the twin-vessel concept is the least effective geometry neutronically. On the other hand, the twin-circular option has some safety advantages as the fuel (and

power) contained in each vessel is smaller. Additional trade-off and cost-benefit studies will be used during the conceptual design phase to assess the most desirable geometry.

Figure 1-10 shows that the small primary vessel sits within an enclosed guard vessel that is also sodium-cooled but on a separate circuit. Note that this figure is not drawn to scale and is used only to depict the principal concept. The heat-removal systems for the primary vessel and the guard vessel are configured to provide natural circulation decay-heat removal in the event of loss of forced flow. In the event of a pipe break in the primary vessel coolant loop, the decay heat can also be transferred to the guard vessel via natural circulation within the primary vessel. The flow of sodium in the guard vessel is sufficient to remove the total decay heat, providing a redundant heat-removal mechanism.

Although not shown in Figure 1-3, the fuel or assemblies can easily be replaced with fuel test assemblies and material irradiation tests. Experimenters would position these assemblies and fuels to optimize the irradiation environment they seek. In the event that an experimenter desires a thermal flux over a small volume (for testing long-lived fission product targets), a reflector position could be replaced with an assembly containing a yttrium hydride moderator to locally thermalize the neutron spectrum.

Depending on the flux level achieved, the small vessel components used in the multiplier will need to be replaced on a one- to three-year interval. In the conceptual design stage, strategies to extend the vessel's lifetime will be pursued. For instance, designing an axisymmetric vessel capable of being rotated periodically will be considered. This will be performed in a manner similar to the target replacement. An inert atmosphere in the hot-cell will allow the safe removal of fuel elements out of the vessel and into storage or removal to a disassembly and packaging area. When fuel needs to be replaced or shuffled after an irradiation cycle or experiment bundles need to be removed the vessel is moved into the hot-cell, and the operations are performed in the inert environment.

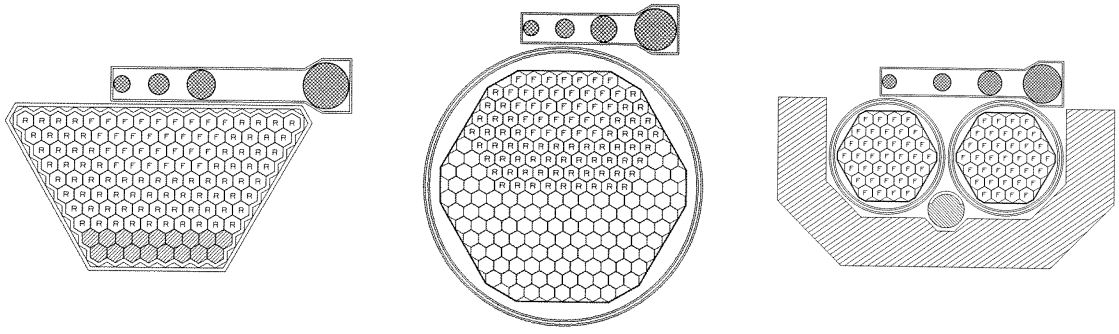

(a) (b) (c)

Figure 1-9. Multiplier vessel options.

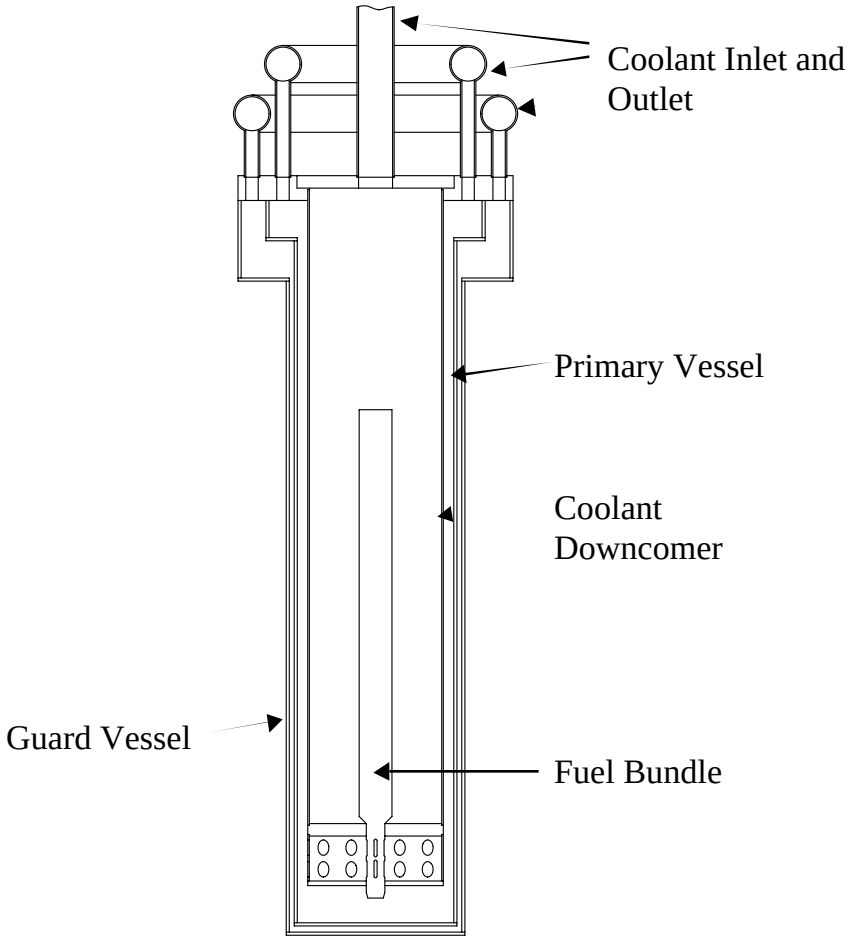

Figure 1-10. Multiplier vessel detail.

1.3.2.2 Thermal-Spectrum System

To demonstrate the flexibility of the facility, an example of a thermal-spectrum multiplier is provided in this section. It is envisioned that the thermal-spectrum multiplier may be used to test advanced fuels and materials, which is part of the facility mission. The design described here consists of a centrally located pressure vessel with a beam entrance window. The beam enters the vessel horizontally. This concept fits within the same irradiation chamber as the fast-spectrum system.

With the beam shut down, the vessel can be opened for access to the target or the fuel blocks. The vessel is the pressure boundary for the pressurized helium atmosphere used to cool the thermal multiplier during operations. The vessel has a beam entrance window that also forms part of the pressure boundary. The vessel operates inside the vacuum atmosphere of the irradiation cell.

Figure 1-11 shows a plan view of the preconceptual vessel design. In the current concept, the vessel is a 6.4-m-high (20.8 ft.) cylindrical structure, 3.5 m (11.6 ft) in diameter, and inserted from one side of the irradiation chamber. The dimensions are subject to change during conceptual design evaluations, however, as the facility mission is further refined with respect to testing needs for the thermal assembly. A flange opening on the downstream side of the vessel allows the removal and replacement of the target in a manner compatible with the sodium-cooled modular ADTF design. A similar flange opening in the upstream side of the vessel accommodates the beam window and allows for its removal and replacement. Both the window and target are designed to attach to a trolley that can be separated from or attached to the vessel by remote means. Seals are formed at the flanges to maintain the pressurized helium atmosphere. To minimize the vessel height, a bolted flat head is used to allow access to the fuel blocks during refueling operations. A flat head is also used in the bottom of the vessel.

A multiplier support barrel surrounds and supports the multiplier, as is shown in Figure 1-11. After entering the vessel, the helium that cools the multiplier flows up in between the vessel and the multiplier support barrel to keep the temperature of the vessel close to the inlet helium temperature. The helium flows from an upper plenum down through the multiplier blocks and exits through the hot duct side, as is shown in Figure 1-12.

To remove the residual heat when the target or window is being replaced, a residual-heat-removal system is needed to keep the temperature in the structures under allowable limits. It is envisioned that when the target or window is being replaced inside the irradiation cell, the atmosphere in the irradiation cell will be equalized with that of surrounding hot-cells by closing a valve down the expander tunnel and breaking the vacuum seals at the end of the trolley. The pressure inside the vessel has to be brought down to the same pressure as the surrounding atmosphere. Conduction, convection, and radiation to a separate heat-removal system may remove the residual heat.

To minimize the cost of the vessel and multiplier support barrel, it is desirable to fabricate them of code-certified, fabrication-proven steels such as SA533 and SA508, type 304 and 316 stainless steels, or others. This is possible if the temperature of the components is kept below the ASME design temperature limit for these materials (700°F to 1,000°F).

As is stated above, this is one option for a thermal-spectrum system, and it is described as an example. An option similar to the fast-spectrum system with two vessels and a windowless beam entry also is a possibility. Additional investigations on determining the most suitable thermal spectrum option will be investigated during the conceptual design.

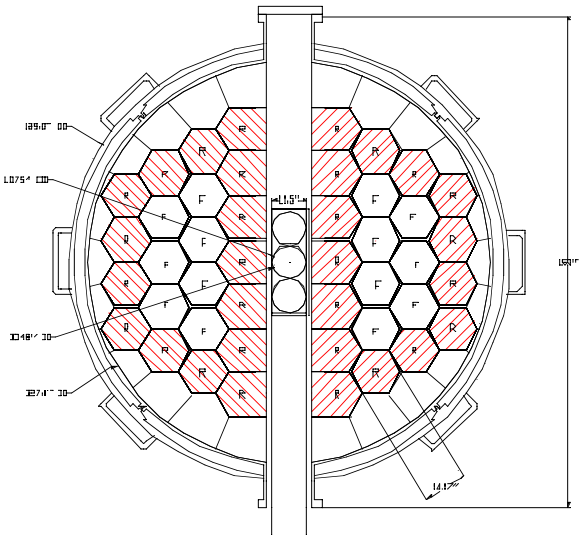

Figure 1-11. Thermal-spectrum modular concept plan view.

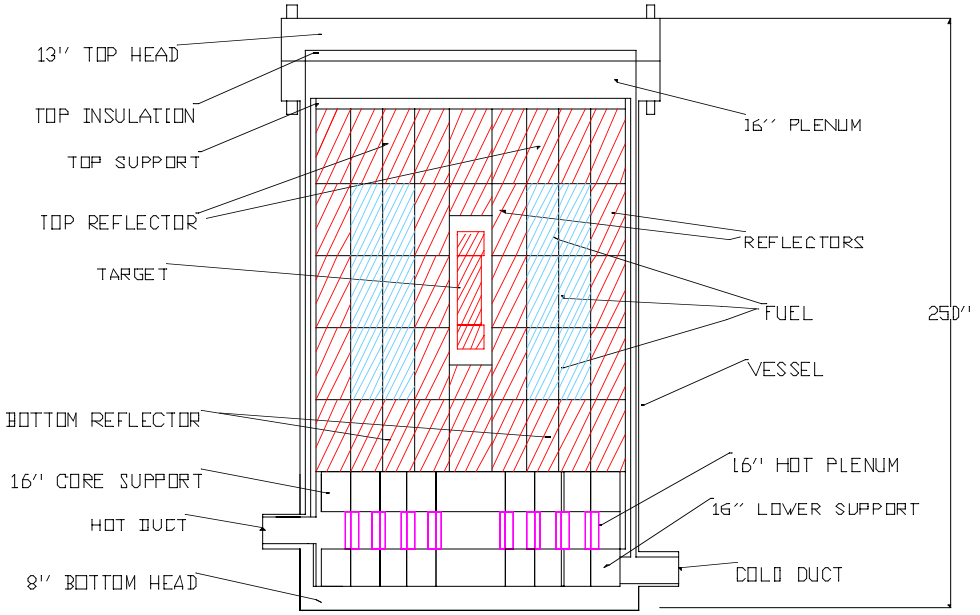

Figure 1-12. Thermal-spectrum modular concept elevation view.

1.3.3 Fuel

For the two options being considered (fast-spectrum or thermal-spectrum), the fuel is vastly different. For the base-case fast-spectrum system EBR-II fuel is assumed, and for the thermal-system, unused Fort Saint Vrain (FSV) fuel is assumed.

1.3.3.1 Fast-Spectrum Multiplier Fuel

The EBR-II fuel was made at the Argonne National Laboratory-West (ANL-West) outside Idaho Falls, Idaho. Approximately 32 subassemblies' worth of fuel slugs is in storage. The equipment used to fabricate the fuel and put it into the assemblies is in storage and can be reconstituted at a reasonable cost (few $M). The facility used to fabricate the fuel is still in operation, performing other fuel-related tasks. Plans are to keep it operating for the future. To operate the ADTF, approximately 60 subassemblies will be required for a full load. It is expected, however, that operation will start with a smaller amount of fuel and low multiplication constants, and then gradually work up to higher power; thus, 30 subassemblies may be sufficient for initial operation. Nevertheless, the fuel fabrication line at ANL-West should be set up starting approximately three years before beginning ADTF operation to provide the necessary fuel.

Because this fuel is qualified and demonstrated for a fast-reactor operation, we plan to use this exact fuel design for our driver fuel. The specifications and dimensions are shown in Table 1-3. These dimensions are consistent with the sketches shown in Figure 1-4 and Figure 1-9. As shown in the table, the uranium enrichment used in EBR-II was 67%. Lower enrichments are possible by blending in more natural uranium. This can be accommodated at the fuel fabrication facility. It is expected that varying the enrichment in the multiplier will be used to flatten the power distribution in the radial direction.

The performance specifications for the EBR-II fuel are summarized in Table 1-4. The environment in the current design is similar to but not identical to the EBR-II. In addition to the typical fast reactor spectrum, there is also some fraction of high-energy particles (scattered protons and spallation neutrons), especially in the row closest to the spallation target. Because of accelerator trips, the fuel and structures will experience a higher thermal cycling rate than in a critical-reactor environment; therefore, in the early phase of operation it is expected that the fuel-operating parameters (e.g., temperature, power density, and maximum burn-up) will be limited to values more conservative than the limits shown in Table 1-4.

Table 1-3. EBR-II Fuel and Assembly Specifications

Feature/Dimension	Value
Fuel slug diameter	0.173 inch
Fuel slug length	13.5 inches
Fuel alloy	U-10w%Zr
Uranium enrichment	67%
Clad diameter	0.230 inch
Clad thickness	0.015 inch
Slug to clad bond material	Sodium
Number of fuel rods per assembly	61
Pin to pin spacer	Wire wrap 0.042 inch diameter
Pin arrangement	Triangular pitch
Assembly duct	Hexagonal
Duct flat to flat distance inside	2.214 inches
Duct thickness	0.039 inch
Hex assembly pitch	2.320 inches

Table 1-4. EBR-II Fuel Performance Specifications

Parameter	Value
Maximum temperature	850°C
Maximum clad temperature	710°C
Maximum linear power	15.2 kW/ft.
Maximum burnup	10 atom %
Maximum fluence	1-2 $\cdot 10^{23}$ n/cm^2
Melting temperature	~1,180°C (solidus), ~1,300°C (liquidus)

1.3.3.2 Thermal-Spectrum Multiplier Fuel

A complete, licensed, replacement core segment (segment 10), consisting of 240 fuel elements was manufactured for the FSV core, but never used. It is now in storage in France. Nine other FSV core fuel segments, which have received various levels of irradiation, are also in storage in Colorado and Idaho and could be used if required. The fuel element is a

hexagonal block of nuclear-grade graphite, 31.22 inches high and 14.172 inches across the flats. The core is comprised of columns of graphite fuel elements stacked six blocks high. The core is cooled by helium gas under pressure, and the gas passes through 108 coolant holes that are drilled through the graphite block. 216 blind holes are also provided for the fuel compacts and lumped burnable poison (LBP), with the six corner blind holes being used for the LBP. The block dimensions and other parameters are summarized in Table 1-5.

Table 1-5. FSV Fuel Element Data

Parameter	Value
Fuel Element	
Cross Section	Hexagonal
Flat-to-flat length, cms	36.07
including gaps between elements, cms	36.10
Side length, cms	20.68
Height, cms	79.25
Area, sq cm	1,126.62
including associated gap, cc	1,128.52
Volume, cc	89,282.30
Graphite volume fraction, %	56.79%
Graphite block density, grms/cc	1.74
Fuel Holes	
Number per element	216
length, cms	78.16
Diameter, cms	1.27
Total volume, cc	21,385.88
Fuel hole volume fraction, %	23.95%
Fuel compact diameter,cms	1.2446
Coolant Holes	
Number per element	108
length, cms	79.25
Diameter, cms	1.59
Total volume, cc	16,941.20
Fuel hole volume fraction, %	18.97%
Fuel Handling Hole	
Diameter, cms	3.51
Height, cms	26.42
Volume, cc	254.92
volume fraction, %	0.29%

The fuel is fully enriched uranium and thorium. The fuel compacts contain separate fissile and fertile TRISO-coated particles bonded together with a carbonaceous matrix. The fissile particles contain a 4/1 Th/U carbide kernel, and the fertile particles contain a pure Th carbide kernel. The TRISO coating contains three types of material: a low-density pyrolytic carbon (PyC), silicon carbide (SiC), and a high-density isotropic PyC. These TRISO coatings have been shown to be a highly impervious barrier to radionuclide release in irradiation tests. These ceramic-coated TRISO fuel particles are also very stable under accident conditions, and can be heated to over 1600°C without failure. They have been tested to essentially complete fissile burnup without loss of integrity.

1.3.4 Heat Removal

Details of the target and multiplier primary heat-removal systems are provided in Section 1.5. Here we provide a general description of the heat-removal systems.

Because the primary coolants for both the target and multipliers will become highly radioactive, the heat exchangers and pumps are located in their respective hot-cells. Secondary coolants are pumped into the hot-cells to provide the necessary heat-removal capability. The heat from the secondary loop is dissipated to the environment through dump heat exchangers. The facility will not use the heat to run a steam cycle and produce electricity. The secondary system is modular so increased heat-removal capability can be added in future facility upgrades up to 100 MW. To support a helium-cooled primary system, the secondary system must have sufficient heat-removal capability with a compatible working fluid. Adequate space in the facility is provided to add this additional heat-removal equipment as well.

For the secondary heat-removal loop of the target and fast-spectrum multiplier systems, we are considering helium as the working fluid. This design will avoid the potential of sodium leaks and fire outside the hot-cell. Because helium is compatible with all conceivable primary coolants, it also provides additional flexibility for future multiplier test options (including water); however, because helium will operate at much higher pressure than the coolant (liquid metal) on the primary side, the heat exchanger tube-break accidents require special attention. The current concept uses an intermediate liquid metal jacket between the helium and liquid metal flows. A layout of the sodium-to-sodium-to-helium heat exchanger is shown in Figure 1-13. A different coolant may be needed on the secondary side when testing a helium-cooled thermal assembly in the multiplier vessel (e.g., organic fluids such as DOW Syltherm).

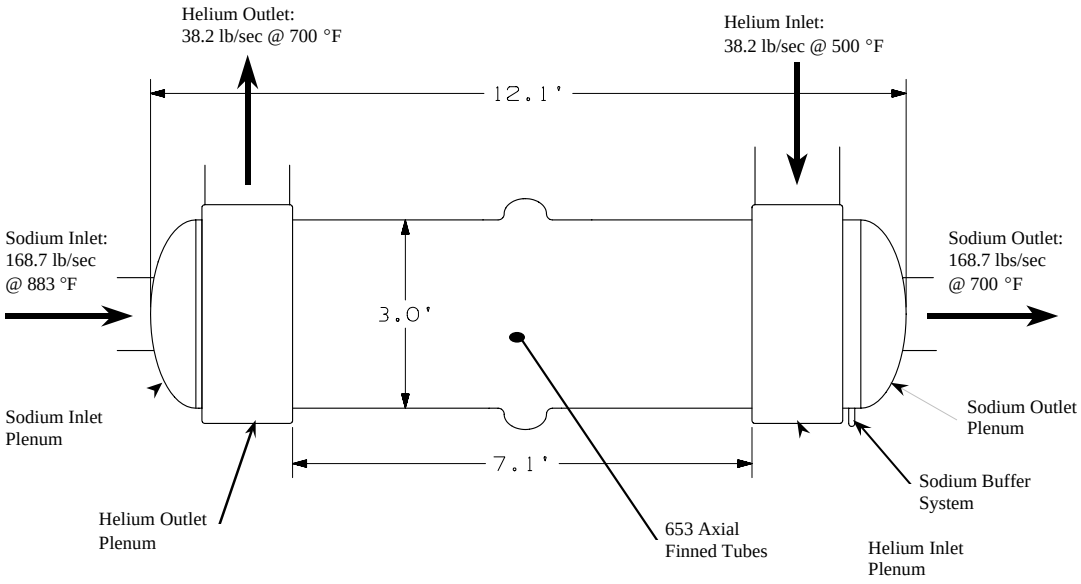

Figure 1-13. Sodium-to-helium heat exchanger.

Although the accelerator will be designed to provide high reliability, a number of beam trips of both short and long duration are expected during the irradiation cycle. The structures and components that make up the primary heat-removal systems for both the target and the multipliers will be designed for the ensuing temperature transients to reduce transient stresses to allowable levels. Components that reach end-of-life because of fatigue will be engineered for easy replacement.

In addition to the heat-removal systems for the target and the multiplier vessels, the shielding surrounding the irradiation chamber requires active cooling. The deposited power in the bulk shield is expected to be low and a gas-cooled system is envisioned for removing the heat, if necessary. The inner lining of the target cell, which will be made of steel, is designed to last the life of the facility. Because of the intense radiation from the target and multipliers, the liner will need to be cooled to maintain a reasonable operating temperature, which is dictated by structural limits. The total heat load is expected to be in the kW range. The preferred heat removal will be performed with a passive system either using natural circulation or heat pipes.

1.3.5 Target and Multiplier Shield Plug and Seal Design

The seals on the target multiplier shield plugs provide the pressure boundary and maintain the necessary vacuum in the irradiation chamber in the windowless design. As such, this arrangement provides an excellent containment boundary that is continuously tested. In the event of seal failure and pressurization of the containment boundary, the beam is automatically shut down. Currently three seal mechanisms are being investigated: elastomer

O-ring face, outboard inflatable elastomer, and inboard inflatable metal seals. During the conceptual design, a trade study will be conducted to determine the optimum seal arrangement.

1.3.5.1 Outboard O-Ring Face Seals

The baseline design for sealing the vacuum within the irradiation chamber incorporates dual elastomer seals with an interseal gas scavenger pump. The gas scavenger vacuum system extracts gases that leak across the seal in contact with atmospheric pressure, creating a low-pressure region between the dual seals resulting in low leakage across the second seal into the vacuum chamber. The seal arrangement is shown in Figure 1-14. The two sets of seals are mounted outboard on a seal carrier plate suspended from the back surface of the module shield by a linkage mechanism. We assume that the seal elastomer compound will not be exposed to excessive radiation at this location and will have a long operating lifetime.

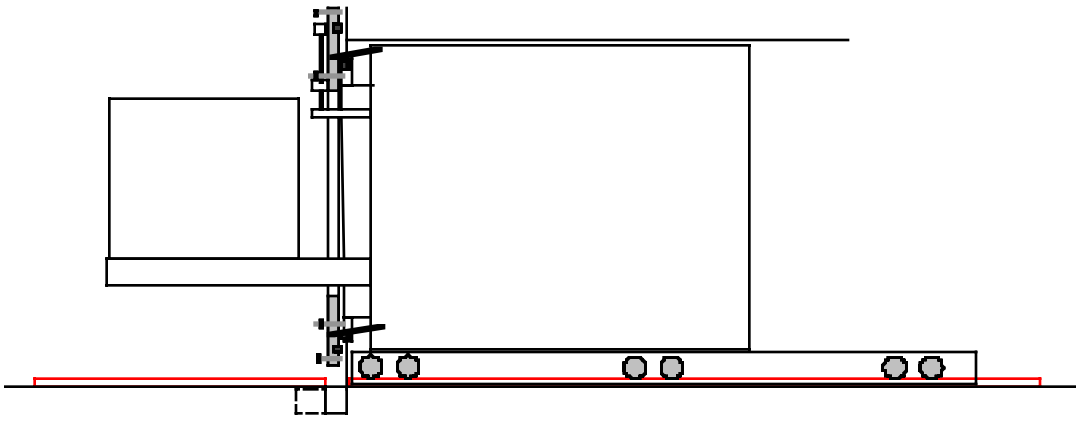

Figure 1-14. Seal carrier plate retracted; dual outboard O-ring.

1.3.5.2 Outboard Peripheral Inflatable Seals

An alternative outboard seal arrangement utilizes dual inflatable elastomer seals with interseal gas scavenging. In this case the seal support plate is not required to move since the seals are retracted from the seal surfaces by deflation. Once the module is inserted, the seals are inflated causing them to expand outward to seal against the inside surfaces of the adjacent building structure. To seal against the building floor, the track incorporates a break and a raised curb.

As with the baseline seal design, a gas-scavenging system extracts leak gas from the interseal space. This arrangement may have a higher leak rate and a lower reliability than the baseline design because of the need for active pneumatic inflation.

1.3.5.3 Inboard Inflatable Metal Seals

A third concept uses dual inflatable metal seals with a leakage-gas-scavenging system located at the inboard shine shield step. The inboard seals must be metal because the radiation level at the inboard location precludes the use of elastomer compounds. This concept utilizes the continuous face of the shine-block step in the building shield against which inflatable seals located on the shield inboard face will be compressed.

The proposed seal design is based on a design being developed and tested for the European Spallation Source (ESS) facility. We are in contact with the principal design engineer in Jülich, Germany, who advises that acceptable quality stainless-steel sheets have been obtained and the fabrication of the prototype seals is now underway. Following fabrication, the full-scale prototype seal will be performance tested. We continue to follow the progress updates. Until the ESS prototype seal data are available, we will not know if the seal performance is adequate.

An advantage of the inboard seal arrangement is that a great deal of vacuum-wetted surface area associated with the outboard elastomer seal designs is removed from the vacuum-chamber space, thereby reducing desorbed gas loads. In the case of the fast spectrum assembly-outer shield plug combination, the area is ~2400 ft^2.

1.3.6 Beam Transport

The proton beam is transported from the end of the accelerator to the target-multiplier building using the standard bending magnet and beam-tube technology employed for the APT design. Vacuum pumps maintain the hard vacuum necessary for low-loss beam transport. Elevation of the beam is identical to that of the centroid of the target so no vertical axis beam bending is required. Before entering the shielded irradiation chamber, a series of beam expansion and/or raster magnets are used to send the beam on a trajectory that provides the desired beam-spot distribution at the front face of the target. Assuming a raster system is acceptable (as was the case for APT), a beam distribution can be provided that is uniform with variations less than 10% over the desired area. Impact of a rastered beam on the neutronic fluctuations and cyclic thermal stresses will be assessed in deciding on the beam expansion strategy.

For the beam to transport to the front face of the target with little or no loss, a relatively hard vacuum is required. To provide this vacuum level in the irradiation chamber without using a beam-entrance window, vacuum pumping will be provided along the beamline, through the expansion chamber, and to the irradiation chamber. Vacuum seals for the target and multiplier inserts in the low-radiation zone on the outside of the shield provide the necessary pressure boundary (see Section 1.3.5). Redundant, fast-acting valves in the beamline outside the shield and upstream of the expansion magnets provide protection for the accelerator beamline in the event of the leak into the irradiation chamber. Any leak into

the irradiation chamber, from either a seal failure or a container failure, automatically shuts down the accelerator, even if the active systems fail because the beam cannot be accelerated without sufficient vacuum. This provides a passive beam shut-down mechanism in the event that either the target container or the multiplier guard vessel fails.

In the preconceptual design assessments, a beam energy of 600 MeV is used. Even though lowering the beam energy to ~400 MeV would result in a less expensive accelerator, a series of sensitivity studies are used to determine the beam energy. The beam power (current) must be increased considerably below 600 MeV to maintain a constant neutron-production rate. For instance, at 400 MeV the beam current must be set to ~27 mA (total power of ~11 MW) to produce the same amount of neutrons as a 600MeV and 13.3 mA beam with a total power of 8 MW. The beam energy also has a strong influence on the power distribution within the target. Figure 1-15 shows how the deposited power density varies as a function of depth in a target for proton beams of varying energy. Below 600 MeV, the peak power density is dominated by the Bragg peak at the end of the proton track. Above 600 MeV, nuclear interactions, combined with an increase in beam divergence as the beam penetrates the target, cause the peak-power density to occur near the front of the target. A corollary to Figure 1-15 is shown in Figure 1-16, where the peak-power density (normalized to power density at 800 MeV) is plotted as a function of beam energy. As is shown in this figure, the peak-power density is considerably higher than the peak-power density at 600 MeV for lower energies. Finally, at low energies there is considerable production loss in the window or structural material used in front of the target material. This is illustrated in Figure 1-17 as percent production loss when a 4-mm steel structure is placed in front of the tungsten or LBE target.

Based on these considerations, the optimum beam energy is determined as 600 MeV. At present the beam current is sized at 13.3 mA to provide an 8-MW total beam power; however, the maximum beam current requirement may be revised when a detailed assessment for the testing needs is performed.

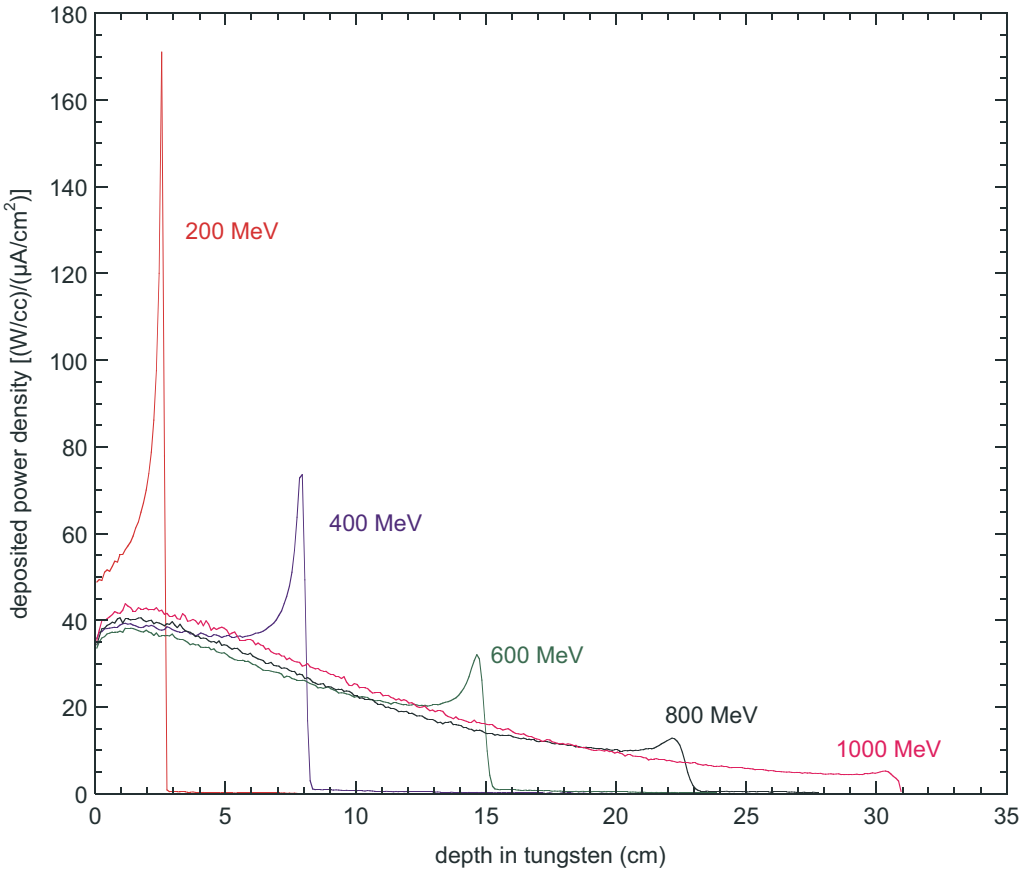

Figure 1-15. Power deposition as a function of beam energy.

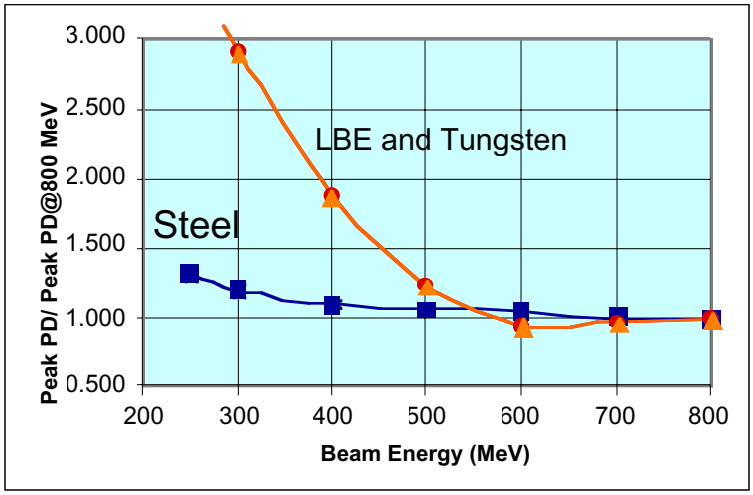

Figure 1-16. Normalized peak power density as a function of beam energy.

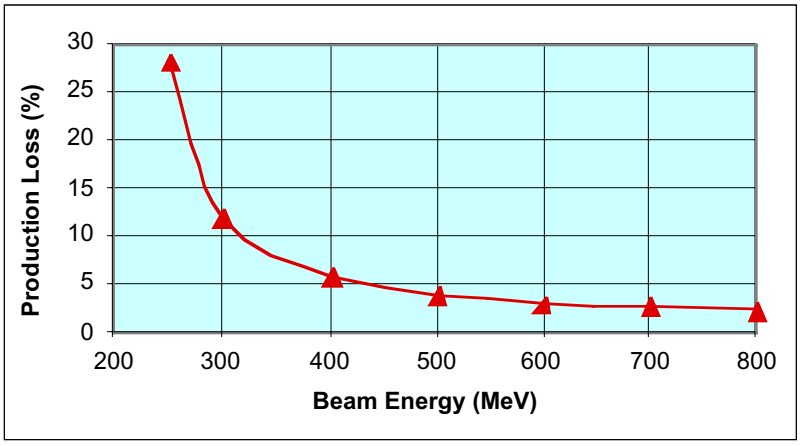

Figure 1-17. Neutron production losses in 4-mm steel as a function of beam energy.

1.4 Nuclear Design Features and Neutronics Performance

The basic layout of the modular target-multiplier system is consistent with that of all accelerator-driven subcritical assemblies: a core consisting of a spallation neutron source, surrounded by a neutron-multiplying blanket fueled by fissile material.

1.4.1 Spallation Target

The heart of the design is the spallation target, which is *split* into a series of vertically oriented heavy-metal-filled pipes arranged along the path of the proton beam. This splitting of the target, combined with horizontal beam insertion, provides real flexibility in terms of optimally distributing the neutron source. The beam is rastered both vertically and horizontally to provide a uniform-current density on target over a 5.9-cm-wide by 38-cm-high area. The beam height is set to provide uniform illumination of the target over a height that is consistent with the active region of the fuel assemblies (34.3 cm). This provides axially uniform leakage of source neutrons from the target into the multiplier, which reduces axial peaking of power density in the fuel elements.

The optimum beam width is a compromise between neutronic and thermal-hydraulic performance. Neutronically, a narrow beam is best because it minimizes parasitic capture in the target and provides the best geometrical coupling between the target and multiplier. There are thermal-hydraulic limits to how narrow the beam can be, however. The beam width is set so the proton-current density on target (60 mA/cm2 for a 13.3-mA beam) provides a safe thermal-hydraulic margin for cooling the heavy-metal target material (our current choice is LBE) and its structural container.

The number, location, and size of the pipes that comprise the spallation target can be adjusted so nearly uniform heat loads in all fuel assemblies that are in closest proximity to the target are achieved. As a starting point, the target has been split into three or four pipes located on the axis of the proton beam path. The pipe diameters increase with depth into the target. This configuration provides fairly uniform neutron production from each pipe, since the quantity of target material increases to compensate for the decreasing neutron production as the beam loses energy while traversing the target.

1.4.2 Multiplier

Some sample calculations for the neutronic performance of fast-spectrum and thermal-spectrum multipliers are provided in this section.

1.4.2.1 Fast-Spectrum Multiplier

The fast multiplier consists of a collection of ^{235}U-loaded fuel assemblies placed as close to the spallation target as practical to achieve optimal neutronic coupling between the target and multiplier. The layout of the modular design has fuel assemblies placed laterally on both sides of the target, with primary and guard vessel walls between the multiplier and

target (see Figure 1-9). In this arrangement, the proton beam never enters the multiplier vessel, so there is no need for a proton-beam window associated with the vessel, which must necessarily be a thin-walled structure to minimize energy loss as the protons pass through it. Instead, only the source neutrons must pass through the vessel walls, and the walls are quite transparent to these fast neutrons. The downside to this arrangement is that the vessel walls are placed in a harsh radiation environment, and the radiation damage to these structural elements dictates frequent replacement of the vessels.

The fuel used in preconceptual design studies is Mark-IIIA fuel as produced for the EBR-II reactor. The fuel is binary metallic U-10w% Zr, clad in stainless-steel tubes. Sodium fills the gap between the fuel pins and the clad. There are 61 fuel pins per hex assembly. The unit cell is hexagonally shaped, 2.32 inches flat-to-flat. Smeared volume fractions in the unit cell are 30.8% fuel, 21.6% stainless steel, and 47.6 % sodium. The active fuel height is 13.5 inches. The Mark-IIIA fuel is 67% enriched in ^{235}U, but in our studies we adjusted the enrichment to achieve the desired reactivity levels.

Two basic multiplier configurations have been investigated: a trapezoid-shaped vessel on each side of the target, and two cylindrically shaped smaller vessels on each side of the target. Specifications call for the multiplier to have a thermal power of 20 MW, upgradeable to 100 MW. The trapezoid includes not only fuel assemblies within the vessel, but also several rows of reflector assemblies, thus, it can easily accommodate higher multiplier power by simply replacing reflector assemblies with fuel assemblies: at 20 MW, there are 60 fuel assemblies; for 100 MW, there are 126 assemblies. For the two-cylinder, the vessels contain only fuel assemblies. At 20-MW multiplier power (i.e., 5 MW in each of the four cylinders), each cylinder has 19 fuel assemblies contained in 13-inch-diameter primary vessels. At 100 MW, this increases to 37 assemblies contained in 19-inch-diameter vessels.

The modular design has the flexibility of operating at different levels of reactivity by simply adjusting the ^{235}U enrichment of the fuel. The trapezoid configuration, operating at 20 MW, appears to be the only design that can successfully operate over the entire specified range of reactivity, $0.8 < k_{eff} < 0.97$. If the two-cylinder configuration is limited to 19 hexes per cylinder, it is not capable of achieving $k_{eff} = 0.97$ because of a lack of sufficient fissile mass. In fact, if the ^{235}U enrichment is limited to 93%, the maximum achievable reactivity is $k_{eff} = 0.91$. With respect to 100-MW operation, the maximum allowable beam current of 13.3 mA limits the minimum reactivity for both configurations. For the trapezoid, the minimum reactivity is 0.94, while for the two-cylinder it is 0.95. The implication of this rather high minimum reactivity is that the fuel may be limited to rather low burnup at 100 MW unless the beam power is increased beyond 8 MW or the fuel has a significant fertile composition.

For the two configurations, results of MCNPX runs are given in Table 1-6. Four variations of each configuration are shown: 20- and 100-MW operation, and low and high reactivity levels. Thermal-hydraulic analyses have not been performed for all of these configurations, and some of them may exceed thermal-hydraulic limits. This is very likely the case for the 100-MW trapezoid configuration, where the hottest hex assemblies have powers exceeding 1 MW. These peak powers may be reduced slightly by creating two fuel zones with different fuel enrichments, or by adding more fuel-hex assemblies. In all cases, fluxes

are higher when the reactivity is lower because the thermal power is proportional to the product of the fissile density and the flux. As the fissile density is increased to achieve higher reactivity, the flux drops to maintain constant power. The trapezoid configuration offers a higher peak and average flux as compared to the two-cylinder configuration because the fuel is more closely packed for the trapezoid. Neutron fluxes in Table 1-6 are limited to neutrons with energies greater than 0.1 MeV. Fluxes over all energies are about 10% higher. Average fluxes are averaged over the entire fuel volume. Target powers for the trapezoid configuration are lower for a given beam current than those of the two-cylinder configuration because, at present, the MCNPX model of the trapezoid target consists of only three pipes, whereas the two-cylinder target has four.

Table 1-6. Results of MCNPX Runs for the Two Configurations

Multiplier Configuration	**Trapezoid**				**Two-Cylinder**			
Multiplier power (MW)	**20**		**100**		**20**		**100**	
k_{eff}	0.8	0.97	0.94*	0.97	0.8	0.91§	0.95*	0.97
^{235}U enrichment (%)	59	85	58	62	73	93	69	72
^{235}U mass (kg)	179	258	369	395	279	355	513	536
Number of fuel assemblies	60	60	126	126	76	76	148	148
Power in hottest fuel assembly (kW)	423	403	1,130	1,110	327	339	888	895
Axial peaking factor for hottest assembly	1.16	1.21	1.17	1.19	1.15	1.16	1.16	1.17
Peak flux, >0.1 MeV (10^{15} n/cm^2/s)	1.4	1.1	3.8	3.6	0.89	0.76	2.5	2.5
Average flux, >0.1 MeV (10^{15} n/cm^2/s)	0.90	0.67	2.2	2.1	0.59	0.50	1.6	1.6
Target power (MW)	3.1	0.60	4.0	1.8	4.4	2.0	5.0	3.1
Beam current (mA)	11.5	1.86	13.3	5.6	12.5	5.0	13.3	8.0

*Minimum k_{eff} limited by a maximum beam current of 13.3 mA.
§Maximum k_{eff} limited by a maximum ^{235}U enrichment of 93%.

Shown in Figure 1-18 is a horizontal slice of the spatial distribution of the neutron flux for the trapezoid configuration with k_{eff} = 0.8 and a multiplier power of 20 MW. Note the flux peaks in the multiplier region at a point fairly close to the spallation target. Figure 1-19 shows a vertical slice for the same system, at the center of the second target pipe. Note the fairly uniform axial distribution of the neutron flux.

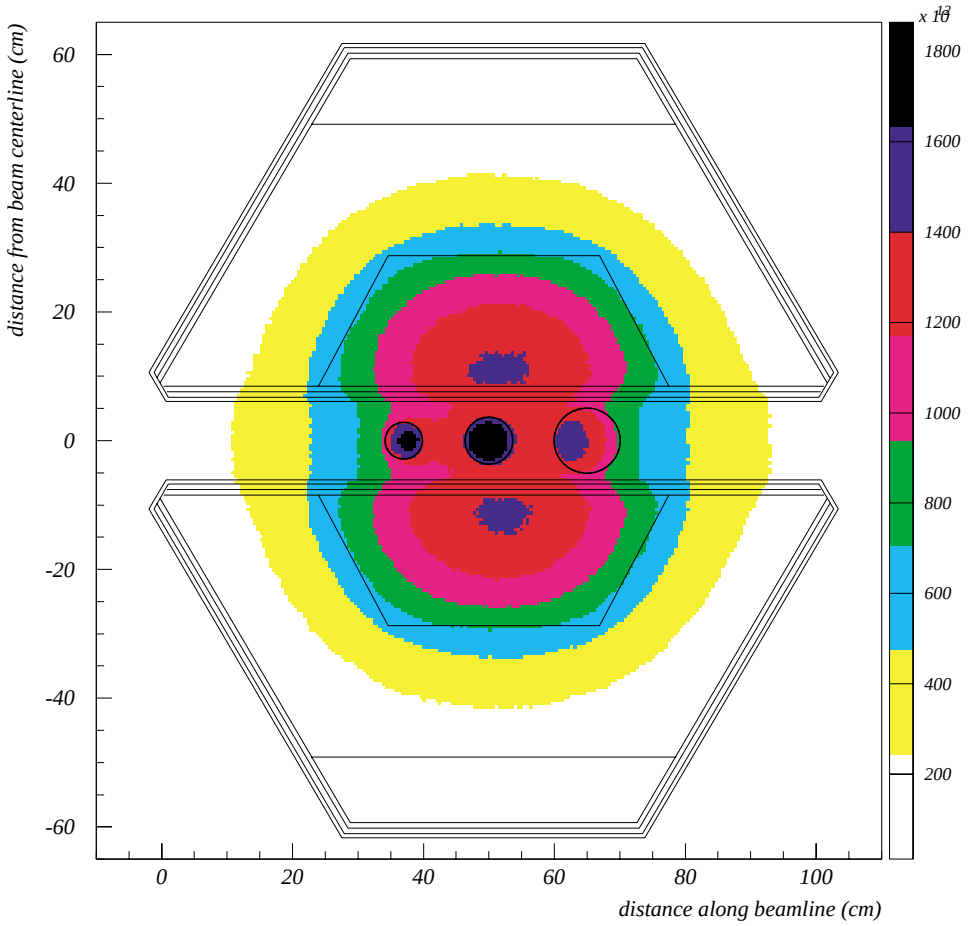

Figure 1-18. Spatial distribution of the neutron flux for the trapezoid configuration at a blanket power of 20 MW and k_{eff} = 0.8 (horizontal cut). Units on the scale bar are n/cm^2/s.

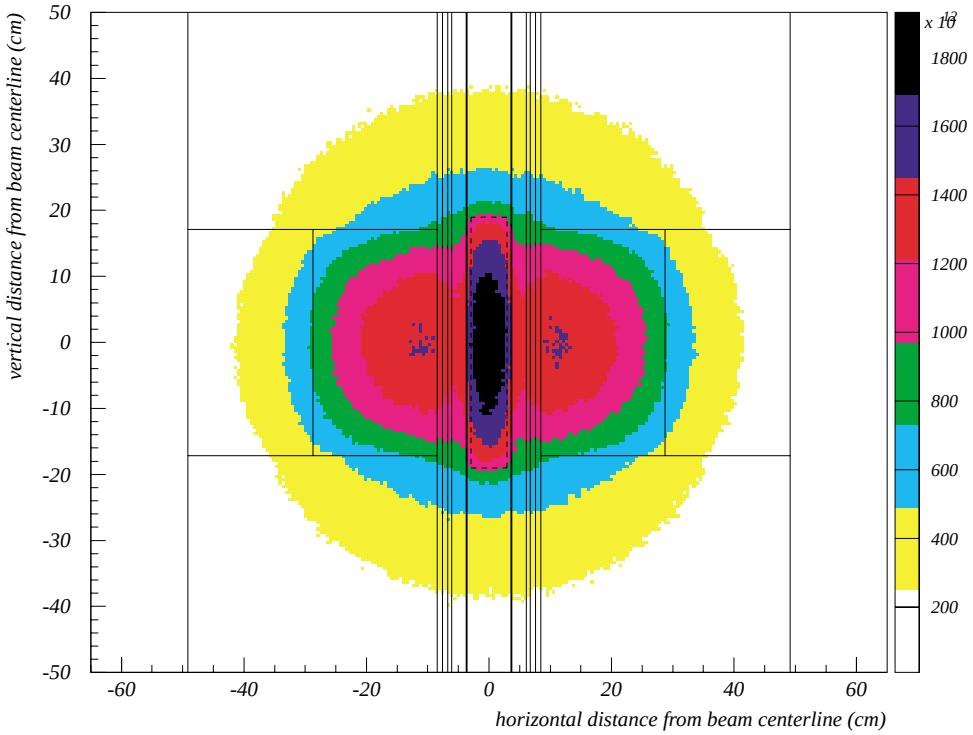

Figure 1-19. Spatial distribution of the neutron flux for the trapezoid configuration (vertical cut). The dashed line indicates the footprint of the rastered beam. Units on the scale bar are n/cm^2/s.

1.4.2.2 Thermal-Spectrum Multiplier

A single configuration of the thermal system has been analyzed up to this point. A number of other layouts have and are being considered, and the basic design allows for a good margin of modification. Primary to all of the thermal-system configurations under consideration is the use of standard GT-MHR graphite fuel and reflector elements. These hexagonal blocks have a flat-to-flat length of 36.07 cm and a height of 79.25 cm. Fuel blocks and reflectors can be easily arranged in various configurations for optimum performance.

The fuel blocks essentially consist of ceramic-coated TRISO fuel particles embedded in a graphite matrix. In an actual fuel element these small (0.0620-cm diameter) particles are packed into *compacts,* which are loaded into fuel *rods*. The fuel assumed in the study is LWR TRU waste, and the relative composition is given in Table 1-7. Other details of these particles can be found in the literature. The rods, along with coolant holes and burnable

poison *rods*, are distributed in an optimized configuration in a graphite block. Although it has been shown that discreet modeling of these fuel blocks is necessary for a proper transport, time constraints dictated that a homogenized fuel/graphite matrix be used. Flux and power tallies should not be affected too much (when considering the overall configuration); however, the calculated k_{eff} will be lower than if discreet modeling was used. Reflectors are essentially graphite blocks and are modeled as such.

Table 1-7. Thermal-Spectrum Multiplier Fuel Composition

Isotope	LWR TRU Waste Contribution (%)
Np-237	4.10
Pu-238	1.20
Pu-239	51.55
Pu-240	23.88
Pu-241	7.99
Pu-242	5.00
Am-241	5.00
Am-242M	0.10
Am-243	1.00
Cm-242	0.00
Cm-243	0.00
Cm-244	0.20
Cm-245	0.00
Total	100.00

The layout considered in the analysis consisted of three vertical layers of fuel blocks, surrounded by one layer (all sides) of reflectors. The fuel blocks are centered vertically at beam center-line, and laterally there is a row of four blocks followed by three blocks. A horizontal slice at beam center-line is shown in Figure 2-11. Thus, there are 21 fuel blocks situated on each side of the target. This configuration is centered in a double wall (1.25 inches of stainless steel assumed for each wall) containment vessel. The overall dimensions are 250 inches high with an outer wall diameter of 139 inches. There is a 13-inch-thick steel head at the top and an 8-inch-thick steel slab at the bottom. The targets were kept the same as the fast design. Other components (supports, plenum, etc.) within the vessel were not included in the transport model.

A preliminary transport calculation was performed for this configuration using MCNPX computer code. The preliminary nature of this calculation must be stressed, since tallies

were generally only determined on a (fuel/reflector) element-by-element basis. Rough vertical subdivision of the fuel elements was performed, so that certain quantities (axial peaking, etc.) may not be an accurate reflection of the true system. The fuel blocks should also be discreetly modeled to achieve a more accurate transport (as is pointed out above). Results of this initial calculation are summarized in Table 1-8, which provides the values for a 20-MW system.

Table 1-8. Results of Preliminary MCNPX Run for the 20-MW System

K_{eff}	**0.92**
Number of fuel assemblies	42
Power in hottest fuel assembly (kW)	718
Axial peaking in hottest assembly	1.11
Target power (MW)	1.15
Beam current (mA)	4.2
Peak flux, >0.1 MeV (10^{15} n/cm^2/s)	0.191

A graphical depiction of the neutron flux in the (horizontal) plane of the beam center-line is shown in Figure 1-20. The flux values are per mA of beam current. As one can see, the neutron flux is distributed in a uniform manner along the beam axis throughout each side of the system.

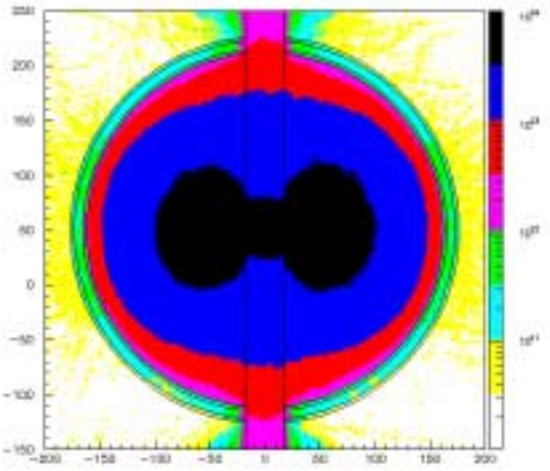

Figure 1-20. Neutron flux per mA beam current in a horizontal plane at beam center line.

1.5 Thermal-Hydraulic Design Features

The modular ADTF target-multiplier uses a horizontal beam entry where the beam strikes the targets with multiplier modules on each side of the targets. The vertical fuel height in the multiplier modules is 34.3 cm (13.5 inches). A beam height of 38 cm was selected. This height is slightly larger than the fuel height to provide a uniform power density along the fuel height. This section describes the primary target design using flowing LBE in vertical pipes and a back-up design using sodium cooling of clad tungsten rings similar to the bundle designs used in the APT project. Three geometric arrangements shown in Figure 1-9 are being considered for the multiplier modules, with all using EBR-II hexagonal assemblies as building blocks.

1.5.1 Target System

The target system includes the in-beam target module and the heat-removal loop. As is shown in Figure 1-7, the target pipes are located between inlet and exit plena. Flow goes from the exit plenum through the loop piping to the heat exchanger and then through the pump and back to the inlet plenum.

1.5.1.1 Target Module

The primary target design uses vertical steel pipes with LBE flowing inside the pipes. Designs were done for a 600 MeV beam with a maximum current of 13.3 mA. The design

constraints are a maximum LBE velocity of 2.0 m/s and a maximum pipe wall temperature of 550°C. Given these constraints, the maximum power density that could be accommodated in the LBE was calculated as a function of pipe size, as is given in Table 1-9. All cases use a LBE inlet temperature of 200°C. At 600 MeV, the power deposited in the LBE is 20 W/cm^3 for each microamp per square centimeter of beam current. So, for example, with a pipe size of 10 cm, the maximum power density in the LBE is 1,193 W/cm^3 so the beam current density can be a maximum of 59.65 microamps/cm^2. For a maximum beam current of 13,300 microamps, the beam area needs to be at least 223 cm^2. With a beam height of 38 cm, this gives a beam width of 5.9 cm. As is shown in the table, the beam width could be somewhat smaller if the locations first struck by the beam are smaller tubes. For this stage of the design the 5.9-cm beam width was used. Also note that, for reduced beam power, the beam spot can also be reduced, making the target even more compact.

Table 1-9. Maximum Power Densities for a Range of LBE Target Pipe Sizes

Inside diameter of pipe (cm)	6	8	10	16
Power density in LBE (W/cm^3)	1357	1268	1193	1029
Current density at 600 MeV .A/cm^2)	67.85	63.40	59.65	51.45
Exit velocity (m/s)	2.0	2.0	2.0	2.0
Exit LBE temperature (°C)	383.0	368.1	356.6	332.7
Maximum tube wall temperature (°C)	550.0	550.0	550.0	550.0

Parameter variations were done for the 10-cm tube for velocity in the tube and peak-power density to determine how much they would have to change to increase the maximum tube-wall temperature from 550°C to 600°C or 700°C. Holding the power density constant, the velocity would have to be decreased from 2.0 m/s to 1.61 m/s and 1.15 m/s to increase the maximum tube wall temperatures to 600°C and 700°C. Holding the velocity constant at 2.0 m/s, the power density would have to be increased by 15% and 45% to increase the maximum tube wall temperatures to 600°C and 700°C.

Calculations have also been done for a back-up target that uses a clad-tungsten ring design similar to the APT target design, except with sodium cooling instead of heavy-water cooling. The initial calculations were done for a bundle containing five clad concentric tungsten cylinders with 0.203 cm (0.080 in.) tungsten thickness, 0.0127 cm (0.005 in.) Alloy 718 cladding, and 0.102 cm (0.040 in.) flow channels between the tungsten cylinders. The Alloy 718 tube is 0.0889 cm (0.035 in.) thick and has an outside diameter of 4.14 cm (1.63 in.). The design constraints are a maximum sodium velocity of 4.0 m/s and a maximum pipe wall temperature of 600°C. The inlet temperature is 200°C and exit temperature is 534°C for the maximum Alloy 718 clad temperature of 600°C. The maximum tungsten power density that gives the 600°C clad-temperature limit is 1,965 W/cm^3. For tungsten at 600 MeV, the power deposition is 37.7 W/cm^3 for each microamp per square centimeter of beam. So for a 38-cm beam height, the beam width needs to be slightly larger for the back-up target, 6.71 cm vs. 5.9 cm. If the back-up target design is chosen,

the size would be optimized for the ADTF beam, probably using larger tube sizes so fewer tubes would be needed to provide the beam width and tungsten effective thickness needed.

1.5.1.2 Target Module Primary Heat-Removal System

The exit temperatures in Table 4-1 assume all of the LBE is directly in the beam. Because part of the flow is outside the beam in the larger pipes, the average exit from these pipes will be decreased from the values given in the table. For calculating loop piping sizes, the average exit temperature from the target pipes was estimated to be approximately 300°C. Since the loop piping is expected to have much longer lifetimes than the in-beam target pipes, a reduced LBE velocity of 1.5 m/s was also used for the loop piping. With a maximum of 5 MW in the target, the loop-piping size would need to be of at least 16.75-cm (6.59 in.) inside diameter (ID) to obtain the 1.5 m/s maximum velocity. The heat exchanger will use helium on the secondary side, with a buffer layer between the walls to prevent the high-pressure helium from entering the LBE loop in the event of a leak. If the back-up target using sodium cooling is chosen, the heat exchanger will then be a sodium-to-helium heat exchanger, again with a buffer layer between the sodium and helium. The helium in the secondary loop is cooled to air or water outside the target-multiplier building. The heat exchanger will be located outside the target tunnel so it can be high enough in elevation to provide natural convection in the target-cooling loop for decay-heat removal.

1.5.2 Multiplier System

The multiplier system includes the multiplier modules and the heat-removal loops. There is a loop for the multiplier modules on each side of the target. Flow goes out of the multiplier modules to the exit plenum, from the exit plenum through the loop piping to the heat exchanger, and then through the pump and back to the inlet plenum.

As is shown in Figure 1-9, three geometric arrangements are being considered for the multiplier modules with all using EBR-II-type hexagonal assemblies as building blocks. The results given here concentrate primarily on the twin-cylinder option with power densities corresponding to 5 MW in each multiplier vessel, with linear scaling of power densities for higher power applications. Representative calculations were done for this type of configuration in which each multiplier vessel contains 37 hexagonal assemblies.

1.5.2.1 Multiplier Vessels

This section describes the thermal-hydraulic results for calculations related to the option with twin-cylinder modules on each side of the target. Each module has the hexagonal assemblies inside an inner hexagonal structure contained inside an inner vessel. A guard vessel surrounds this inner vessel, with a flow space between the vessels. For the fueled part of the module, flow goes downward between the hexagonal structure surrounding the assemblies and the inner vessel, and then back up through the hexagonal assemblies. A separate loop provides flow to the annulus between the inner vessel and guard vessel that has a much smaller power removal requirement. The flow in this separate loop goes down-

ward in half of the annulus between the vessels and back up in the other half of the annulus. This guard-vessel flow helps provide cooling of the inner vessel, and also provides a potential means of removing decay heat for the lower power multiplier modules if there is loss of flow in the main cooling loop.

Calculations were done for the highest power hexagonal assembly for the 5-MW total module power case and then for a higher power that caused the 4-m/s sodium velocity limit to be reached. The geometry of the assembly is given in Table 1-3. The sodium inlet and exit temperatures were used the same as for EBR-II, 371.1°C (700°F) inlet and 472.8°C (883°F) exit. As is shown in Table 1-10, for the power densities corresponding to 5 MW in the module, the maximum sodium velocity is 1.6 m/s. This design can use increased powers up to 12.5 MW per module (50 MW total) before the 4 m/s velocity limit in sodium is reached. Table 1-10 shows that the peak clad and peak hexagonal wall temperatures remain below 500°C, even at the highest power level.

Guard-vessel conditions were calculated for full power operation at 5 MW, 12.5 MW, and 25 MW. Both the inner and outer vessels are 0.635 cm (0.25 in.) thick, and the flow annulus is 1 cm (0.394 in.) thick. The inner vessel ID is 43.815 cm (17.25 in.), and the guard vessel ID is 47.085 cm (18.54 in.). Calculations were done for both full power and for decay power. For decay power the power densities in the vessels were 1% of full power, and the decay power from all of the fuel assemblies (1% of the modules steady-state power) was assumed to be conducted out through the inner vessel to the guard vessel flow. In more detailed calculations, the ANS decay curve will be used. The 1% estimate is approximately the decay heat corresponding to two hours after shut down. The inlet sodium temperature was 371.1°C and the sodium velocity was 4 m/s in all cases. Table 1-11 shows the peak temperatures in the inner vessel and guard vessel for the three power levels for full power and decay-heat removal. All are below 600°C.

Table 1-10. Peak Temperatures in Hexagonal Assembly for 5 MW and 12.5 MW in Module

Power in module (MW)	5	12.5
Maximum velocity (m/s)	1.6	4.0
Fuel power density (W/cm^3)	656.5	1644.7
Hexagonal wall power density (W/cm^3)	23.4	58.7
Peak clad temperature (°C)	483.6	498.8
Peak fuel temperature (°C)	507.6	558.2
Peak hexagonal wall temperature (°C)	473.3	474.1

Table 1-11. Temperatures in Inner Vessel and Guard Vessel for Full Power and Decay-Heat Removal

Module power at full power	5 MW	12.5 MW	25 MW
Full power peak inner vessel temp (°C)	395.1	430.7	489.2
Full power peak guard vessel temp (°C)	413.4	475.8	577.7
Decay power peak inner vessel temp (°C)	409.5	466.7	560.9
Decay power peak guard vessel temp (°C)	373.1	376.1	381.0

1.5.2.2 Multiplier Module Primary Heat-Removal System

Coolant flows out of the multiplier modules to the exit plenum, from the exit plenum through the loop piping to the heat exchanger, and then through the pump and back to the inlet plenum. The heat exchanger transfers the power from the primary loop sodium through a buffer layer to the secondary side helium. The buffer layer prevents a direct leak from the higher pressure helium side into the sodium primary loop. The helium in the secondary loop is cooled to air or water outside the target-multiplier building. The heat exchanger will be located outside the multiplier tunnel sufficiently high in elevation to provide natural convection in the loop for decay-heat removal.

Pipe sizes were calculated using a 4-m/s velocity limit. For a 5-MW module and a total of 10 MW in the two modules on that side of the target, the pipe IDs would need to be at least 12.1 cm (4.76 in.) coming out of the module and 17.1 cm (6.74 in.) after the pipes from the two modules join. For the highest power possibility (100 MW total), there would be 25 MW in one module and a combined 50 MW in both modules on one side of the target. The corresponding pipe IDs would need to be at least 27.1 cm (10.6 in.) coming out of the module and 38.3 cm (15.1 in.) after the pipes from the two modules join. There is a separate heat-removal loop for the guard vessels and the reflector module (if it is separate). These loops will be designed during the conceptual design.

1.5.3 Shield Heat Removal

A heat-removal system will be provided for the relatively low temperature shield regions. One possibility is to use a gas cooling system. The power generation in the shield region is expected to be lower than the target and multiplier systems. A heat-removal sizing study for this system will be performed during the conceptual design.

1.6 Structural Design Features

The design of the ADTF target and multiplier systems is based primarily on the science and technology that has evolved over the past 30 years in the development of spallation sources for materials and nuclear science research. The wealth of knowledge and experience in materials, design, and safety from the nuclear reactor field is also applied. This

section presents a basic overview of the structural components, the structural requirements, and the identified candidate materials.

1.6.1 Structural Components

Of all the components within the ADTF, those of most interest are located in or adjacent to the spallation target. These components, which are subjected to high-energy protons and spallation neutrons, receive the most radiation damage during the fuel irradiation cycle and therefore warrant careful consideration with respect to materials and design geometries used. The major components of the target and multiplier systems located in the high-energy proton and neutron spectrum regions are identified and briefly described below.

1.6.1.1 Target (Spallation Neutron Source)

The proton beam, either rastered or expanded, enters the irradiation chamber and impacts the target structure. This target structure, which contains the neutron source material, is designed to sit directly in the proton beam and will therefore have the highest radiation-damage rates. The function of the neutron-source material is to produce spallation neutrons efficiently; therefore, materials with high atomic numbers and low neutron-absorption cross sections are preferred. There are currently two candidate materials for use as the neutron source: tungsten and LBE.

1.6.1.2 Multiplier Vessels

The multiplier vessels sit adjacent to the target. The multiplier vessels are double-walled and contain fuel assemblies, reflector assemblies, control rods, and coolant. These vessels serve as the primary and secondary coolant and containment boundaries for the fuel assemblies. Being located in such close proximity to the target and therefore to the proton beam, it is anticipated that the vessels will experience fairly high radiation damage during operation.

1.6.1.3 Fast Fuel Assembly Structure

The fuel assemblies are comprised of 61 EBR-II-type fuel-pin assemblies packaged within a thin-wall hex can structure that holds the pin assemblies in place and serves as an upflow coolant channel. Like the multiplier vessels, the fuel assembly structures are also located in a high-radiation-damage area.

1.6.1.4 Thermal Fuel Assembly Structure

The coating layers of a TRISO particle have specialized functions; in composite, however, they provide a high-integrity pressure vessel, which is extremely retentive of fission products. The purpose of the buffer layer is to provide a reservoir for fission gases released from the fuel kernel and to attenuate fission recoils. The main purposes of the inner pyrocarbon coating are to provide a smooth regular substratum for the deposition of a high-integrity SiC coating and to prevent Cl_2 and HCl from permeating the fuel kernel during the

SiC deposition process; therefore, a major benefit of the IPyC coating is realized during particle fabrication. The most important coating in a TRISO particle is the silicon carbide, which provides most of the structural strength and dimensional stability and serves as the primary barrier to the release of fission products, particularly the metallic fission products. The outer pyrocarbon coating (OPyC), which shrinks under irradiation, produces a compressive stress in the dimensionally stable SiC, which partially compensates for the tensile stress in the SiC, which may be induced by the internal gas pressure. The OPyC coating has also been shown to effectively retain fission gases in fuel particles with defective or failed SiC layers at temperatures up to about 1,800°C.

1.6.1.5 Irradiation Chamber Shielding

Surrounding the irradiation chamber is a region containing both permanent and movable shielding. This shielding serves to protect workers and minimize the activation of equipment located in the adjacent hot-cells. It is anticipated that the shielding that directly faces the irradiation chamber will require active cooling.

1.6.2 Structural Requirements

The design of the system components located within the target and multiplier regions will conform to applicable design codes and standards. A supplemental structural design criteria will be developed and used to establish permissible stress values that take into account any known or predictable degradation of material performance caused by the effects of irradiation, coolant selections, or operating temperatures.

It is anticipated that many components of the target and multiplier systems will last the lifetime of the plant. Some components, like the target structure and the multiplier vessels, are expected to have shorter lives and will be designed to facilitate easy replacement when necessary. Currently, it is anticipated that the target will be replaced at a frequency no greater than every three months and the multiplier vessels annually.

For a 5-MW LBE target configuration, it is anticipated that the structure's operating temperature falls between 200°C and 550°C. The operating temperature range for the multiplier vessel is on the order of 350°C to 600°C. Both the target and multiplier components will be subjected to a peak fast-spectrum flux greater than 1×10^{15} n/cm^2-s. It is also anticipated that the modular system will allow testing of different primary coolants so potential materials corrosion and/or erosion issues may arise. All of these potential environmental effects will be considered in the selection of materials for, and the design of, various system components.

1.6.3 Material Candidates

Material selection criteria for the various candidate materials encompass broad categories related to performance, safety, cost, environmental impact, and experience. Specific selection criteria include effects of irradiation on material properties and performance (strength, thermal properties, fatigue, creep, crack growth, fracture, corrosion resistance, material lifetimes, swelling, embrittlement), fabricability (machining, joining, inherent

flaws), availability, cost, and operational experience. Table 1-12 lists the current candidate materials and their relative advantages and disadvantages.

The materials ED&D Program will be able to provide much needed data on the effects of irradiation on material properties for the expected proton and neutron spectrum.

Table 1-12. Candidate Materials

Material	Component Use	Advantages	Disadvantages
Zirconium-based alloys (Zr-4)	fuel cladding	low parasitic neutron capture, LWR experience	low strength at very high temperature, exothermic oxidation with hydrogen release
Austenitic Stainless Steels (304, 316)	target structure, multiplier vessels, fuel assembly structure, coolant lines, support structures, shielding	moderate strength at elevated temperatures, reactor experience	moderate neutron capture
Ferritic Martensitic Steels (HT-9, 9Cr-1Mo)	target structure, multiplier vessels	high strength at elevated temperatures, high K, low a, resistance to swelling in irradiation environment, reactor experience	moderate neutron capture

1.7 Safety Features

The design strategy for the modular concept embraces the safety-by-design principal. During all phases of the design, safety features will be designed initially into the system rather than as an afterthought. For the modular design, the goal is to provide an overall level of safety that meets or exceeds that of advanced nuclear systems. Several features are currently used to meet that goal, and are summarized below. After an initial hazard analysis, it is expected that additional safety features will be incorporated into the conceptual design.

In general, when an upset condition develops the safety strategy is to

1. detect the event;
2. shut down the beam;
3. remove the decay heat;
4. contain any radiological releases during the event; and
5. prevent criticality for all conceivable scenarios.

1.7.1 Beam Shut-Down

For subcritical systems, the beam acts as the power switch for the multiplier. With the beam off, the multiplier power quickly reaches decay-heat levels with a time transient behavior similar to that of a critical reactor. In reactor terms, it can be thought of as an instantaneous control rod because it takes only microseconds to shut off once the trip signal is received.

There are several ways to shut down the beam, including turning off power to the accelerating cavities or the injector or losing vacuum in the beam tube. The easiest way is to turn off the beam at the injector. There are several essential components that must be energized for the injector to function. If any of them is de-energized the beam will be stopped. We will use these basic features to provide diverse and redundant beam shut-down. This system is fail-safe and will be implemented as a safety-class feature into the facility. Categorically, we anticipate three layers of beam shut-down systems to provide against transients without beam shut-down:

1. The first layer is an active system, in which the beam is shut down based on signals generated by temperature, flow-rate, and pressure measurements in various parts of the target-multiplier systems. For APT, an active shut-down system with conditional failure frequency less than 10^{-6}/yr was designed.
2. As the primary back-up, semi-passive shut-down systems are being envisioned for liquid metal systems. For example, to protect against a loss-of-flow incident in the multiplier, a simple permanent-magnet flow meter may be used in the primary sodium loop. The electric current created by the flowing sodium in the magnetic field acts as a flow switch and is connected directly to the injector. The current must be on for the injector to operate. The resulting fail-safe mechanism protects against any type of accident that causes flow to be reduced or to cease in the primary heat-removal system. Similar signals can be used in the guard vessel and target.
3. Another inherent safety feature of the modular configuration is derived from the fact that the irradiation chamber environment is connected directly to the accelerator vacuum. Active systems will shut the beam down in the event of loss of vacuum in the irradiation chamber or the beam pipe itself. In the extremely unlikely event that a breach in the primary cooling systems occurs and automatic shut-down fails to function, beam shut-down will occur naturally because it cannot be accelerated without sufficient vacuum. This provides a passive beam shut-down mechanism in the event the multiplier guard vessel, the target, or the vacuum seals leak. Obviously, the design objective is to assure that the active systems reliably work prior to the point where the transients proceed to a point at which internal vacuum can no longer be sustained.

The horizontal removal of the heavy components provides an added safety benefit as drop accidents in the irradiation chamber are eliminated. Once the components are in the hot-cell, lifting of sub-components will take place and there is a potential of drop accidents in the hot-cells. The consequences of the drops in the hot-cell are less severe, however, and the possibility of damage to other systems (other multiplier vessel or target, etc.) is eliminated.

1.7.2 Decay-Heat Removal During Postulated Accidents

To preclude the possibility of accidental, melt-driven criticality for all credible accidents, the fuel-assembly geometry is maintained by providing diverse and redundant decay-heat removal. The heat-removal system for the primary vessel is configured to provide natural circulation decay-heat removal in the event of loss of forced flow.The flow of sodium in the guard vessel is also sufficient to remove the decay heat, providing a redundant heat-removal mechanism for both loss-of-flow and loss-of-coolant events in the primary system. A more detailed assessment of the decay-heat removal strategies for a variety of design basis accident initiators continues and additional design features will be implemented as detailed assessments of the design basis accidents are developed. Table 1-13 provides a qualitative assessment of decay-heat-removal strategies for the design basis accidents.

Table 1-13. Decay-Heat-Removal Strategies for Various Design-Basis Accidents

Target	
Loss-of-flow (in primary)	Natural circulation in the primary loop.
Loss-of-offsite power	Natural circulation in the primary. However, an ultimate heat sink is needed. We are investigating the use of passive means (e.g., heat pipes) to transfer the decay heat to structures with large thermal inertia (e.g., shields). If the heat can be removed passively for > 1 h, an active system (e.g., blower) can be started reliably (diesels or batteries).
Loss-of-heat sink	Similar to loss-of-offsite power.
LOCA	For LBE, most of the decay heat is in the coolant. Coolant will spill over cold surfaces and freeze. The target will radiate its heat to the surrounding cold structures. If the target pressure boundary fails at high temperature, the coolant will spill and freeze. For tungsten option, we prevent oxidation at high temperatures by maintaining an inert atmosphere.
Heat exchanger tube break	Heat exchanger has an intermediate jacket (e.g., LBE-to-LBE-to-helium) to prevent pressurization of the LBE loop by high pressure helium gas.
Multiplier	
Loss-of-flow (in primary)	Natural circulation in the primary loop.
Loss-of-offsite power	Natural circulation in the primary. However, an ultimate heat sink is needed. We are looking at heat pipes to transfer the decay heat to structures with large thermal inertia (e.g., shields). If the heat can be removed passively for > 1 h, an active system (e.g., blower) can be stated reliably (diesels or batteries).
Flow blockage	Detection by temperature measurements at the assembly exit. Activity and fission gas monitoring in the coolant. Decay heat will be passively moved to open flow regions.
Loss-of-heat sink	Similar to loss-of-offsite power.

Table 1-13. Decay-Heat-Removal Strategies for Various Design-Basis Accidents (Continued)

LOCA in primary vessel loop	Decay heat is transferred by internal natural circulation to the guard vessel interface. Forced cooling in guard vessel is sufficient to remove the total decay heat.
LOCA in guard vessel loop	Decay heat in guard vessel wall is transferred to the primary vessel by conduction. Forced cooling in primary vessel is sufficient to remove the total decay heat.
Primary vessel breach	Detected by differential pressure change between primary and guard vessel loops. Forced flow continues to remove decay heat.
Guard vessel breach	Decay heat on guard vessel wall is radiated to primary vessel. Forced flow continues in the primary vessel.
Heat exchanger tube break	Heat exchanger has an intermediate jacket (e.g., sodium-to-sodium-to-helium) to prevent pressurization of the sodium loop by high-pressure helium gas.

1.7.3 Containment

The irradiation chamber and its shield form the containment boundary for the target-multiplier. Because a good vacuum level is required to operate the multiplier, the integrity of this system is being checked continuously during operation. The hot-cells offer excellent containment of upsets in the cooling loops. Because they operate in an inert argon atmosphere, coolant leaks can occur without the possibility of sodium fire. We are considering the use of helium in the secondary loop, as was discussed previously; thus, no liquid metal will exist outside the hot-cell.

In addition to the irradiation chamber and the hot-cells, the building provides additional containment. All releases from the building will be through a stack of HEPA filters. Additional protection will be provided by the HVAC system, condensers, and liquid waste catch tanks.

Quick-closing valves will protect releases to and through the accelerator tunnel.

1.7.4 Criticality and Overpower

To prevent over-power events, physical constraints are used in the injector to prevent the accelerator current from exceeding a preset value for the run cycle. The multiplier segments are designed so the multiplier is in its most reactive position during operation. Physical constraints on the vessels prevent the segments from moving closer together; therefore, the fuel cannot reach criticality unless reconfigured because of melting and pooling of the fuel.

During extremely unlikely events (beyond design-basis events), if fuel melting occurs, design features will be planned so strong neutron absorbers can be introduced into the irradiation chamber to prevent criticality. We plan to place catch tanks made of materials

with high melting temperatures and that contain strong neutron absorbers (e.g., boron-carbide) under each multiplier vessel as an added feature.

1.8 Operational Features

As a user facility, the intent is to provide as much simplicity as is possible in its operations without compromising the mission needs and safety. The horizontal movement of the target and multiplier modules in and out of hot-cells provides considerable operational robustness. Engineering details for the target and multiplier vessel replacement operations will be further developed during the conceptual design. At this stage, some concepts are developed for these activities.

The trolleys for the target and the vessels will be rolled in and out using wheel assemblies on rails. Dry film lubricated bearings can be used in high radiation areas near the multipliers. There are a number of motive force approaches, most of which were used on the APT project. The set of wheel assemblies near the outside of the shield plugs can be powered to provide the motive force. The motor drive can be located outside the shield plug in a low-irradiation environment with a pinion drive extending in to the wheels. As an alternative, either a worm-screw drive or a rack-and-pinion drive could be used. The motor driving the pinion could be located outside the shield plug. The rack would be located in the floor.

The target replacement activities are more straight forward than the activities associated with the multiplier vessels. Design concepts are still being evaluated with respect to the following aspects of the multiplier vessel replacement:

1. During replacement the decay heat must be removed by an active cooling system. This requires that flexible connections must be provided for the primary heat exchanger. Such connections can be on either the primary or the secondary side.
2. To extend the vessel life, we are looking into options of rotating the vessel in the hot-cell and re-using it for multiple cycles. The side of the vessel facing the spallation target is expected to see higher radiation damage than the sides away from the target; therefore, the vessel lifetime can be extended if a uniform radiation damage can be achieved by rotating the vessel periodically. A number of different concepts are being evaluated to design a rotation scheme while keeping the fuel inside the vessel cooled.
3. The driver fuel is disposable. It is desirable to expose the test fuels to high fluences, however, which may require that the fuel be moved from one vessel (that reaches the end of its life) to a new vessel in the hot-cells. Engineering details of how such fuel movement will be done, while adequately removing the decay heat, are being developed. Similar concepts also apply to driver fuel if it is used through multiple cycles. Finally, moving fuel position within a given vessel may be desirable in some of the tests; thus, we will be developing a general fuel-handling scheme during the conceptual design.
4. Temporary and permanent storage of the disposed fuel is also an issue that is being addressed. There are pros and cons of using the hot-cell for temporary storage for a large quantity of fuel. The movement of the fresh and used fuel in and out of the hot-cells requires further evaluations.

During conceptual design, the instrumentation, testing, and maintenance requirements will also be developed for various parts of the target-multiplier system.

When the facility first becomes operational, it is expected that the initial operations will be aimed mostly at target and materials testing, with little or no fuel in the multiplier vessels. Subsequently, multiplier vessels with small quantities of fuel will be introduced to initiate the target-multiplier coupling tests at low power (≤ 20 MW) and low reactivity. Finally, high-power (> 20 MW) and high-reactivity (multiplication factor > 0.9) tests will be performed as part of the proof-of-performance testing for transmutation. Additional data and operational procedures will be developed during the initial phases as we move towards the higher power tests.

1.9 Major Engineering Development and Demonstration Activities

Many aspects of the proposed design rely on previously demonstrated or fairly well advanced technologies. Additional research aimed at engineering development and demonstration (ED&D) during the preliminary and final design is needed in some areas, however. The Core Technology Plan, which will be generated in parallel with conceptual design activities, will include a detailed discussion of specific ED&D activities relevant to the conceptual design. A qualitative listing of potential ED&D tasks relevant to the modular design is provided in this section. It is important to note that ED&D needs depend on the design options pursued and the sensitivity studies conducted during conceptual design.

1.9.1 Materials Behavior, Corrosion, and Structural Design Criteria

One major ED&D issue is the structural properties of irradiated materials. Previous studies conducted under the APT ED&D Program demonstrated that irradiation in a spallation spectrum (high-energy neutrons and protons) affects the materials differently than the irradiation in a fission spectrum (lower-energy neutrons); therefore, in addition to displacement per atom (dpa), the energy spectrum is also important in defining the structural design criteria. For high-energy irradiation, almost all existing data are for low-temperature irradiation. Additional experiments must be conducted over the temperature range of interest using a high-energy beam with high enough current to provide the neutron and proton spectrum over an adequate material volume.

Another structural issue that requires further investigation is corrosion. It is known that corrosion is affected by the presence of a high-energy proton beam. Corrosion studies in the beam are therefore required for all target options considered. In-beam corrosion experiments for the considered target option will be needed.

For the LBE target, a more fundamental understanding of its corrosive properties is needed. Data on the corrosion of different material samples of interest can be obtained in an LBE loop (outside the beam) to develop and implement a corrosion control strategy (i.e., oxygen control). The effect of spallation (mainly hydrogen generation) must also be

quantified on oxygen control used to passivate the structure surfaces. While some of these tests can be conducted in experiments outside the beam using (for example) hydrogen injection into the coolant, the in-beam experiments are needed to properly simulate the hydrogen generation in the solids and its impact on the surface oxide layer.

The experiments listed above are primarily aimed at the target technology; however, the issues for the subcritical multiplier components that are exposed to high-energy spectrum also must be addressed in similar experiments.

1.9.2 Fuel Behavior

The preconceptual design is based on using a known fuel type for the subcritical multiplier (e.g., the EBR-II fuel used in the current set of analyses). The neutron spectrum in regions near the spallation target will be biased to higher-energy neutrons than the previously tested spectrum. During early phases of facility operations, a conservative approach is anticipated and considerably less burn-up than specified limits will be imposed on the fuel. Nonetheless, an early irradiation of some small fuel samples in a high-energy spectrum near a spallation source would provide data that can be used to start ADTF operations. Post-irradiation examination of the fuel samples irradiated near a spallation source and the comparison with results of reactor irradiation will provide the needed data to characterize the effect of high-energy irradiation on the fuel performance.

1.9.3 Thermal-Hydraulic Design

Depending on the design configuration for the target, local heat-transfer-coefficient measurements may be needed. This issue becomes more important if the design configuration deviates substantially from the conventional geometries (e.g., the use of micro-channels for tungsten targets).

As discussed in Section 6 for the safety features, the design relies on natural circulation for decay-heat removal. In addition to natural circulation in the primary loop for both the target and multiplier assemblies, in some of the postulated accident scenarios, internal natural circulation within the primary multiplier vessel also is needed. Using properly scaled geometry, the internal and external natural circulation experiments using electrical heating will provide the needed data. Note that the natural circulation for an LBE target requires a more difficult test design because the decay heat is mainly in the coolant.

If multiple parallel flow paths connected through a common manifold are used to tailor the flow distribution to power distribution (especially when there is a fairly non-uniform power distribution), a hydraulic model of prototypic size may be required to demonstrate that the required flow distribution is achieved.

If composite materials are used in the design (e.g., clad tungsten target), the behavior of the interface must also be quantified through a series of thermal-cycling experiments simulating the frequent beam interrupts.

1.9.4 Beam Shut-Down

It is expected that the design will rely on a number of fail safe schemes to shut the beam down in the event of an upset condition caused by power-coolant mismatch. One concept is a direct electrical current input to the injector circuit (e.g., using the magnetic field created by liquid metal coolants, or a direct conductivity through a coolant column). These concepts and their reliability must be tested and the Low-Energy Demonstration Accelerator (LEDA) injector may provide a good test bed when the shut-down scenarios are properly mocked up.

1.9.5 Beam Current Control

The beam current must be maintained within a predetermined safety envelope for each test; within the given envelope the capability of varying the beam current to compensate for reactivity losses may be desirable for some of the experiments, however. These capabilities must be built into the accelerator control system design and must be tested.

1.9.6 Nuclear Codes and Data

The design and safety will rely heavily on computational methods; therefore, based on the results of sensitivity studies, benchmark data may be needed over the appropriate range of parameters to verify the computational results:

1. power generation,
2. decay heat, and
3. spallation and activation products.

These benchmarks are mainly aimed at the spallation target performance behavior and the content of additional tests will depend on the target technology that is used; for example, considerable benchmark data already exist for tungsten to guide the preliminary design. A similar set of data, however, does not exist for LBE. The existing cross-section data for different technologies (especially for LBE) must also be reviewed and improved if necessary. The improvement may require additional evaluations and, perhaps, some additional measurements.

The work described above is mainly aimed at target technology. For the multiplier, a known fuel type with a known geometric arrangement will be used. The spectrum near the spallation source is different (biased towards higher energy neutrons) than the reactor spectrum, however; thus, some high-energy cross-section measurements and evaluations may be needed in support of the multiplier work. Likewise, for a sodium-cooled target and/or multiplier, the high-energy cross-sections of sodium require an evaluation. The need for cross-section improvements in different materials will be guided by sensitivity studies performed during conceptual and preliminary design phases.

1.9.7 Purification/Clean-up Systems

If on-line purification of the target and multiplier coolants is needed, the design of such a purification and clean-up system must be demonstrated at a proper scale using in-beam experiments. Some of these tests could also be done using surrogates. Likewise, for recycling the coolant (e.g., LBE) after target replacement, the clean-up system and its effectiveness must be demonstrated at the proper scale.

1.9.8 Spallation Products and Dose Conversion Factors

The APT assessments have shown that, the dose-conversion factors for a number of spallation products do not exist. The development of such a database can be accomplished by proper evaluations and would be very beneficial in establishing the safety bases for the facility operations.

1.10 Summary and Conclusions

The modular target-multiplier system concept is described in this report. The main advantage of the modular concept is in its flexibility that is needed to meet the various mission needs. Scoping calculations performed to date for the neutronic, thermal-hydraulic and structural performance show the feasibility of the presented concept. Additional structural assessments and design criteria are being developed to estimate the components' lifetimes. An initial safety assessment shows that a high level of safety can be provided in the current concept. A wide variety of design basis accidents can be adequately mitigated via the use of passive systems and/or well-developed and highly reliable active systems. Some of the operational details need to be worked out and those items will be addressed in the conceptual design. An initial list of ED&D activities needed to support the preliminary and final design also is included.

In conclusion, the modular design concept provides the needed flexibility to meet the different mission objectives while providing an adequate parametric range for a variety of target and multiplier tests.

It is also envisioned that the modular concepts can constitute the first station of a multi-station approach. In this approach, the first station would be a dedicated facility for target, materials and small quantities of fuel testing. As such the first station would not need a large fission power. For fuel testing, thermal power level on the order of few megawatts and a low multiplication factor (k_{eff}) would be adequate. The large-scale accelerator-target-blanket coupling tests would be performed in the second station, where fission powers up to 100 MW and multiplication factors in excess of 0.9 would be achievable.

The modular design concept described in this report would readily apply to the design of the first station, where the multiplier vessels would be down-sized to accommodate fuel assemblies. This facility will provide the capability of testing various spallation target options at high power.Vertical insertion of material test tubes into and near the target region is also possible. Such material test tubes would contain small material samples and

operate at fairly low powers (less than 1 MW) and would have their own small, dedicated heat-removal systems.

2 Sodium-Cooled Fast-Spectrum Vessel Multiplier Option

2.1 Design Description

2.1.1 Overview

The sodium-cooled fast-spectrum vessel target-multiplier system is designed for 100-MW (thermal) operation but is expected to be operated at 20 MW for a considerable time to gain confidence in the operability and controllability of the system as a whole. It uses a primary coolant loop located in a sodium pool contained in a double-walled vessel. A subcritical multiplier assembly is housed inside an inner vessel that is part of the primary coolant loop. Initially, the fuel for this assembly will be fully qualified metallic fuel of the type used in the Experimental Breeder Reactor Number Two (EBR-II), which was operated by the Argonne National Laboratory (ANL) at its Idaho site for over 25 years, but gradual changeover to prototypic Accelerator-Driven Transmutation of Waste (ATW) fuel is anticipated at some stage during the lifetime of the Accelerator-Driven Test Facility (ADTF). Two in-vessel primary Na pumps circulate the Na through the fuel assemblies and through an in-vessel heat exchanger that rejects heat to a secondary Na system. The ultimate heat sink will be a Na-to-air heat exchanger that would discharge heat to the atmosphere.

The multiplier assembly, consisting of fuel and reflector assemblies, forms a cluster surrounding or partially surrounding an accelerator tube that contains the spallation target and may also house a buffer region to mitigate the effects of very-high-energy neutrons on nearby structures. Absorber rods in the multiplier fuel region may be used for fine regulation of neutron multiplication, and hence, power level, and for burnup compensation. Fuel-handling is via a rotating plug in the vessel cover and a rotating offset gripper, with transfer of fuel assemblies to the in-vessel storage baskets for removal of decay heat before withdrawal from the pool. Provision is made for three semi-permanently installed loops for developmental testing of ATW fuels under prototypic thermal-hydraulic and neutronic conditions with any potential ATW coolant (presumably Na, He, or Pb-Bi.) Assemblies containing structural material samples or encapsulated developmental fuel may be placed anywhere in the multiplier and reflector regions for irradiation and may be handled the same as fuel assemblies. Instrumented assemblies may be included as well, if provisions are initially made for them (i.e., access holes through the rotating plug and multiplier-assembly vessel cover.)

Two concepts have been developed for the configuration of the multiplier assembly and the accelerator tube. In one the multiplier occupies an annulus around a vertical accelerator tube that penetrates the overhead rotating plug and the center of the removable cover of the inner multiplier vessel. In the other, the multiplier forms a C-shaped cluster around the end of an inclined accelerator tube that penetrates the edges of the fixed double-walled vessel cover and the removable inner vessel cover. A trade study is being conducted to determine which of these concepts should be chosen for continued design development. A third alternative, using horizontal entry through the double-walled vessel, was consid-

ered but rejected as increasing, rather then decreasing, the engineering and handling complexity inherent in the other two.

Since time constraints permitted only limited design and analysis of this system, dimensions and operating parameters typical of the EBR-II design and operating experience were used in this preconceptual activity wherever new analyses were unavailable for presentation. The distinction between 20- and 100-MW operation will be noted wherever appropriate or should be apparent from the context of the discussion.

Since a basic program strategy is to minimize cost and technical risk, there is a very strong incentive to utilize existing technology for the ADTF. The EBR-II design was used as the starting point for this preconceptual design effort.

2.1.2 Facility Layout

A simplified layout of the facility concept using vertical accelerator entry into the target-multiplier assembly is shown in Figure 2-1. The accelerator is located in a long hall, covered by an earthen berm for shielding, leading to the building housing the subcritical multiplier system. Inside this building, a set of bending magnets (two 45° bends are shown) directs the beam downward to the target-multiplier assembly, which is located at the bottom of a reinforced concrete shaft constructed in an excavated pit. The difference in elevation between the accelerator and the target-multiplier assembly is necessary to provide vertical clearance for handling the portion of accelerator tube that penetrates the target-multiplier system for replacement of the spallation target, accelerator beam tube, and/or window structures. (This handling will be discussed in Section 2.1.9.) An alternative configuration may be to bend the beam upward from the long hall through a concrete silo-like structure next to the target-multiplier building, bend it again to a horizontal path across an upper floor of the building, and then down into a target-multiplier system that is located at or near grade. The choice between these two alternatives would, of course, be made primarily on the basis of relative costs.

In the inclined-entry concept shown in Figure 2-2, the accelerator is again housed in the same type of earth-covered hall, but should not require locating the target-multiplier assembly in a shaft, nor any long up-and-down beam legs, as necessary for the vertical-entry concept, since the length of the in-pile accelerator tube is not only shorter, but inclined, and hence can be handled in a much shorter structure.

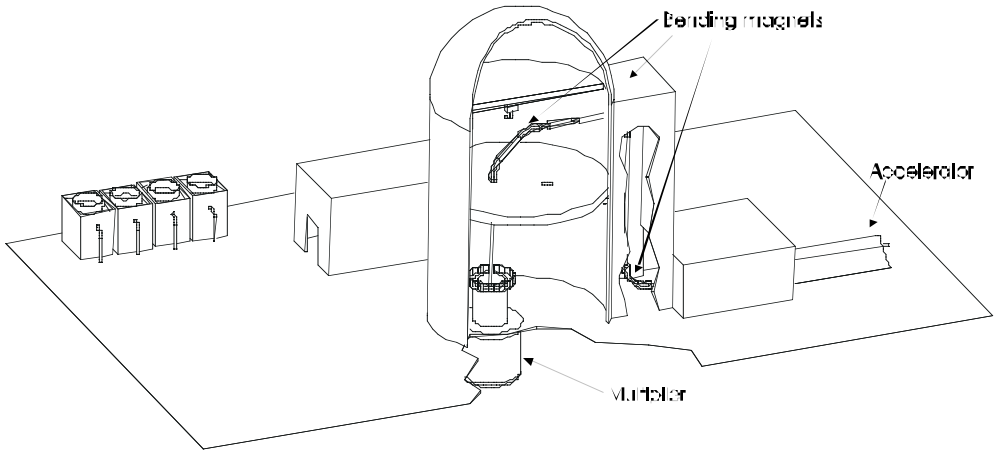

Figure 2-1. Concept for an ADTF with vertical entry of accelerator/target tube into subcritical multiplier.

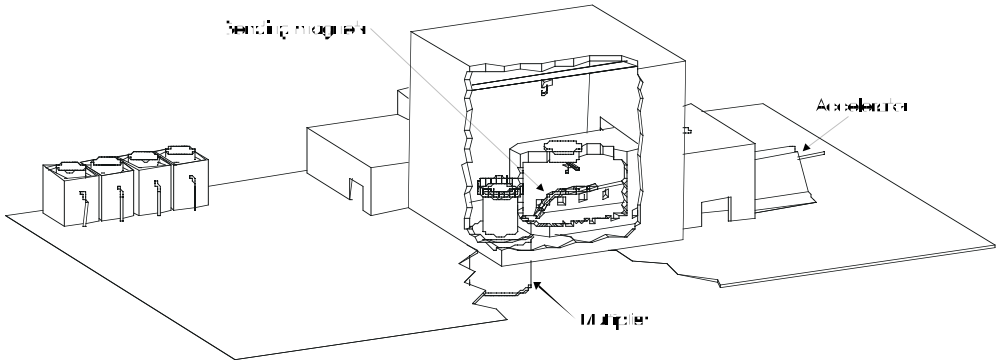

Figure 2-2. Concept for an ADTF with inclined entry of accelerator/target tube into subcritical multiplier.

2.1.3 Primary System Configuration

The Target and Multiplier System (TMS) is housed in a double-walled vessel (i.e., primary and guard vessels.) The double-walled vessel is about 30 ft deep and 26 ft in diameter for the vertical-entry concept, as shown in Figure 2-3 and Figure 2-4, and about 30 ft in diameter for the inclined entry concept, as shown in Figure 2-5. This vessel houses the fueled multiplier assembly with its spallation target inside an inner vessel that rests on a support structure that transfers the load to the primary vessel wall, along with two primary Na

pumps (one shown), a heat exchanger, and fuel storage baskets (not shown). The pumps and heat exchanger are suspended from the vessel cover with overhead access for maintenance. The double-walled vessel and its cover are top supported. The accelerator tube also occupies space in the inclined-entry concept, leading to the slightly larger diameter of the double-walled vessel.

A rotating plug in the cover allows positioning of a rotating offset gripper (not shown) over any portion of the multiplier assembly for fuel-handling. Also penetrating this rotating plug are control rod drives, struts for suspending the removable cover of the inner multiplier vessel (for fuel-handling) and experimental loops. The rotating plug and the surrounding concrete structure comprise a shielded cell that houses the upper parts of the experimental loops, which will become radioactive during operation. The various tubes and shafts that extend down to the multiplier assembly pass through this cell. The interior of this cell is ~17-ft high to provide vertical clearance for various experimental loop-handling operations. In the vertical entry concept, the accelerator tube also passes through this rotating plug.

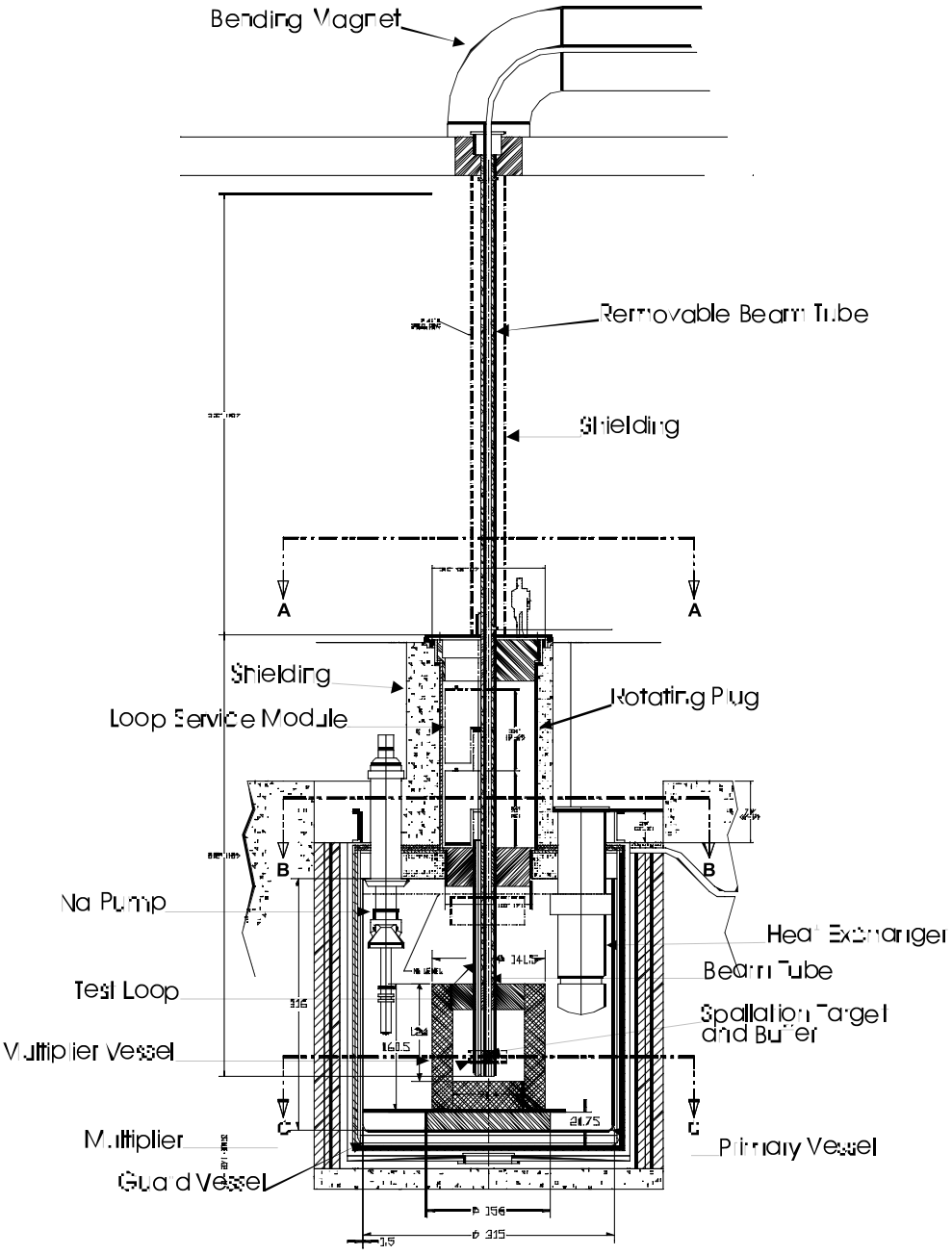

Figure 2-3. Vertical section of ADTF Na-cooled target-multiplier with vertical accelerator entry.

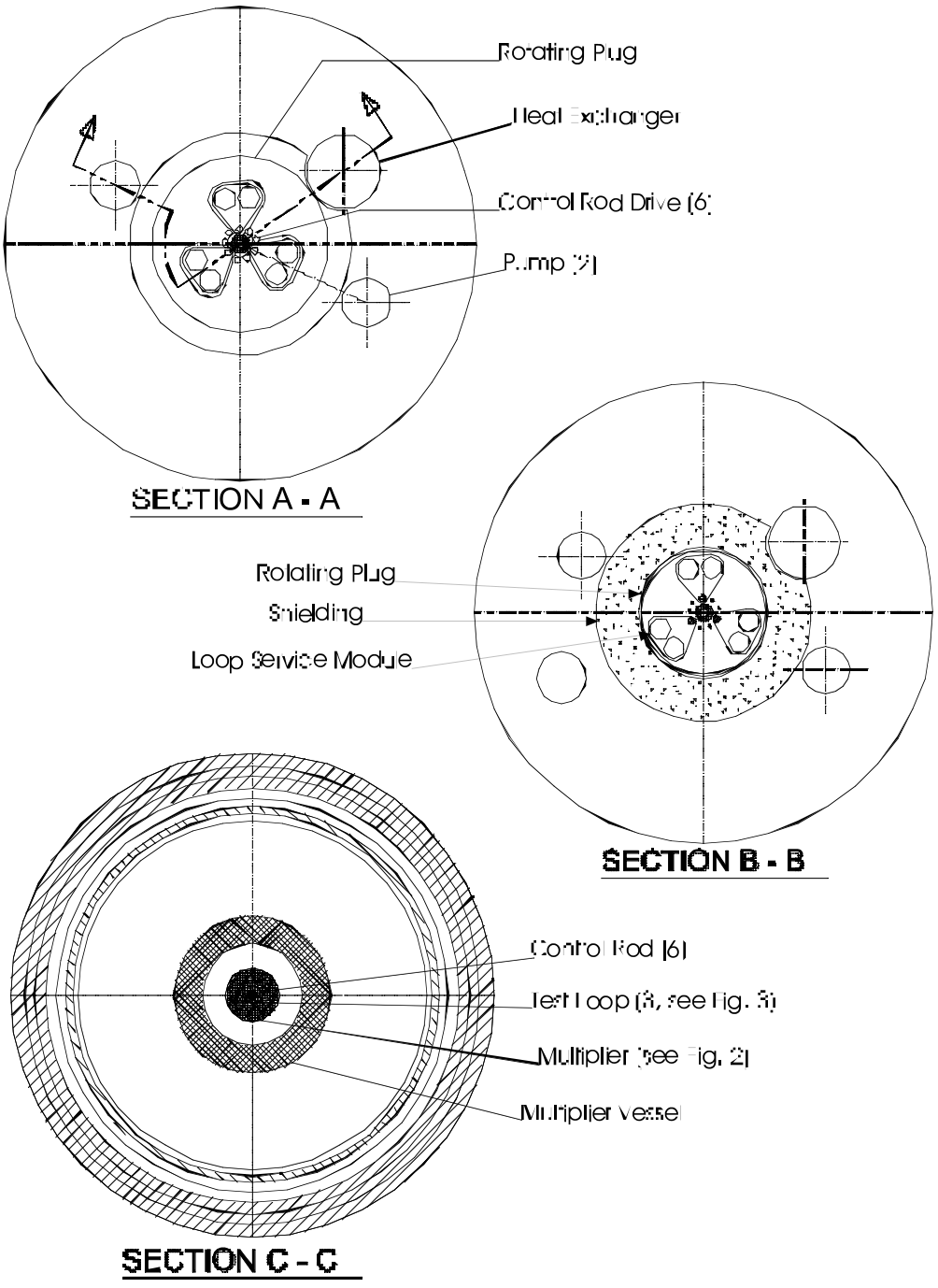

Figure 2-4. Horizontal sections of Figure 2-3.

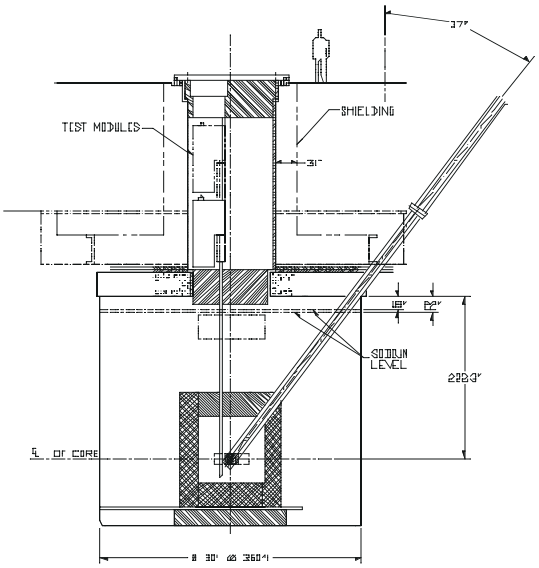

Figure 2-5. Vertical section of ADTF Na-cooled target-multiplier system with inclined accelerator entry.

The sodium pool consists of ~60,000 gallons of sodium. Two primary pumps draw cool sodium from this large pool at a rate of ~14,650 gpm and discharge it through pipes into a plenum at the bottom of the inner vessel that houses the multiplier assembly. Hot sodium is discharged from the multiplier vessel via a plenum at the top and through a pipe to the heat exchanger. The heat exchanger discharges directly back into the pool. At this time operating temperatures have not been firmly established, but multiplier inlet and outlet temperatures of approximately 700°F and 880°F, respectively, are expected. The fuel region in either multiplier assembly incorporates 75–85 fuel assemblies for operation at 20 MW and 110–130 for operation at 100 MW. Since each assembly would generate 0.8 to 0.9 MW at design power with the standard enrichment of 67%, the multiplier must be operated at a derated power or the enrichment must be lowered for 20-MW operation.

2.1.4 Multiplier Assembly

The fuel region in the multiplier assembly for the vertical entry concept takes on a somewhat triangular shape (see Figure 2-6) and is surrounded by reflector assemblies to fit within a 48-inch-diameter envelope inside the multiplier vessel inside the primary vessel. The annular region between this envelope and the vessel is filled with fast neutron shielding and moderator. The multiplier design configuration for operation at 20 MW incorporates 81 fuel assemblies similar to EBR-II Mk-IIIA assemblies. The hexagonal assemblies measure 2.29 in. across flats and contain 61 U-10%Zr fuel rods 0.230 in. in diameter mounted on a 0.272-in. triangular pitch with a 13.5-inch-long fuel column. This

number of assemblies is necessary to allow a double layer around the ~17-inch-diameter accelerator target/buffer tube and a single layer around each experimental loop. As is shown in Figure 2-6, for operation at the rated power of 100 MW, the multiplier would contain an additional 45 assemblies, for a total of 126, and could be operated at closer to nominal design conditions. The 45 additional assemblies would replace 45 reflector assemblies used in the 20-MW configuration.

Preliminary calculations of neutron fluxes for this configuration yielded ~8×10^{14}n/s·cm^2 (>0.1 MeV) and ~2×10^{13}n/s·cm^2 (thermal) at 20 MW. These calculations were done for a critical system, however, and fluxes could be increased by lowering k_{eff} (by lowering enrichment) of the multiplier and increasing proton beam intensity to maintain the 20-MW multiplier power. This is discussed in more detail in Section 2.2.

Three experimental loops are placed in cavities toward the apexes of the triangular fuel region. They may be as large as 6.50-inch-diameter if the adjacent fuel assemblies are reduced in size by flattening two adjacent flats of the hexagonal shape; otherwise 4.875 in. is the maximum diameter. Six control rods are located along the flats of, and partially embedded in, the triangular fuel region.

For the concept using an inclined accelerator tube, the multiplier is more C-shaped, as shown in Figure 2-7. It contains 72 of the same assemblies as above for 20-MW operation and 110 for 100 MW. Control rods are not shown in this figure, but can be accommodated more readily than in the vertical-entry concept because of the additional room in the fuel region and the freer overhead access afforded by the removal of the accelerator tube to the side. Preliminary physics calculations for this type of configuration are also discussed in Section 2.2.

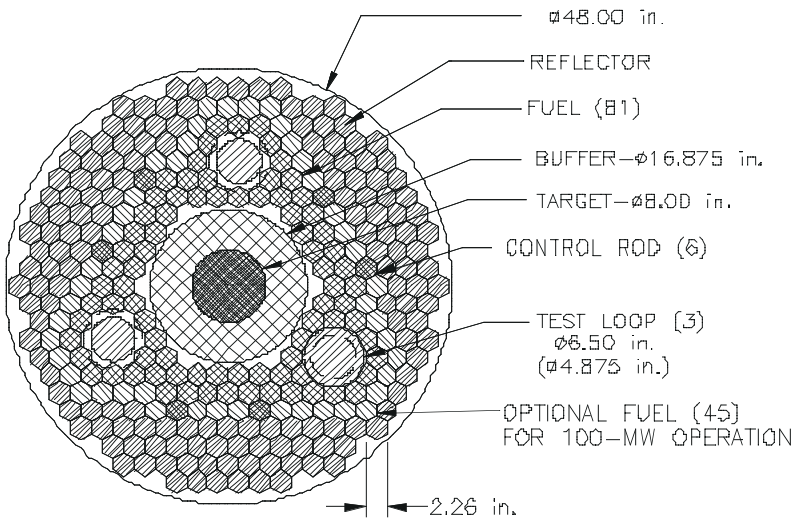

Figure 2-6. Multiplier for vertical-entry ADTF concept.

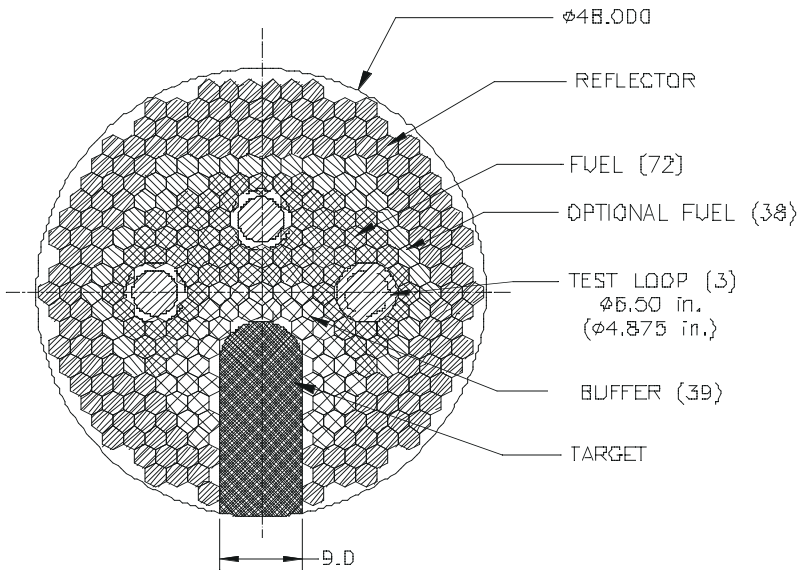

Figure 2-7. Multiplier for inclined-entry ADTF concept.

Again three loops are shown, although the three-fold symmetry of the triangle-shaped multiplier fuel region of the vertical-entry concept has degenerated into the two-fold symmetry of the slotted fuel region. If a reduction to two loops is acceptable, it may be desirable to

remove the center loop, which is in line with the target tube, and move the side loops inward toward that space.

2.1.5 Accelerator Interface and Target

The vertical-entry accelerator tube penetrates the system through a hole in the double-walled vessel cover's rotating plug and a corresponding hole in the cover of the multiplier vessel. For this study, it was assumed that the target is 8 in. in diameter and is surrounded by a 4-in.-thick buffer to reduce the flux of very high-energy neutrons impinging on the innermost fuel assemblies. One possible target is composed of lead-bismuth, which has a eutectic point of 258EF and will be molten at the Na pool temperature. It could be circulated through an external loop for cooling, although preliminary calculations have shown that it may be possible, using proper design, to cool with the flowing Na coolant. On the other hand, a tungsten target would be solid at operating temperature and would be easier to contain and to cool with flowing Na than the molten Pb-Bi. Further study may reveal that these dimensions may not be optimal, but these design refinements should be easily incorporated. The only significant constraint may be the dimensional quantization implied by the dimensions of the standard fuel assemblies, although it may be feasible to change the number of fuel rods in an assembly; changing the rod dimensions would probably require a much more extensive fuel qualification program.

Vertical entry requires a removable section of accelerator tube that extends ~46 ft above the rotating plug in the vessel cover. It connects to a tube that penetrates an upper floor upon which is mounted the fixed magnets that bend the proton beam from a horizontal path to the vertical section extending down into the multiplier system. A single 90E bend is shown in Figure 2-3; it is likely that two 45E bends will be used (as in Figure 2-1). The vertical section of tube will need massive shielding assemblies surrounding it to allow access to the area during operation. Less will be needed during shut-down, e.g., for fuel and experiment handling, or if the area is designated for no personnel occupancy during operation. The removable section may be shortened somewhat by segmenting the in-core section of the accelerator tube and/or by pivoting the bending magnets, but either would complicate design and handling of the shielding and the tubes themselves.

The inclined-entry accelerator tube penetrates the system through a hole near the edge of the double-walled vessel cover and a corresponding hole in the cover of the multiplier vessel near its edge. This concept not only frees up access area directly over the multiplier, but also removes the requirement for the rotating seal that the penetration of the vertical tube through the rotating plug brought about. In this case, the in-core section of the accelerator tube need only be ~33-ft long, and handling is accommodated in a hot-cell-like structure, greatly mitigating the handling problems of the vertical-entry concept, especially with a pivoting bending magnet structure. This alleviates the requirement for a removable tube section and allows entry of the main accelerator tube at about grade level (see Figure 2-2.)

The interface between the accelerator/target with the multiplier will be more complex here because of the angled entry into the inner multiplier vessel and the multiplier itself. Filler pieces will be needed in the multiplier both above and below the canted accelerator tube

and Na flow paths will have to be provided for cooling of these filler pieces and of the tube. Provision for a W target may be accommodated quite simply by making it into sodium-coolable assemblies handled identically to multiplier fuel/reflector assemblies. It should be possible to design a Pb-Bi target similar to that used in the vertical-entry concept. For both types of target, it is anticipated that the buffer will consist of fuel-like assemblies.

2.1.6 Experimental Loops

The experimental loops are packages containing the equipment necessary to circulate coolant through an assembly of test fuel, remove the heat generated in the fuel, and monitor the thermal-hydraulic and neutronic conditions of both the coolant and the fuel. This would include a pump (for liquid coolants) or fan (for gaseous coolants) and a heat exchanger, along with associated instrumentation. While the in-core section of the loop and the coolant would be subject to neutron activation, the services to the package loop, including the coolant to the secondary side of the heat exchanger, would not be. At this preconceptual stage of design, the loops are the same for either accelerator entry concept; divergence in the two designs may be expected to take advantage of the additional space directly over the multiplier afforded by the inclined-entry concept.

The loops will be semi-permanently mounted on a movable platform inside the cell in the rotating plug in the cover of the vessel of the target-multiplier system and extend down through the multiplier vessel cover into the fuel region. Normally, only a test train that contains the fuel assembly under test would be removed from the loop; the loop itself would only be removed if it becomes inoperable for some reason (e.g., a failed pump) or if radiation damage limits to the tube are reached. The loops are also raised and withdrawn from the multiplier assembly during fuel-handling (see Section 2.4.1).

Although no detailed design of a loop for the ADTF has been done, past experience indicates that the service module at the top might need to be ~8-feet high to house the necessary components. The total length of the loop would need to be ~30 ft. for the in-core tube to penetrate through the fueled region of the multiplier. A cross section of a concept for the fuel bundle of such a loop is shown in Figure 2-8. Here it is assumed that the fuel under test has the same dimensions as the multiplier fuel and is cooled by Na (note that this is not as redundant as it might at first seem, since this allows testing of fuel under thermal-hydraulic conditions independent of the multiplier itself). Such a configuration will allow testing of a 217-element fuel bundle containing approximately 16 kg of heavy metal. Fuel assemblies for other coolants, would, of course, be of different sizes, but should contain comparable masses of fuel.

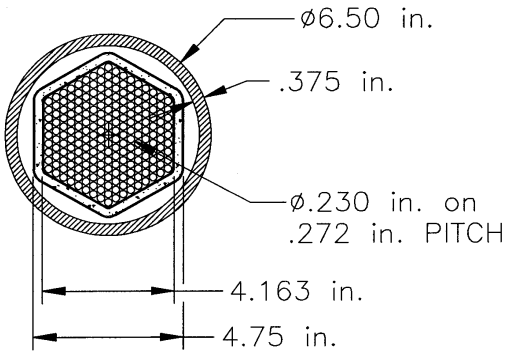

Figure 2-8. Horizontal section of fuel bundle in test-loop concept.

2.1.7 Satisfaction of General Requirements

A comparison of the capabilities and characteristics of the current Na-cooled ADTF concepts (there should be no significant differences between the vertical- and the inclined-entry) with the general requirements for the ADTF is presented in Table 2-1. This table is fairly self-explanatory, but the neutron fluxes and the fuel irradiation quantities bear further comment. As alluded to above, the requirements for high flux and high k_{eff} are mutually exclusive at a power of 20 MW. At 100 MW, the flux and k_{eff} goals should be met or nearly met concurrently. With respect to test fuel quantities, the 16 kg represents only that amount of fuel in an individual loop. Combining the fuel capability of a loop or loops with multiplier fuel (perhaps in irradiation capsules) raises the irradiation capability many-fold.

2.1.8 Technology Status

Technology risks for the Na-cooled ADTF option should be low in most areas. Sodium technology is very mature and has been used successfully in many reactors worldwide. Operational problems have indeed occurred in some of the Na-cooled reactors, but no catastrophic or severe failures have occurred. Maintenance technology for sodium systems is also well developed, and recoveries from system failures have been demonstrated. Fuel and assembly design and performance has been well characterized and fully qualified in EBR-II, which served as a test-bed for Na-cooled, metal-fuel reactor technology and generated electricity for sale on the local grid for over 25 years. Fuel-handling techniques also have been well characterized and fully qualified in EBR-II and other reactors, and the present handling strategy represents only a small deviation from those methods. Moreover, designs of major pieces of equipment can be duplicated or adapted from proven LMR designs for use in ADTF, and considerable equipment is on hand from EBR-II that can be used in ADTF (e.g., a spare heat exchanger is in storage at ANL-W).

Table 2-1. Sodium-Cooled ADTF Performance Vs. Requirements

Target-Multiplier Requirement	Goal	Concept Capability
Produce neutrons with prototypical spectrum using high-energy proton beam and subcritical multiplier	20 MW thermal power initially, eventually 100 MW; k_{eff} 0.8 to 0.97	20 MW with derated lineal power density, 100 MW at rated power with additional assemblies; k_{eff} 0.8 to 0.97
Provide peak neutron flux with representative ATW spectrum and level	>0.1 MeV: ~3-5 $\times 10^{15}$ n/s·cm^2 Thermal (<0.1 eV): ~1-2 $\times 10^{13}$ n/s·cm^2	At 20 MW: >0.1 MeV: ~0.8 $\times 10^{15}$ n/s·cm^2 Thermal: ~0.2 $\times 10^{14}$ n/s·cm^2 At 100 MW: >0.1 MeV: ~2.5 $\times 10^{15}$ n/s·cm^2
Irradiate fresh/irradiated/recycled ATW fuel samples in representative conditions	Up to 40 kg, at up to 3 $\times 10^{15}$ n/s·cm^2, prototypical thermal and hydraulic conditions	~ 16 kg multiplier-type fuel in Na coolant per loop non-fuel-failure; less in fuel-failure tests
Provide coolant loops for testing ATW representative assemblies in all coolant environments	At least 2 closed loops to test representative fuel assemblies and coolants	3 loops: Na, He, Pb-Bi, each with independent thermal and hydraulic control
Provide ATW prototype materials irradiation environment	Window: 30-100 :A/cm^2 protons, Multiplier: Near target ~44 dpa/yr, 80 appm/yr H, 10 appm/yr He; Far from target: ~40 dpa/yr	Materials may be irradiated in any inner row fuel assembly position(s) close to buffer, any other position(s) far from target
Capability to test prototype spallation targets	Prototypical ATW liquid Pb-Bi and He-cooled W Targets	Targets are independent of multiplier system
Demonstrate integrated ATW system behavior	Control reactivity, power and power distribution under all operating conditions	Multiplier system includes 6 control rods and grid spaces for optional fuel assemblies
Allow for controlled transient testing	Conditions to allow validation of safety codes and analyses	Thermal hydraulics and control system will allow transient tests
Maximum reliance on passive safety strategies	Depend on passive safety systems	Na-cooled metal-fueled critical systems shown to be passively safe under many conditions. Passive safety of coupled target/subcritical multiplier needs further work.

There are some engineering design challenges, however. The compactness of the Na-cooled fast multiplier makes placement of requisite test, operations, and fuel-handling components on the cover difficult, especially for the vertical-entry concept. While the Pb-Bi and W targets will be extensively tested in the near term, engineering of the accelerator beam tube for insertion, sealing, and removal through the rotating cover will be challenging. As was mentioned above, shielding of components above the cover to allow for

routine operations and recovery from off-normal operations will require complex design and extensive detailed planning of operations. Some of these difficulties will be alleviated if the inclined-entry option is chosen, but the multiplier design (e.g., cooling and handling) will be complicated somewhat.

2.1.9 Remote-Handling and Operations

Handling of fuel, experimental loops, and the accelerator/target interface tube are the main handling activities that affect system design. We will discuss each of these in the order stated, since the requirements imposed by each build up in that order. In doing this, the reasons for various dimensions given above should become clear.

2.1.9.1 Fuel-Handling

To remove fuel assemblies from the multiplier, the cover of the multiplier vessel must be raised by the length of an assembly plus some allowance for the gripper equipment and clearances for movement of the fuel. This turns out to be ~8 ft for assemblies of EBR-II length. Movement of the rotating plug then allows the gripper to be positioned at any azimuthal position around the multiplier, while rotation of the gripper around its shaft axis allows positioning at any radial position, thus allowing any assembly to be picked up. The gripper assembly will need to be designed with a hold-down mechanism to maintain the surrounding assemblies in place when the gripper lifts an assembly. Once the assembly is removed from the multiplier, the gripper passes it on to a transfer arm, which places it into a storage basket. A separate mechanism extending through a penetration outside the rotating plug is used to remove the elements from the basket to a fuel coffin resting on the operating floor.

Control rod drives are disconnected from their respective rods, allowing rotation of the plug with the rods fully inserted into the multiplier. Since loops must also be withdrawn from the multiplier to allow movement of the rotating plug, the inside cell height must accommodate this, making it ~17 ft high. This cell height, plus the thicknesses of its floor and ceiling, must be added to the length of the in-core portion of the accelerator tube to give its total length, which is ~46 ft.

2.1.9.2 Experimental Loop Handling

As was discussed above, loops are semi-permanently mounted inside the cell comprising the rotating plug. They are installed and removed through penetrations in the roof of this cell, the other side of which constitutes the operating floor above the target-multiplier system (See Figure 2-3; although this figure depicts the vertical entry concept, the situation for the inclined-entry is substantially the same.) After irradiation, they would be withdrawn into a shielded coffin that would adapt to the penetration. Although not requiring the shielding, the same coffin would probably be used for installing new loops. A test train containing irradiated fuel would be withdrawn into the same coffin after removing the penetration plug and unbolting a closure flange on the top of the loop using remote-handling techniques.

2.1.9.3 Accelerator/Target Handling

Replacement of the vertical in-core accelerator/target tube involves lateral displacement of the removable tube section mentioned above and vertical withdrawal of the lower section into a bottom-loading coffin mounted to the top of the rotating plug. Since its length is ~46 ft, it must be raised that distance; hence the removable section of accelerator tube and the coffin must be that long, and the underside of the upper floor upon which are mounted the bending magnets must be that height above the operating floor. Details for handling with segmented tubes and pivoting bending magnets have not been developed as yet.

The copious amounts of shielding around the removable section, necessary for protection of personnel against the backshine from the neutron spallation source at the center of the multiplier (the pipe forms a very effective streaming path) during operation, will make this a rather difficult design and handling problem. If steel is used, as seems probable because of activation problems with lead, the outer envelope of this shielding will encompass not only the loop access ports, but possibly the control rod drives and fuel-handling equipment as well (see the horizontal sections of Figure 2-3.) Cavities for this equipment can certainly be built into the shielding, but servicing of, e.g., control rod drives during shut-down will require its removal and replacement by a thinner shield, perhaps of lead, to protect workers from the accelerator tube itself, since it will have become activated during operation. If the area is an exclusion area during operation, the shielding requirements will be significantly less, but a change from steel during operation to lead during shut-down will probably still be necessary.

In this vertical-entry concept, it is assumed that the target and buffer will be attached to the accelerator tube, although that may not necessarily be the case for a W target. It may also be possible to locate the window, through which the protons must pass in going from the evacuated accelerator tube to the capsule containing the target, in a spool-piece above the double-walled vessel cover and replace it as a cartridge, as necessary, independently of accelerator/target replacement and/or multiplier fuel-handling.

In the inclined-entry concept, the bending magnet is pivoted to the side, so that no removable tube segment is needed, and the in-core tube is withdrawn along its axis into the hot-cell surrounding it by some convenient means (e.g., a cable or chain winch or a rack-and-pinion gearing arrangement along the tube) onto rollers mounted on rails. It would then be uprighted and withdrawn into a bottom-loading coffin mounted to a port in the roof of the cell. This type of operation has been well developed for the Lujan Center spallation neutron source at LANSCE. It might be suggested that the vertical-entry concept be handled in a like manner. It would be difficult, however, to implement the hot-cell capability atop the rotating plug with the multitude of other equipment handling (e.g., control rod drives, experimental loops, etc.) that must be done there.

Target and window handling will be similar to the vertical-entry case, except that the W target, in the shape of multiplier fuel/reflector assemblies, will be much easier. Handling of the filler pieces above and below the inclined accelerator tube may be handled by attaching adapters and then handling them as fuel/reflector assemblies.

2.2 Physics

The neutron-physics analyses that have been performed for the preconceptual design of the sodium-cooled ADTF are discussed in this section. Analyses have been performed to investigate the influence of core configuration (i.e., the physical layout of the target and multiplier regions) on the ability of the sodium-cooled ADTF to achieve the specified requirements and/or goals for the ADTF program. The parameters of primary consideration in these neutron-physics analyses were the core multiplication factor, thermal power, and the neutron-flux level in the experimental test loops.

The sodium-cooled ADTF can meet the requirements of a subcritical facility with a multiplication factor in the range 0.8 to 0.97, operating at a multiplier power of 20 MW. The multiplier power level can also be upgraded to 100 MW by increasing the number of fuel assemblies. Operating at 20 MW, the fast (>0.1 MeV) neutron-flux in the three test loops is ~1×10^{15} n/cm^2/s, not quite meeting the project goal of 3×10^{15} n/cm^2/s. Operating at the design level of 100 MW will increase the fast flux to ~2.5×10^{15} n/cm^2/s. Further refinements in the core design may provide an even greater flux level for testing of ATW fuel and cladding.

2.2.1 Core Model

The accelerator beam delivers high-energy protons to the spallation target. The neutron source produced by the spallation reactions drives the subcritical multiplying region. The configuration of the assemblies in the multiplier region is strongly influenced by the direction from which the proton beam-tube enters the core and the location of the target. In the preconceptual design phase of the sodium-cooled ADTF, two distinctly different configurations, the so-called vertical- and inclined-entry layouts are considered. To date, most of the physics analyses have been performed for the vertical-entry layout.

In the vertical-entry layout, the beam-tube penetrates the multiplier vessel cover above the center of the core and the target/buffer is located in the center of the multiplying region. A representative radial cross section of the core in this layout is provided in Figure 2-9. For low-power operations, the number of multiplier assemblies must be minimized to achieve the neutron-flux levels desired in the ADTF. The annular configuration of the multiplier assemblies has a relatively high neutron leakage, however; with a smaller multiplier region, the project requirement for the multiplication factor (>0.8) becomes an important consideration. Several variations of this configuration, with different target/buffer sizes and number of multiplier assemblies have been analyzed.

In the inclined-entry layout, the beam-tube also penetrates the multiplier vessel cover, but from an off-center position. Because the beam-tube enters from the side (and above) the target/buffer cannot be completely surrounded by multiplier assemblies, as depicted in Figure 2-10. Although this layout has the advantage of lower neutron-leakage from the multiplier region because of the more compact configuration (thus allowing fewer assemblies), there is the apparent disadvantage of greater leakage of neutrons from the spallation-source from the side facing away from the multiplying region. The test loops are also not all in the same neutron-flux environment.

The following core components are represented in the neutron-physics model: a spallation-target, a neutron-buffer region, a multiplier region, test loops, and a reflector region. A discussion of each of these components and how they were modeled in the neutron-physics analyses is provided below. Although it is anticipated that the final sodium-cooled ADTF design will include a system of movable rods for reactor control, these were not modeled in the present work.

To date, analyses have been performed assuming a lead-bismuth (Pb-Bi) spallation-target. The use of tungsten as a target material may be preferable from a fabrication standpoint; as will be discussed below, this modification would not disqualify the present work. The target was modeled as Pb-Bi at full density (10.4 g/cm^3). In those calculations in which the target-beam interface was explicitly modeled, a voided region (reduced Pb-Bi density) was used to represent the proton beam.

A buffer region is placed between the target and multiplier to soften the energy spectrum of the neutron-source reaching the multiplier region and reduce material damage from high-energy neutrons. Pb-Bi was also assumed for the buffer because it is a good reflector with a low absorption cross section.

The EBR-II Mk-IIIA driver assembly has been chosen as the multiplier assembly in the sodium-cooled ADTF. This choice makes use of existing technology and takes advantage of the many years of operating experience accumulated for the Mk-IIIA. The Mk-IIIA is a hexagonal bundle of 61 U-10Zr fuel elements clad in stainless steel; each assembly contains ~4.5 kg HM. The fuel enrichment of the Mk-IIIA in EBR-II was 66.9 without ^{235}U; for the sodium-cooled ADTF the use of multiplier assemblies at this enrichment, and several others, has been investigated. The Mk-IIIA has a stainless steel hexagonal wrapper with an outer flat-to-flat dimension of 2.29 inches; the assembly pitch in EBR-II was 2.32 inches and was also applied here. This assembly pitch has been applied for all other core components as well, although they may not be in a strictly hexagonal geometry in the ADTF (e.g., the target, buffer, and test loops will likely be circular).

The modeled multiplier assembly length was 55 inches, which extends from the lower to the upper axial reflector of the Mk-IIIA assembly. The as-built (cold, unirradiated) active fueled-length of each element is 13.5 inches. Experience in EBR-II revealed that the U-10Zr fuel expands axially because of temperature and fission-induced swelling; radial expansion is inhibited by the fuel clad. The magnitude of this axial growth increases with burn-up; consistent with EBR-II analysis, an average axial growth of 6.9% was assumed in the present work, giving an active fueled-length of 14.43 inches (36.66 cm). Figure 2-11 presents an axial cross section of the core model for the vertical-entry layout; the positioning of components in the radial direction is for illustrative purposes only and does not represent their precise position in the full (three-dimensional) core model.

The test loops in the ADTF will be used to conduct irradiation experiments in a prototypical ATW environment. It is proposed that the test loops should accommodate potential coolants for the ATW such as Na, He, or Pb-Bi. In the present work, the test loops were filled with Pb-Bi. For all configurations studied, three test loops were modeled.

The multiplying region will be surrounded by reflector assemblies to improve neutron economy and to reduce radiation damage of the multiplier vessel. These assemblies were

modeled as a mixture of stainless steel (85%) and sodium (15%), similar to the reflector design in EBR-II.

2.2.2 Calculations and Results

The DIF3D computer code was used to compute the neutron-flux and multiplication factor for the many configurations of the sodium-cooled ADTF investigated here. The code's nodal diffusion technique was used in the present work; a finite-difference option is also available. The neutron balance equations can be solved for homogeneous (i.e., critical) and external source-driven problems. Calculations were performed using a three-dimensional (hexagonal-Z), full-core model. The REBUS-3 fuel-cycle analysis code, coupled with DIF3D, was used to perform depletion analyses of the ADTF.

Nuclear data in nine broad energy groups are employed; these data were previously derived for analysis of EBR-II. When deriving broad-group data, a maximum neutron energy must be assumed based on the energy spectrum in the system and available data; neutron-induced reactions at energies higher than this cutoff energy are not modeled, but are considered rare. While the cutoff energy of the broad-group data used here (14 MeV) is sufficiently high for a system driven by a fission-neutron source, special consideration must be made for the harder energy spectrum of the source in an accelerator-driven system. This is discussed later in this section.

Table 2-2. Performance Parameters at Beginning-of-Life for 20-MW sodium-cooled ADTF (vertical-entry layout)

Case	# Rings in Target/buffer	Fuel form*	# Multiplier assemblies	Enrichment (w/o U^{235})	k-eff	Multiplier flux ($x10^{15}$ $n/cm^2/s$) Average	Peak
case01	6 (21.4 in OD)	U-10Zr	93	66.9	0.81	0.59	0.77
case02	6 (21.4 in OD)	U-10Zr	93	95.0	0.97	0.44	0.57
case03	4 (13.4 in OD)	U-10Zr	69	90.0	0.97	0.62	0.81
case04	3 (9.3 in OD)	U-10Zr	87	66.9	0.97	0.64	0.88
case05	2 (5.4 in OD)	U-10Zr	45	66.9	0.79	1.19	1.70
case06	4 (13.4 in OD)	U-28Pu-10Zr	69	53.0	0.96	0.74	0.97
case07	4 (13.4 in OD)	U-28Pu-10Zr	69	66.9	0.97	0.71	0.93

*In U-28Pu-10Zr, the Pu isotopics is weapons-grade (Pu-239=0.937, Pu-240=0.057, Pu-241=0.003, Am-241=0.003).

An initial series of homogeneous, diffusion theory calculations for the 20 MW, vertical-entry ADTF at beginning-of-life (i.e., all fresh fuel) was performed to assess the tradeoffs between fuel enrichment, target/buffer size, and fuel form on the multiplication factor and neutron-flux magnitude. The homogeneous calculations provided simplified and consistent comparisons of performance parameters for a variety of core configurations; in the multiplier region and test loops, the neutron-flux computed by homogeneous and source-driven calculations are nearly the same when the target is located in the center of the multiplying region. The results of these cases are presented in Table 2-2. In the table, the

 # Rings in Target/Buffer is the number of full hexagonal rings used to represent the target/buffer region; the number in parentheses is the largest target/buffer that could be accommodated in that space. The layout shown in Figure 2-9 was adjusted by increasing/decreasing the size of the target/buffer and appropriate repositioning of the fuel assemblies and test loops. In these cases, the target-beam interface was not modeled; the void region indicated in Figure 2-11 was filled with Pb-Bi at full density.

For a given core configuration and fuel form, increasing the enrichment causes an increase in k_{eff} but a decrease in the multiplier neutron-flux required to generate the specified power level (compare case01 and case02). We also observe that decreasing the size of the target/buffer while maintaining the same number of multiplier assemblies (compare case01 and case04) increases k_{eff} while having little effect on the neutron-flux level; the eigen value increased significantly in case04 (relative to case01) because of the lower neutron-leakage in the more compact configuration while the flux level increased only slightly because of the small decrease in the number of multiplier assemblies. This suggests that by reducing the size of the target/buffer region and loading either fewer or lower-enriched multiplier assemblies, even higher flux levels may be attained while still meeting the project requirement for minimum multiplication factor (>0.8). This conclusion is supported by case05. Other considerations, such as the need for adequate space to accommodate necessary reactor components and the larger target/buffer needed for higher power operations, will likely preclude this approach as a means for increasing the neutron-flux level, however.

Another means for increasing the neutron-flux level is to use a more reactive fuel form, such as weapons-grade Pu in the ternary fuel U-28Pu-10Zr. Case03 and case07 have nearly the same k_{eff}, but the flux is higher in case07. Although not indicated in Table 2-2, the fuel volume fraction was reduced slightly in case07 (to 0.285 from 0.301 for all other cases); using a more reactive fuel reduces the fissile content needed to achieve a specified k_{eff}, thus increasing the flux.

Table 2-3 presents the results of calculations performed to assess the effect of fissile-material depletion in the multiplier region for the 20 MW ADTF. A three-batch, equilibrium fuel cycle was assumed with a core residence-time for each batch of 820 full-power days (i.e., 3 years at 75% capacity factor). Just as for the results presented in Table 2-2, a homogeneous diffusion theory calculation was used for the flux solution. The three cases presented all used U-10Zr fuel at 66.9 w/o U-235; cases at other enrichments revealed trends similar to those observed in Table 2-2. Neutron-flux levels in the multiplier region and the test loops (all of which are in the same flux environment) are reported at the end of the equilibrium cycle (EOEC); this represents the core state at which the neutron-flux is highest for a fixed reactor power level.

Table 2-3. Performance Parameters for 20-MW Sodium-Cooled ADTF with Depletion (vertical-entry layout)

					Flux at EOEC (x10 ^{15} n/cm ^{2}/s)			
	# Rings in	# Multiplier	k-eff		Multiplier	Test loops		
Case	Target/Buffer	assemblies	BOEC	EOEC	Average	Average	Peak	Peak-fast
cased1	6 (21.4 in OD)	93	0.79	0.78	0.62	0.55	0.76	0.64
cased2	5 (17.4 in OD)	81	0.81	0.80	0.71	0.64	0.87	0.74
cased3	4 (13.4 in OD)	69	0.81	0.80	0.83	0.77	1.03	0.87

As expected, k_{eff} is lower at BOEC than at BOL (compare cased1 with case01 in Table 2-2), and lower still at EOEC. The flux in the multiplier region increases with fuel burn-up; the lower fissile content at EOEC compared with BOL requires a higher neutron-flux to achieve the same reactor power. The same trends that were evident at BOL were observed, namely, reducing the size of the target/buffer increases k_{eff}, while reducing the number of multiplier assemblies increases the flux.

For the vertical-entry layout, decreasing the size of the target/buffer and multiplier regions may not be a practical approach to increasing the neutron-flux because of physical space limitations. One way already introduced to free up space is to use an inclined-entry for the accelerator beam-tube. The results of an equilibrium-cycle depletion of the inclined-entry layout with 77 assemblies in the multiplying region (as depicted in Figure 2-10) are presented in Table 2-4. The operating conditions are the same as for the vertical-layout cores: 20 MW, three-batch core, and 820 FPD residence time. The fuel form is U-10Zr.

Table 2-4. Performance Parameters for 20-MW Sodium-Cooled ADTF with Depletion (inclined-entry layout)

				Flux at EOEC (x10 ^{15} n/cm ^{2}/s)						
	Enrichment	k-eff		Multiplier	Test loop(s) A			Test loop B		
Case	(w/o U ^{235})	BOEC	EOEC	Average	Average	Peak	Peak-fast	Average	Peak	Peak-fast
cased4	53.0	0.79	0.77	0.95	0.77	1.16	0.99	1.15	1.50	1.29
cased5	66.9	0.89	0.88	0.78	0.63	0.95	0.83	0.94	1.22	1.07

The more compact configuration results in lower neutron-leakage, increasing k_{eff} (compare cased5 with cased2 in Table 2-3). For the same fuel enrichment, the neutron-flux in the multiplier region also increased slightly compared with cased2 because of the fewer number of multiplier assemblies. Decreasing the fuel enrichment is again seen as a means to increasing the neutron-flux; cased4 provided the highest flux levels for all cases analyzed at 20-MW operations.

The results in Table 2-4 verify that the test loops in the inclined-entry layout are not all in the same neutron-flux environment. Test loop B, which is located more in the center of the multiplier region, experiences a higher flux and has a smaller peak-to-average flux ratio than the other test loops (1.3 vs. 1.5). A better balance can likely be achieved by relocating the “A” test loops more inside the multiplying region.

Figure 2-12 and Figure 2-13 provide spatial distributions of the total neutron-flux at the mid-plane of the fueled region for cases representing the vertical- (cased1) and inclined-entry (cased5) layouts. These cases are based on the configurations shown in Figure 2-9 and Figure 2-10. The target/buffer, multiplier region, and test loops are outlined. The flux map in Figure 2-13 was rotated by the software that produced the figure (it does not at first glance appear to agree with Figure 2-9), but the flux values themselves are correct. The peak multiplier flux in the vertical-entry layout (Figure 2-12) occurs in positions adjacent to the target/buffer; one would expect the peak flux to occur in the same positions in a source-driven evaluation of this configuration. For the inclined-entry layout (Figure 2-13), the peak flux occurs within the multiplier region, away from the target/buffer; in a source-driven evaluation of this configuration, one would expect the peak location to move to the buffer-multiplier interface.

The results presented above are all based on homogeneous diffusion theory calculations. A more accurate evaluation of the neutron-physics parameters in the ADTF requires an external-source diffusion theory model, however. The cases presented in Table 2-5 used the EOEC conditions of cased1 as a basis for evaluating the vertical-entry layout of the ADTF as a source-driven system.

Table 2-5. Comparison of Homogeneous and Source-Driven Solutions for 20-MW sodium-Cooled ADTF at EOEC (vertical entry layout with 21.4-inch OD target/buffer)

		Homogeneous solution				*Source-driven solution*			
		(No void)	*(90% void)*			*(90% void)*			
				Multiplier Flux			*Multiplier Flux*		
				(x10 ^{15} n/cm ^{2}/s)			*(x10 ^{15} n/cm ^{2}/s)*		*Source-*
Case	*Target size*	*k-eff*	*k-eff*	*Averag*	*Peak*	*k-source*	*Averag*	*Peak*	*importance* *
cases1	2 rings	0.7839	0.7754	0.62	0.79	0.7237	0.61	0.90	0.76
	(5.4 in OD)								
cases2	3 rings	0.7839	0.7656	0.62	0.79	0.7060	0.62	0.90	0.74
	(9.4 in OD)								

* Source-importance = (1-1/k-eff)/(1-1/k-source)

The target and buffer were explicitly represented in these cases. The two cases used two and three full hexagonal rows to represent the target region while maintaining a fixed outer dimension (six rows) for the buffer region. The void region above the target (i.e., the beam-tube) was modeled as Pb-Bi at 10% of full density (90% void fraction). A preliminary set of scoping calculations at higher void fractions revealed the short-comings of nodal diffusion theory to properly compute the neutron-flux in voided regions. Transport theory may be needed to accurately represent the voided region.

To clearly understand the difference between using a homogeneous vs. source-driven model, it was necessary to repeat the homogeneous solution, but with an explicit representation of the target and buffer (specifically, the void region). Including the void region decreases the k_{eff} of the system, as it provides a leakage path for neutrons; increasing the size of the void region (larger beam-tube) further decreases the k_{eff}. Although not indicated

in Table 2-5, the computed multiplier and test loop flux levels are not affected by the presence of the void region.

The source-driven solution was obtained by providing a neutron-source at a magnitude that yielded a total reactor power of 20 MW. The spatial- and energy-dependence of the source was representative of that which might be produced in an accelerator-driven system. The use of other target materials (e.g., W vs. Pb-Bi, which was used here) with different neutron-diffusion properties may slightly alter the flux level in the target, but not the overall conclusions.

The energy distribution of neutrons produced directly by the spallation reaction is harder than the typical energy distribution of fission neutrons; roughly 20% are born at energies higher than 14 MeV, which is the cutoff energy for the broad-group data used here. Previous work tracked the transport of high-energy source-neutrons in an accelerator-driven system to the point at which they dropped below the 14 MeV cutoff. A space- and energy-dependent neutron-source that accounts for all neutrons but with a maximum energy of 14 MeV can be constructed. For this work, a simplified source located only within the target region is utilized; comparisons indicate good agreement with the more detailed distributed source results. Future analyses may include a more accurate representation of the neutron-source and the treatment of high-energy neutron transport, but will not contradict the trends observed here.

The multiplication factor of the source-driven model, ksource (computed as the ratio of fission-neutron production to absorption plus leakage losses), is significantly lower (~7%) than the multiplication factor of the homogeneous model, k_{eff}. The so-called source-importance is also included in Table 2-5 and provides a measure of the relative importance of external-source to fission neutrons for driving the system. There is an inverse relationship between the source-importance and the accelerator beam-current; as the source-importance decreases, the beam-current must be increased for the multiplier to produce a specified power. Increasing the size of the void region (larger beam-tube) has little effect on the source-importance.

The source-driven model predicts a larger neutron-flux gradient than the homogeneous model; the peak-to-average flux is 1.46 vs. 1.27. This is expected as the source-driven problem shifts the power density toward the buffer-multiplier interface. This also has the effect of decreasing the flux level in the test loops, however. Increasing the size of the target area (moving the source closer to the multiplier) causes only a slight increase in the multiplier flux gradient. Figure 2-14 provides the spatial distribution of the total neutron-flux at the mid-plane of the fueled region for cases2 (9.4-inch OD target). Comparing Figure 2-14 with Figure 2-12, we observe the somewhat larger flux gradient in the multiplier region and a lower flux level in the test loops for the source-driven solution. Although the flux level in the target/buffer region is significantly higher in the source-driven solution, we observe that the flux distribution within the multiplier is within a few percent of the homogeneous solution; the trends observed in the earlier part of this study will hold for the source-driven system.

Source-driven solutions were not obtained for the inclined-entry layout in the present work because of the unavailability of a representative neutron source for this geometry; they will

be completed in future work. The following trends are anticipated when these analyses are complete:

1. The peak flux in the multiplier region will shift to the buffer-multiplier interface.
2. The flux level in the test loops will be slightly lower than that reported in Table 2-4 for a given reactor power level and multiplier arrangement and enrichment.
3. The source-importance for the inclined-entry layout will be lower than that for the vertical-entry, although the presence of reflecting materials on the side of the target facing away from the multiplier will reduce target leakage.

The design power for the facility is 100 MW. The analyses performed were all done using a multiplier power of 20 MW, since it is likely the facility will initially be operated at this lower power level. Increasing the multiplier power requires an increase in the size of the multiplier region (replacing reflector with fuel assemblies) to maintain the power density and lineal heat rate within the design limits for the heat-removal system. Even so, it is anticipated that higher flux levels will be achieved at 100 MW operation since at 20 MW we are operating at a derated power level.

A core configuration for 100 MW operation was developed by adding 51 multiplier assemblies to the layout shown in Figure 2-9 (bringing the total to 144 assemblies). The equilibrium-cycle results for this configuration (using homogenous diffusion theory) are presented in Table 2-6. The results are based on a three-batch core, 820 FPD residence time, U-10Zr fuel, and an enrichment of 66.9 without ^{235}U. A comparison of cased6 with cased1 in Table 2-3 shows an increase in k_{eff} caused by a decrease in neutron leakage relative to the fission source. An increase in the flux levels in all regions is also observed, with a peak fast-flux in the test loops near the project goal of 3×10^{15} n/cm^2/s. The lineal heat rate in the multiplier assemblies is 311 W/cm, compared with 97 W/cm at 20 MW operations. By comparison, the Mk-IIIA lineal heat rate in EBR-II was ~350 W/cm.

Table 2-6. Performance Parameters for 100-MW Sodium-Cooled ADTF with Depletion (vertical-entry layout)

					Flux at EOEC (x10 ^{15} n/cm ^{2}/s)			
	# Rings in	# Multiplier	k-eff		Multiplier	Test loops		
Case	Target/Buffer	assemblies	BOEC	EOEC	Average	Average	Peak	Peak-fast
cased6	6 (21.4 in OD)	144	0.86	0.82	2.28	2.27	2.95	2.48

2.3 Heat Transport

2.3.1 Primary Coolant Circuit

The primary coolant circuit is in many ways similar to that of a sodium-cooled reactor. The fuel is contained inside sealed steel-clad rods. The rods are wire-wrapped and tightly arranged inside hexagonal cans to form fuel assemblies. These assemblies are aligned vertically in a tight hexagonal array. The target region is located at the center of the accel-

erator and is surrounded by the buffer region, which is, in turn, surrounded by the fuel region. Liquid sodium flows in parallel paths through all of the fuel assemblies. There is a common lower coolant plenum that provides sodium coolant to each fuel assembly. All of the coolant that passes through the fuel assemblies merges into a common upper plenum in the multiplier vessel and is transported through a single exit coolant pipe to the shell-side of a large sodium-to-sodium counterflow heat exchanger.

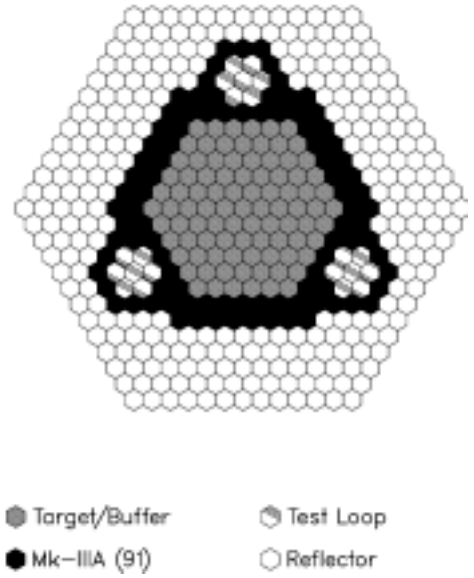

Figure 2-9. Representative core configuration for vertical entry of the accelerator beam-tube in the sodium-cooled ADTF.

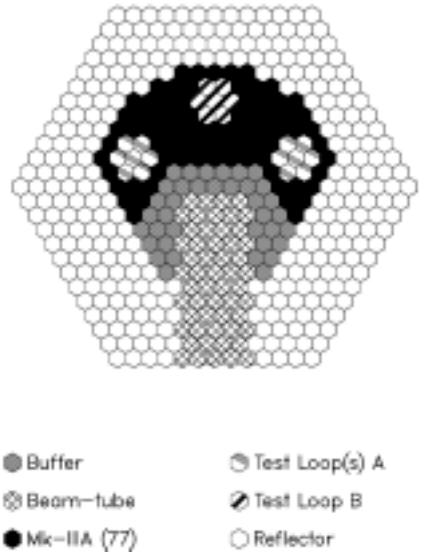

Figure 2-10. Representative core configuration for inclined entry of the accelerator beam-tube in the sodium-cooled ADTF.

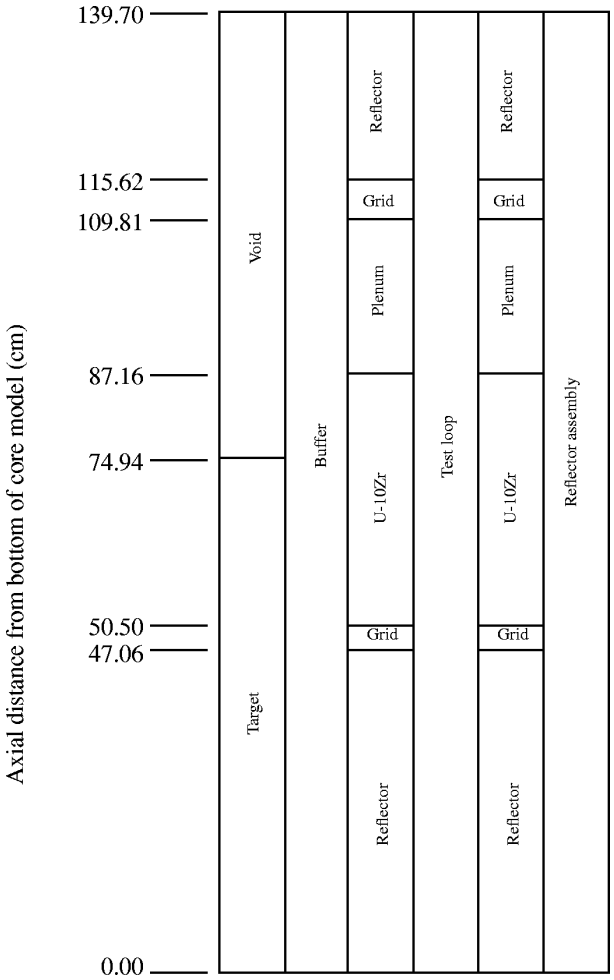

Figure 2-11. Axial cross-section of core components in the sodium-cooled ADTF as modeled for neutron-physics analyses.

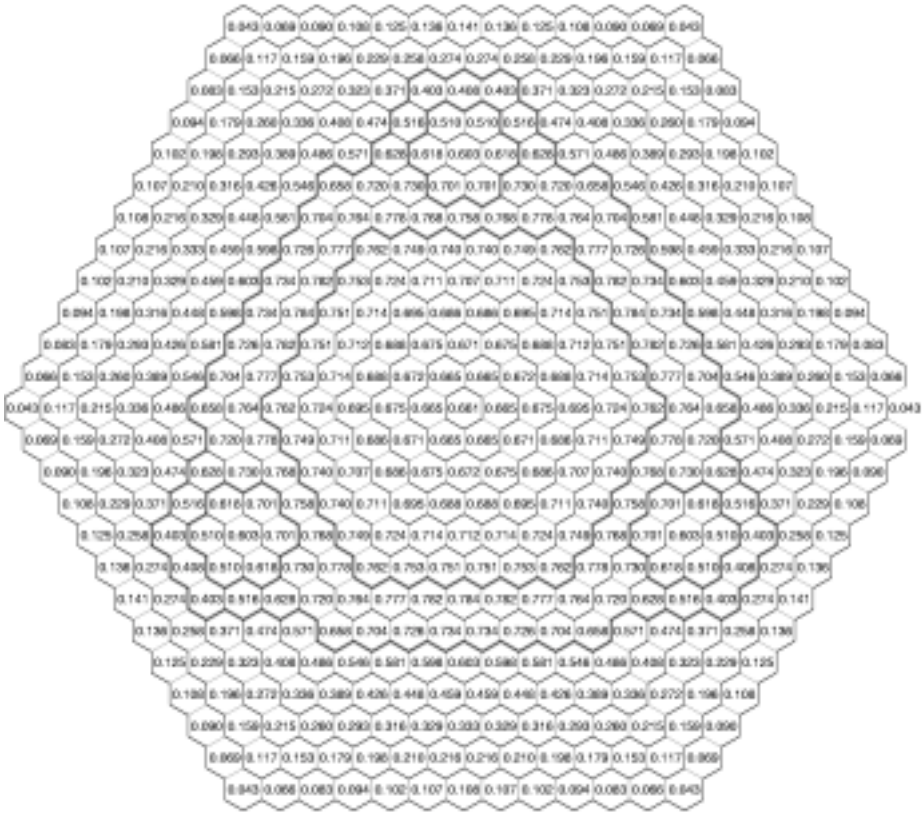

Figure 2-12. Spatial distribution of total neutron-flux ($\times 10^{15}$ n/cm^2/s) at fuel mid-plane for cased1 at EOEC (homogeneous solution).

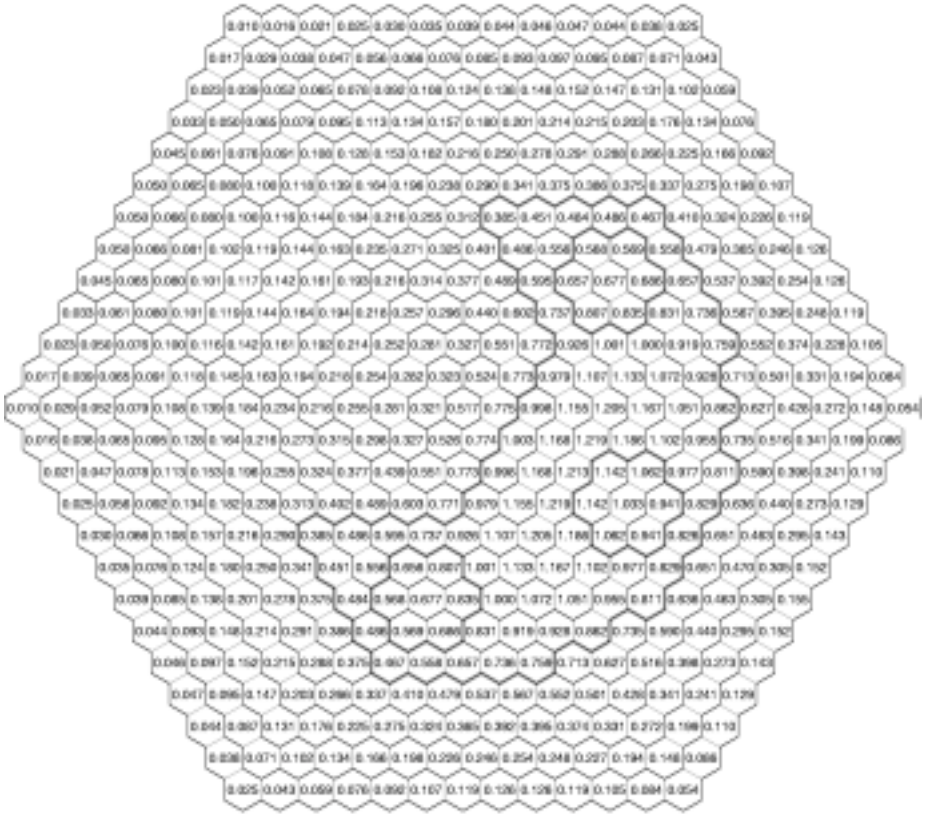

Figure 2-13. Spatial distribution of total neutron-flux ($\times 10^{15}$ n/cm^2/s) at fuel mid-plane for cased5 at EOEC (homogeneous solution).

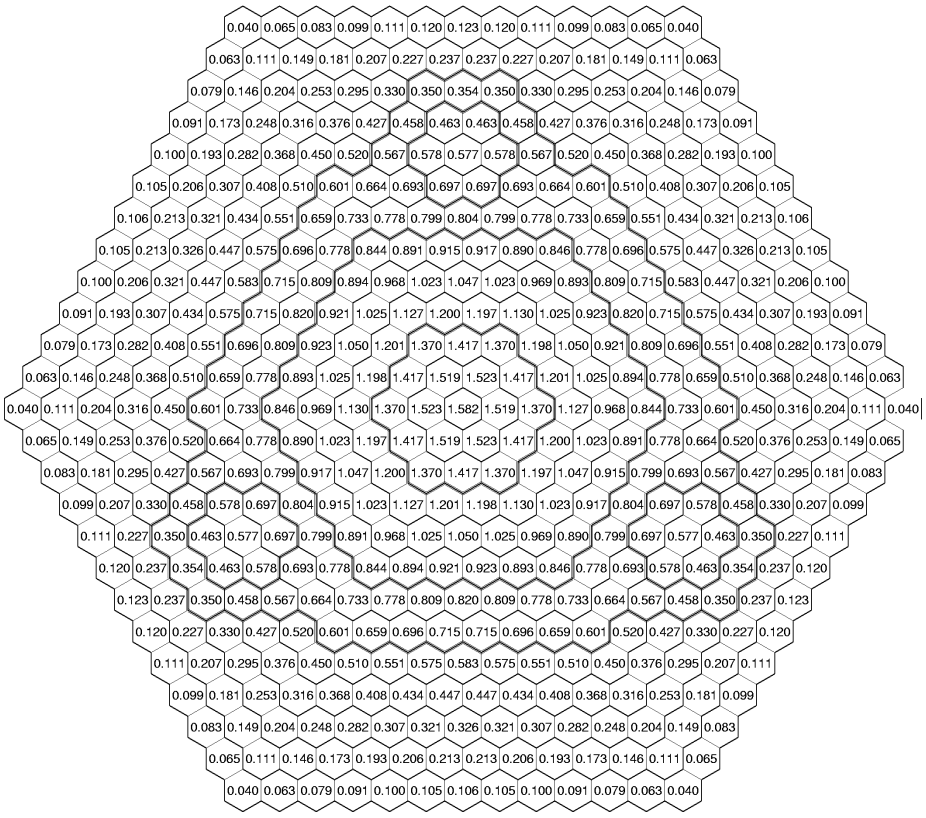

Figure 2-14. Spatial distribution of total neutron-flux ($\times$ 10^{15} n/cm^2/s) at fuel mid-plane for cases2 (source-driven solution).

The multiplier vessel is located in a large pool of sodium. The coolant exits the shell-side of the heat exchanger into the pool. Two large centrifugal pumps, one on each of two inlet pipes, draw sodium from the pool and transport it to the accelerator lower coolant plenum. The accelerator driven subcritical multiplier is designed for 100 MW of thermal power although it will initially operate at 20 MW. The inlet temperature to the plenum is initially selected at about 700°F and the temperature at the upper plenum about 880°F. To remove 100 MW of power and have a 180°F temperature rise from the inlet to the outlet plenum the combined flow from the two main centrifugal sodium pumps would have to be approximately 14,650 gpm. This flow rate was calculated assuming that the sodium density is that of 800°F sodium.

For 20-MW operation the primary flow rate could be reduced to 20% of that used for 100 MW operation. This would maintain the 880°F outlet temperature, and keep core temperatures close to their nominal (100-MW operation) values, and thus allow operation at this temperature range to be understood before operation at 100 MW is attempted. It would also reduce power consumption. A potential difficulty is that the pumps would have to be

designed to run properly for long periods of time at two widely different flow rates. This could potentially impact the design of the lower hydrostatic bearing of the pumps.

The multiplier will use previously qualified EBR-II fuel. The operating temperatures selected for the ADTF multiplier are those at which the EBR-II fuel operated. These relatively high sodium temperatures will also facilitate heat transfer to the atmosphere. For an ATW with electricity production option, relatively high sodium temperatures are required for thermal efficiency. It is a requirement for the ADTF to operate at conditions prototypical of the ATW facility. The high sodium temperatures in the ADTF would ensure meeting this requirement. A disadvantage of higher temperatures is that structural materials are subject to more fatigue when they are cycled over wider temperature ranges during start-up and shut-down. Since sodium freezes at 208°F and there is a greater tendency for sodium oxides to precipitate at temperatures approaching the freezing point, operation near this temperature would be unacceptable. The nominal cold shut-down temperature for EBR-II was about 400°F, and this could represent a lower limit.

2.3.2 Cooling the Target and the Buffer

One concept for cooling the target and the buffer would rely on transverse heat transfer. This, which is sometimes called *radial heat transfer*, would essentially conduct heat transversely from the target and the buffer to the surrounding fuel assemblies where the heat would be carried away by the flowing sodium. This probably is not a viable concept because the power generated in the target can be up to about 8 MW and the temperature differences from the center to the periphery of the target is expected to also be very high; a special cooling system for the target may be needed. It may be possible to design a solid tungsten target to fit into several assembly hexagonal cans and cool it by patterning the buffer design after the fuel assemblies and connecting the buffer assemblies to the multiplier common lower and upper coolant plena. For a liquid lead-bismuth target, cooling may be accomplished by allowing the lead-bismuth to flow to a heat exchanger or by imbedding a sodium-cooling coil in the target to transport the heat to a heat exchanger. The buffer cooling would be accomplished by either (1) radial heat transfer to the adjacent fuel assemblies, (2) in a manner analogous to the solid tungsten target, or (3) some, yet undetermined, means.

2.3.3 Heat Removal from the Primary Circuit to the Atmosphere

All of the heat transferred to the primary sodium by the fuel, and possibly by the buffer and the target, is transferred to the large counterflow heat exchanger. From there the ultimate heat sink is the atmosphere. In an ATW designed to produce electric power, about a third of the energy will be converted to electricity when the turbine is online. Since the primary-circuit heat exchanger is submerged in a pool of liquid sodium, it is unacceptable to use water or air as the secondary-side coolant. Air and water both can chemically react with sodium and generate large amounts of heat. This can pose a hazard to the radioactive primary system and its fuel assemblies in the event of a heat exchanger structural failure;

therefore, an intermediate loop of essentially non-contaminated sodium would be used to transfer the heat out of the primary pool. A second heat exchanger, or set of heat exchangers, is needed to remove the heat from the secondary sodium. Air will be used to transfer the heat from the secondary sodium to the atmosphere, following the concepts used in the Fast Flux Test Facility (FFTF).

2.4 Remote-Handling and Operations

Handling of fuel, experimental loops, and the accelerator/target interface tube are the main handling activities that affect system design. We will discuss each of these in the order stated, since the requirements imposed by each build up in that order. In doing this, the reasons for various dimensions given above will be explained.

2.4.1 Fuel-Handling

To remove fuel assemblies from the multiplier, the cover of the multiplier vessel must be raised by the length of an assembly plus some allowance for the gripper equipment and clearances for movement of the fuel. This turns out to be ~8.5 ft for assemblies of EBR-II length. Movement of the rotating plug then allows the gripper to be positioned at any azimuthal position around the multiplier, while rotation of the gripper around its shaft axis allows positioning at any radial position, thus allowing any assembly to be picked up. The gripper assembly will need to be designed with a hold-down mechanism to maintain the surrounding assemblies in place when the gripper lifts an assembly. Once the assembly is removed from the multiplier, the gripper passes it on to a transfer arm, which places it into a storage basket. A separate mechanism extending through a penetration outside the rotating plug is used to remove the elements from the basket to a fuel coffin resting on the operating floor.

Control-rod drives are disconnected from their respective rods, allowing rotation of the plug with the rods fully inserted into the multiplier. Since loops must also be withdrawn from the multiplier to allow movement of the rotating plug, the inside cell height must accommodate this, making it ~17 ft high. This cell height, plus the thicknesses of its floor and ceiling, must be added to the length of the in-core portion of the accelerator tube to give its total length, which is ~46 ft, as noted in Section 2.1.5.

2.4.2 Experimental Loop Handling

As was discussed above, loops are semi-permanently mounted inside the cell comprising the rotating plug. They are installed and removed through penetrations in the roof of this cell, the other side of which constitutes the operating floor above the target-multiplier system (See Figure 2-3; although this figure depicts the vertical entry concept, the situation for the inclined-entry is substantially the same.) After irradiation, they would be withdrawn into a shielded coffin that would adapt to the penetration. Although not requiring the shielding, the same coffin would probably be used for installing new loops. A test train containing irradiated fuel would be withdrawn into the same coffin, after removing the penetration plug and unbolting a closure flange on the top of the loop using remote-handling techniques.

2.4.3 Accelerator/Target Handling

Replacement of the vertical in-core accelerator/target tube involves lateral displacement of the removable tube section mentioned above and vertical withdrawal of the lower section into a bottom-loading coffin mounted to the top of the rotating plug. Since its length is ~46 ft, it must be raised that distance; hence the removable section of accelerator tube and the coffin must be that long, and the underside of the upper floor upon which are mounted the bending magnets must be that height above the operating floor. Details for handling with segmented tubes and pivoting bending magnets have not been developed as yet.

The copious amounts of shielding around the removable section, necessary for protection of personnel against the backshine from the neutron spallation source at the center of the multiplier (the pipe forms a very effective streaming path) during operation, will make this a rather difficult design and handling problem. If steel is used, as seems probable because of activation problems with lead, the outer envelope of this shielding will encompass not only the loop access ports, but possibly the control rod drives and fuel-handling equipment as well (see the horizontal sections of Figure 2-4.) Cavities for this equipment can certainly be built into the shielding, but servicing of, e.g., control rod drives during shut-down will require its removal and replacement by a thinner shield, perhaps of lead, to protect workers from the accelerator tube itself, since it will have become activated during operation. If the area is an exclusion area during operation, the shielding requirements will be significantly less, but a change from steel during operation to lead during shut-down will probably still be necessary.

In this vertical-entry concept, it is assumed that the target and buffer will be attached to the accelerator tube, although that may not necessarily be the case for a W target. It may also be possible to locate the window, through which the protons must pass in going from the evacuated accelerator tube to the capsule containing the target, in a spool-piece above the double-walled vessel cover and replace it as a cartridge, as necessary, independently of accelerator/target replacement and/or multiplier fuel-handling.

In the inclined-entry concept, the bending magnet is pivoted to the side, so that no removable tube segment is needed, and the in-core tube is withdrawn along its axis into the hot-cell surrounding it by some convenient means (e.g., a cable or chain winch or a rack-and-pinion gearing arrangement along the tube) onto rollers mounted on rails. It would then be turned upright and withdrawn into a bottom-loading coffin mounted to a port in the roof of the cell. This type of operation has been well developed for the Lujan Center spallation neutron source at LANSCE. It might be suggested that the vertical-entry concept be handled in a like manner. It would be difficult, however, to implement the hot-cell capability atop the rotating plug with the multitude of other equipment handling (e.g., control rod drives, experimental loops, etc.) that must be done there.

Target and window handling will be similar to the vertical-entry case, except that the W target, in the shape of multiplier fuel/reflector assemblies, will be much easier. Handling of the filler pieces above and below the inclined accelerator tube may be handled by attaching adapters and then handling them as fuel/reflector assemblies.

2.5 Safety Characteristics

This section presents a preliminary assessment of the safety features and the safety challenges associated with the ADTF concept. No analyses have been completed of the ADTF sodium pool concept; thus, the assessment is based on previous analyses of similar systems backed by engineering judgement. The thermal design and power limits of the facility are governed by the unplanned transients, or upsets, rather than by the anticipated normal, mostly steady-state, operation. The preliminary assessment is divided into several parts as follows:

- Operational Considerations of a subcritical reactor;
- Response to Protected Transients;
- Response to Unprotected Transients;
- Decay-Heat Removal;
- Fuel Qualification;
- Loop Safety Assessment; and
- Impact of the Target/Buffer.

2.5.1 Operational Considerations

The concept of an accelerator driven subcritical multiplier will require a reevaluation of operational safety. Small reactivity insertions will not represent the problem that they would in a critical reactor, where a small reactivity insertion would result in a increase in power until compensated by negative reactivity feedbacks inherent in the design. In a subcritical multiplier, small reactivity additions will cause the power to increase and stabilize at slightly higher power even if the inherent feedbacks in the design of the core are negligible. In a subcritical multiplier the power is a strong function of the beam power with the inherent feedbacks of the design potentially providing secondary effects in terms of maintaining stable operation.

Another issue is the impact of beam trips on safety and availability. The present accelerator designs have not been challenged to reduce the beam trips or interrupts. The design life of a reactor facility is often governed by the thermal transients to which the structures are exposed. Based on the current operational experience of accelerators the induced thermal transients could severely limit the structure life of the ADTF; a major challenge of the design and testing will be to increase the reliability of the accelerator while at the same time reducing the sensitivity of the subcritical multiplier structural life to thermal transients.

The issue of start-up of a subcritical multiplier will also present new design challenges to the accelerator. The start-up of a subcritical multiplier will require a continuously variable beam power or a multiple small stepwise increases in power. This will represent a design issue for the accelerators. The safety implications will require assurance against large stepwise increases.

2.5.2 Response to Protected Transients

A significant safety advantage of a subcritical multiplier is an improved response to protected transients. Given a signal to shut-down the accelerator, the time constant for a beam trip is significantly faster than for the insertion of a control rod. Because of the subcriticality of the assembly, the response to reactivity insertions is also improved. A negative impact is that the faster shut-down of the target-multiplier will increase the induced thermal stresses. This will need to be addressed with increased reliability of accelerators combined with accommodating the design of the multiplier structures. A significant design issue will be the extent that safety grade equipment extends into the accelerator.

A typical protected transient will be a loss of flow with accelerator shut-down. This is analogous to loss of flow with scram in a power reactor. For this category of accident there would need to be two modes of protection. The primary one would be a flow trip. In the even more unlikely event that the primary trip failed to function properly, a secondary one, a temperature trip, would shut down the accelerator.

2.5.3 Response to Unprotected Transients

In an appropriately designed sodium-cooled critical reactor, the negative feedbacks (Doppler, radial, axial expansion, etc.) can be sufficient to drive the reactor to zero power for various unprotected events such as limited reactivity insertions, loss of flow, and loss of heat-sink events. This response cannot be extrapolated to a subcritical multiplier. A satisfactory response can be expected for limited reactivity insertions and loss of off-site power. The unprotected loss of flow event, however, could represent a design challenge for a subcritical multiplier. In this case the design of passive means to shut down the accelerator or to divert the beam power needs to be investigated. This is likely to be a major design issue for the ADTF. Concepts being considered could rely on the temperature increase in the coolant causing a valve to open, or a bimetallic switch to activate causing the beam to limit the power input to the target. The issue will be the time response of these systems. Another means could rely on the bottom plate of a liquid (lead-bismuth) target that could melt and allow the target to flow away. This would shut down the accelerator by effectively destroying the target. The recovery could be both difficult and costly. The impact of passive accelerator shut-down devices on the shut-down reliability of the accelerator will need to be studied. Accelerator overpower transients may need to be investigated as well. These transients will depend on the accelerator design.

2.5.4 Decay-Heat Removal and Natural Circulation

The primary normal method of removing the decay heat will be through use of the normal sodium-to-air heat exchanger. This system will be an active system requiring power to remove the heat; a completely passive back-up decay-heat-removal system is desirable.

The three primary requirements of successful passive decay-heat removal are

1. removal of the decay heat from the core by natural circulation,
2. a large thermal mass to accept decay heat from the natural circulating sodium, and
3. a highly reliable passive heat transfer device to remove heat from the sodium pool that serves as the thermal mass and the transfer to an ultimate heat sink.

Short-term decay-heat removal covers the time span immediately after an accelerator shut-down caused by an upset condition or otherwise. During the coastdown of the primary pumps after the accelerator has been shut down, the fuel coolant temperatures go to a nearly uniform value throughout the primary circuit. The buoyancy forces in the fuel assemblies may not provide adequate flow in all fueled (and buffer and target) assemblies to remove the decay heat, which is at its highest immediately after a shut-down. The desirable solution is a completely passive system. This could be accomplished by increasing the pump coastdown, or designing for higher differential elevation of the thermal centers to increase natural circulation. A less desirable solution is to have an auxiliary pump attached to the multiplier outlet coolant pipe. This pump would run all of the time and have a battery back-up that would provide sufficient energy to provide flow immediately after an accelerator shut-down. After the decay heat levels are sufficiently low and the coolant temperature heads are sufficiently well established the auxiliary pump operation could be temporarily curtailed as the batteries as depleted.

Long-term decay-heat removal is concerned with walk-away safety following a severe incident, such as one caused by a seismic event. For the short-term case, there is no need to be concerned about decay-heat removal from the primary pool. The very large heat capacitance of the double-walled vessel and its contents prevents any significant primary pool sodium temperature rise in the short term; however, when the time interval is weeks or months, the primary pool sodium temperature potentially could rise tens or hundreds of degrees. One could consider removing this energy via the normal heat-transport system. During (for example) a seismic event, however, the intermediate loop piping could be severed or essential parts of the heat-transport system may be inoperable. Any method used must be totally passive and not rely on an external power source. The EBR-II employed two bayonet-type shut-down coolers in the primary tank sodium. Each circulated NaK coolant via natural convection between a bayonet cooler in the primary tank and a NaK-to-air heat exchanger attached to the exterior of the primary containment building. The air-side of these heat exchangers also relied on natural circulation for flow. NaK was used as the coolant because it is liquid at room temperature. The ADTF could use a Direct Multiplier Auxiliary Cooling System based on this system. Another system under consideration is the naturally circulating Multiplier Vessel Air-Cooling System [MVACS (similar to the RVACS of the General Electric PRISM Design)]. This system would circulate air, via natural convection, past the exterior of the guard vessel. The guard vessel surrounds the primary vessel and is capable of containing a sodium leak through the wall of the primary vessel. The space between the guard vessel and the primary vessel wall would be filled with an inert gas.

2.5.5 Fuel Qualification

A requirement for consideration of an ADTF concept is that the fuel to be used in the initial several multiplier cores must be fully qualified. The goal in the sodium-cooled pool concept is to use the driver fuel developed and qualified for EBR-II. The chosen fuel for the ADTF is the EBR-II MkIIIA fuel. The best sources of fuel for the multiplier blanket of the ADTF are existing inventories of fresh fuel for FFTF or EBR-II. These fuels were qualified for operation of FFTF and EBR-II, and although the ADTF environment is not the same, enough is known about the performance of those fuels in a fast spectrum to prepare a safety case for ADTF operation, with some informed extrapolation to the conditions of the ADTF. The fuel can be qualified for ADTF operation through a surveillance program that examines fuel subassemblies operating under representative and aggressive conditions in the ADTF to ensure that fuel behavior is as expected and remains bound by the envelope of the safety case. During this surveillance period, the ADTF can be operated in a manner such that the fuel is not exposed to the most severe conditions (e.g., by operating initially at lower-than-rated power and then incrementally increasing power) until the fuel is demonstrated to perform reliably and predictably.

2.5.6 Loop Safety Assessment

Large experimental loops in sodium systems have been operated in the past and extensive experience has been acquired. For example, the Sodium Loop Safety Facility was a large loop that allowed the testing of up to 37 elements in the Engineering Test Reactor. Numerous tests were performed in TREAT Reactor Facility in Idaho. The experimental loops will be designed in accordance with the lessons learned in those tests. Based on the experience of the previous designs, no specific safety-related issues related to experimental loop operation are expected in the ADTF.

2.5.7 Impact of the Target/Buffer

At this preliminary stage, design of the target buffer region needs additional maturity before an evaluation can be completed. The safety evaluation will be completed during the conceptual design phase. The potential of potential material interactions between the sodium and the coolants in the target will be investigated.

3 Preconceptual Design Description of Accelerator Systems

The ADTF accelerator is designed to meet the performance goals of the facility by providing:

1. An 8-MW beam at 600 MeV output energy, implying a 13.3-mA continuous wave proton current. This requirement follows from Section 3.2 that gives the maximum neutron production capacity of the ADTF as a function of proton beam energy and potential other uses.
2. A beam shut-off capability that is consistent with meeting the facility safety-class requirements.
3. Beam entry to the target-multiplier, beam-spot size, beam-transverse pattern, and beam-exit window that are consistent with safety and target-multiplier restrictions.
4. Beam-loss that is low enough to allow unrestricted hands-on maintenance on the accelerator components when the proton beam is off.
5. A beam-interrupt rate and temporal format that is consistent with target-multiplier performance and component lifetime.
6. A beam-current amplitude control that is consistent with target-multiplier power control and sub-system design.
7. Accelerator availability during scheduled operations that is consistent with facility operations.
8. The capability through upgrades or additions to the accelerator to meet the tritium production goals.
9. The capability through upgrades or additions to the accelerator to support isotope production.
10. A high-energy beam transport (HEBT) that incorporates the possibility of additional beamlines or an extension of the accelerator.

The majority of the ADTF linac design can be directly derived from the work done on the APT plant accelerator, significantly reducing the design effort required. The layout of the 1030-MeV, 100-mA APT linac and beam-transport system is shown below (Figure 3-1) in conceptual form. A nominal sketch of the ADTF linac layout and beam-transport system is shown below it in Figure 3-2 for comparison.

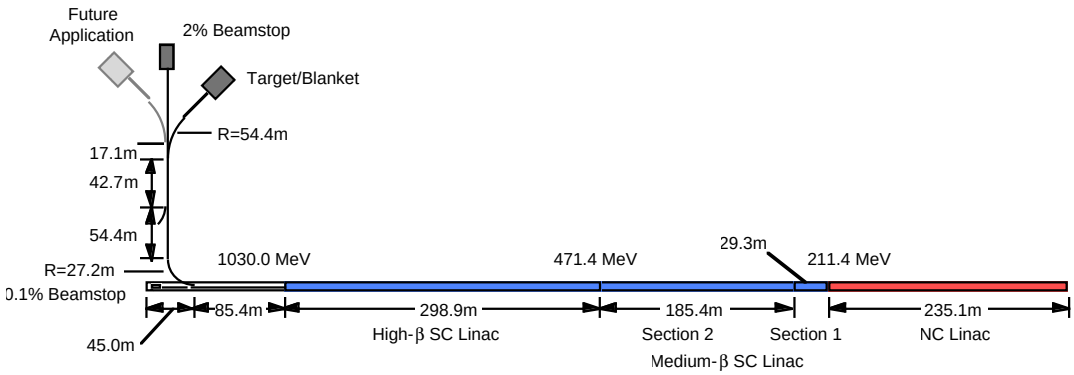

Figure 3-1. Sketch layout of APT accelerator and beam-transport system.

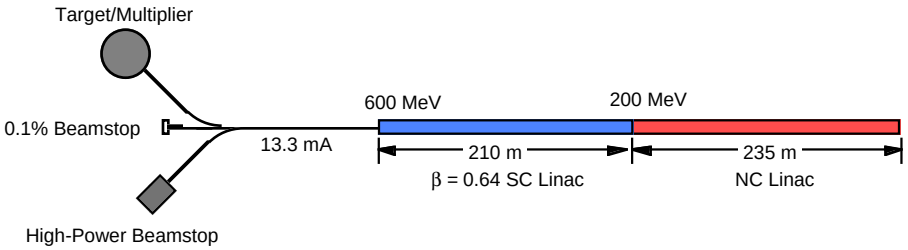

Figure 3-2. Sketch layout of nominal ADTF accelerator and beam-transport system on same scale as APT.

The overall design of the linac is driven strongly by available cavity accelerating gradients, beam dynamics, and beam-loss considerations. This leads to a design with a tight-focusing channel and large-aperture accelerating cavities. Superimposed on this framework are the additional requirements of safety, reliability, availability, and maintainability.

Following a 75-keV proton injector that contains a microwave-driven ion source, the ADTF linear accelerator uses normal-conducting water-cooled copper structures to accelerate the 13.3-mA continuous-wave proton beam up to an energy of approximately 200 MeV, and niobium superconducting accelerating cavities to the final energy. To smoothly and efficiently accelerate the proton beam without loss, several different accelerating structures are used, each optimized for a specific energy range. The 200-MeV low-energy (LE) linac consists of a 6.7-MeV radio-frequency quadrupole (RFQ), a coupled-cavity drift tube linac (CCDTL) to about 100 MeV, and a coupled-cavity linac (CCL). The high-energy linac (from 200 MeV to 600 MeV) consists of elliptical superconducting cavities grouped into

cryomodules. The RFQ operates at a frequency of 350 MHz. All subsequent accelerating structures operate at 700 MHz. High-power continuous-wave microwave generators (klystrons) supply the RF power to drive the structures and accelerate the beam.

3.1 Accelerator Reliability

To minimize effects caused by thermal transients, the ADTF target-multiplier assembly may impose a new accelerator requirement that was not specified for APT, high-beam reliability. Beam reliability differs from availability. Availability is defined as the integrated amount of charge delivered to the target over some fixed period of time, typically a year. Reliability has to do with the number and duration of beam interrupts in that interval. In addressing beam reliability issues for ADTF, the preliminary thermal analysis that has been done to date has been focused on Na and Pb-Bi liquid-metal-cooled multipliers. Other target-multiplier technologies may have different beam reliability requirements.

3.1.1 Fault Durations and Impacts on Target-Multiplier Assembly

Preliminary analysis of fault time scales indicates that beam-interrupt periods can be divided into three characteristic time intervals, for which there appear to be different impacts on the target-multiplier' assembly. For liquid-metal-cooled systems, the shortest meaningful thermal response time, which is for the fuel elements (load pads), appears to be about 0.3 seconds. Temperature changes would only be a few degrees Celsius for beam interrupts of this length or shorter, so this class of interrupts is transparent to the target-multiplier.

Various structural elements of the target-multiplier have longer thermal time responses, ranging from seconds to about 100 seconds. The number of thermal cycles that can be tolerated by various parts of the target-multiplier before significant damage occurs is different from element to element, and depends on the temperature differences that develop following a beam interrupt; for example, the fuel assemblies can tolerate more than 10,000 cycles, but other elements are far less tolerant. Modifications can be incorporated into the target-multiplier design that reduces the impact of beam-trip-induced thermal cycling; however, some of these may negatively affect target-multiplier performance.

For interrupts lasting longer than 0.3 seconds, the present consensus is that the beam power should not be restored immediately. The target-multiplier components need to be able to cool down for a minute or so after a *noticeable* beam interrupt to minimize thermal stress. Following this cool down, there could be a ramped restart lasting a few minutes. If the beam were off too long (more than 100 sec, for instance) some of the long-time-constant elements of the target-multiplier are affected, and the waiting time before restoring the beam may be longer. It could take several hours to return the target-multiplier to operation. There is therefore an identifiable beam-interrupt interval stretching roughly from 0.3 sec to 100 sec. To avoid excessive impact on availability, as well as stress on the target-multiplier components, the frequency of these *midrange* beam interrupts needs to be

reduced below what it is in the LANSCE accelerator (of order 10^4/yr) by between one and two orders of magnitude.

For faults more than 100 seconds, thermal effects in the sodium-cooled target-multiplier concept may limit the number of such interrupts to less than 30/year. For example if such an interrupt required a multi-hour restart, then overall availability could be affected. The impact of long beam interrupts remains a question that still needs to be resolved. The 100-second time period separates interrupts not requiring a lengthy target-multiplier restart from those that do is somewhat arbitrary as noted above. It might be higher or lower depending on the design of the target-multiplier.

A tolerable interrupt spectrum (rates, durations) and the resultant impact on accelerator design will be refined in the conceptual design phase. A design goal is to also make the target-multiplier more fault tolerant than is presently assumed, and thus reducing the impact of these time constraints on the accelerator design.

3.1.2 Influence of Beam Reliability Requirements on Accelerator Design

While ADTF beam reliability requirements need more resolution in terms of what will be acceptable to assure transmuter performance and component lifetimes, it is clear that reduction of the interrupt rate in comparison with those in existing accelerators will be a significant driver for the linac design. Preliminary indications are that design goals should seek a reduction in the total number of annual interrupts by more than an order of magnitude, and also should seek to shorten the duration of many of these interrupts to less than the roughly 300-millisecond response time discussed above.

A high-reliability accelerator design would include an appropriate mix of the following principles and approaches. Attaining the right balance among these that achieves the ADTF reliability goals for minimum cost will be the task of trade studies during conceptual design.

1. The superconducting linac, which is made up of individually driven accelerating units, should have a fault-tolerant beam dynamics design. Beam operation can be continued after the failure of an accelerating unit (cryomodule or RF station) by retuning neighboring units to make up the energy shortfall. Improvements in fast control electronics may now make this a practical approach to eliminating most of the beam interrupts attributable to the superconducting linac.
2. Critical equipment, such as RF stations in the normal-conducting low-energy linac, the injector, etc., should have an appropriate level of redundancy. This will limit the beam-off time when interrupts do occur to periods lasting from a few seconds to a few minutes. With a very high level of component redundancy, it would be possible to ride through most faults, but the capital cost tradeoff could be high.
3. Critical equipment should be designed and specified to operate in a conservative regime (in terms of voltages, power densities, thermal management, etc.), one that is well below maximum performance limits, and should be tested to considerably higher levels than needed for operation. This will provide a long mean time between failures (MTBF), which will reduce the need for redundancy.

4. Spurious equipment shut-downs caused by sensitive noise-susceptible protection circuits can be reduced to a very low probability.
5. Diagnostics should be integrated into critical equipment that provides advance warning of end-of-life or impending failure, so that the equipment can be repaired or replaced at a scheduled maintenance time.

3.2 Injector System

3.2.1 Introduction

This section describes the H^+ injector that will be used in the ADTF facility. This injector will, with minor modifications, use the same technology as that developed for the Low-Energy Demonstration Accelerator (LEDA) of the APT Project. The LEDA injector, shown in Figure 3-3, has been successfully demonstrated for two years at proton beam outputs of up to 110 mA , with a normalized rms emittance of less than 0.2 mm-mrad. This is considerably better performance than required for ADTF, and will be suitable for an upgrade to APT performance, if needed. Injector modifications and tuning parameters will be investigated as part of the ED&D Program.

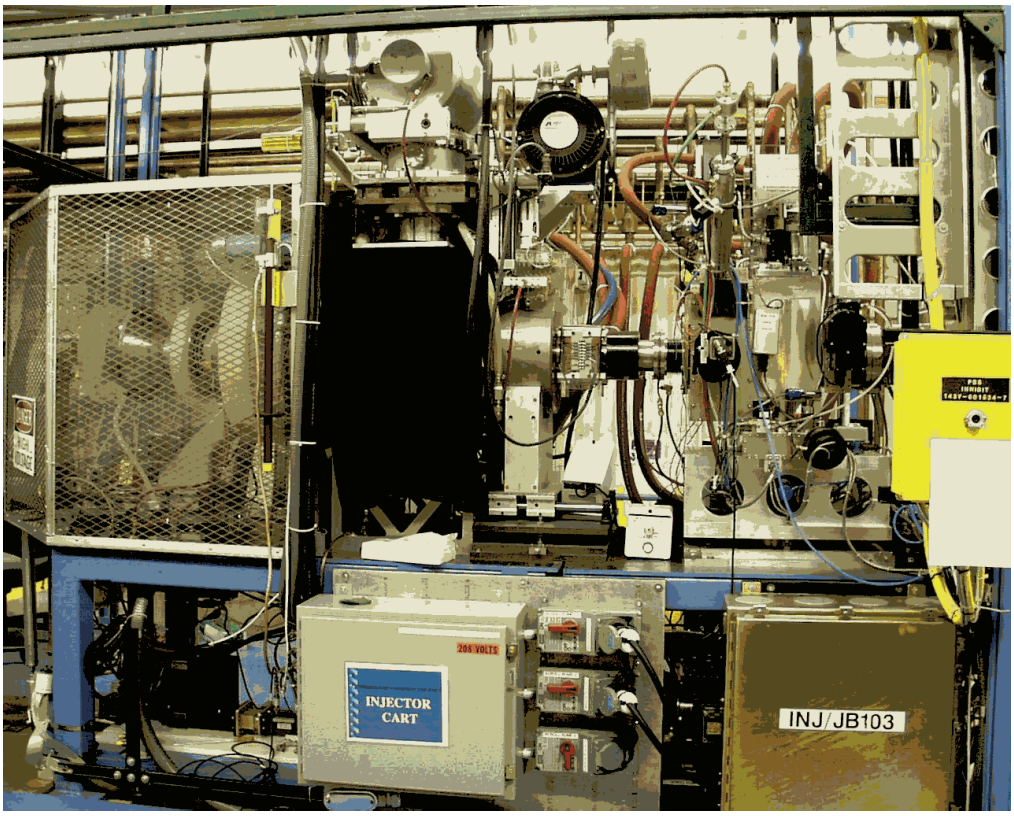

Figure 3-3. Photograph of LEDA H^+ injector including LEBT (Low-Energy Beam Transport)

3.2.2 Design Description

The injector system, shown in Figure 3-4 and described in detail in the APT document PPO-A11-G-SYD-X-00001, has three principal parts: the ion source, high-voltage ion-beam extraction system, and low-energy beam transport (LEBT). The ion source produces a hydrogen plasma in an RF discharge chamber using a low-power 2.45-GHz microwave source. The discharge chamber resides in an 875-gauss axial magnetic field, and is held at 75-kV positive potential with respect to a grounded extractor electrode. A continuous beam of protons, up to 110-mA, is drawn from the chamber by the extraction electrodes

The LEBT is a 2.8-meter-long transport section that matches the proton beam into the RFQ. Using a pair of solenoid lenses and magnetic steering elements, the LEBT focuses and transports the beam, diagnoses its characteristics, removes unwanted ions (H_2^+, H_3^+), and tailors it optically for insertion into the RFQ. High-speed vacuum pumps are attached to the LEBT to exhaust the flow of hydrogen escaping from the ion source.

The injector normally provides a continuous beam output. It must also provide low-average-current, pulsed beams for accelerator commissioning and tuning, however. Tests at LEDA have shown that the injector is capable of producing pulses suitable for RFQ acceptance as short as 100 ms. For APT, injector current was optimized for operation near 100 mA. Injector optimization for the lower currents required for the ADTF accelerator will be part of the ED&D Program.

The LEDA program demonstrated injector availability of 99% for a one-week period, which satisfies APT plant requirements. The injector reliability needed to meet ADTF beam reliability goals needs further consideration, and will be addressed during conceptual design.

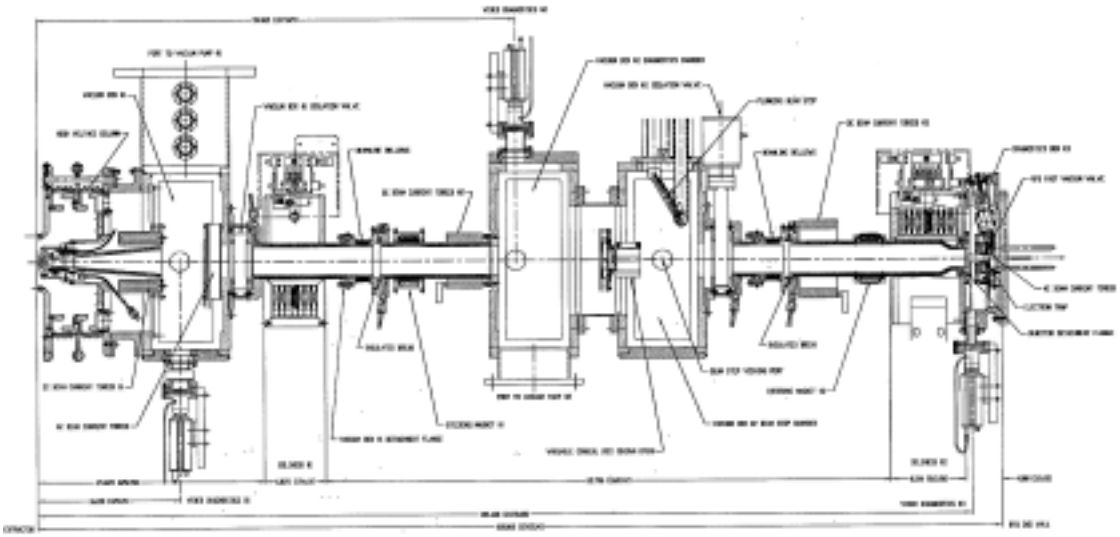

Figure 3-4. Overall layout of Injector and LEBT.

3.2.3 Beam Current Control and Safety

Control of the transmuter fission power output and safe operation of the target-multiplier assembly places significant requirements on the control of the accelerator beam current. First, the beam power delivered to the target-multiplier must be limited to a designated safe maximum. Second, the beam must be tripped very rapidly in the event of an excess-power spike, local overheating, or other problem in the target-multiplier assembly (as was designed for APT).

The target-multiplier is a driven subcritical reactor that will operate within a permitted fission power envelope. Since the fission power is proportional to the number of spallation neutrons produced by the incident beam, the linac output current needed to operate the target-multiplier within this power envelope is a function of its k_{eff}. Performance diagnostics (neutron flux, fuel and coolant temperature, etc.) will be distributed throughout the target-

multiplier assembly, providing a fast-response read-out of its specific power level. The most effective way to provide beam current control will be worked out during conceptual design, but an approach that appears straightforward would be to place a beam collimating system in the injector LEBT, backed up by precision current-measuring diagnostics in the HEBT. The multiple and independent beam-current limiting and adjustment hardware would be integrated into a safety-class system.

A hard-wired safety-class beam trip with a less than one-millisecond response time will be provided, as in APT, to abort the beam quickly in the event of off-normal conditions or malfunctions in the target-multiplier or beam delivery interface. The ultrafast beam trip can be implemented through several channels, but the simplest is by shutting off the injector. As in the case of the APT target protection arrangements, the diagnostics, beam-trip mechanisms, and HEBT/transmuter interface closures would involve a mix of safety-class and safety-significant hardware.

3.3 Low-Energy Linac System

3.3.1 Introduction

The low-energy linac system is the second section of the ADTF accelerator. The front end of the LE linac is based on LEDA (Figure 3-5). The LE Linac System accepts a continuous proton beam from the Injector, forms it into bunches, accelerates the bunched beam, and delivers it to the high-energy (HE) linac. The LE Linac consists of three different types of water-cooled copper accelerating structures, a radio-frequency quadrupole, a coupled-cavity drift tube linac, and a coupled-cavity linac. Collectively, these structures are referred to as the normal-conducting linac to reflect the fact that their internal cavity surfaces have normal, significant copper resistive losses.

The RFQ bunches the 75-keV continuous proton beam from the injector at a frequency of 350 MHz and accelerates it to an energy high enough for injection into the CCDTL. The CCDTL and CCL subsystems continue to accelerate the bunched proton beam to the energy appropriate for injection into the HE Linac System.

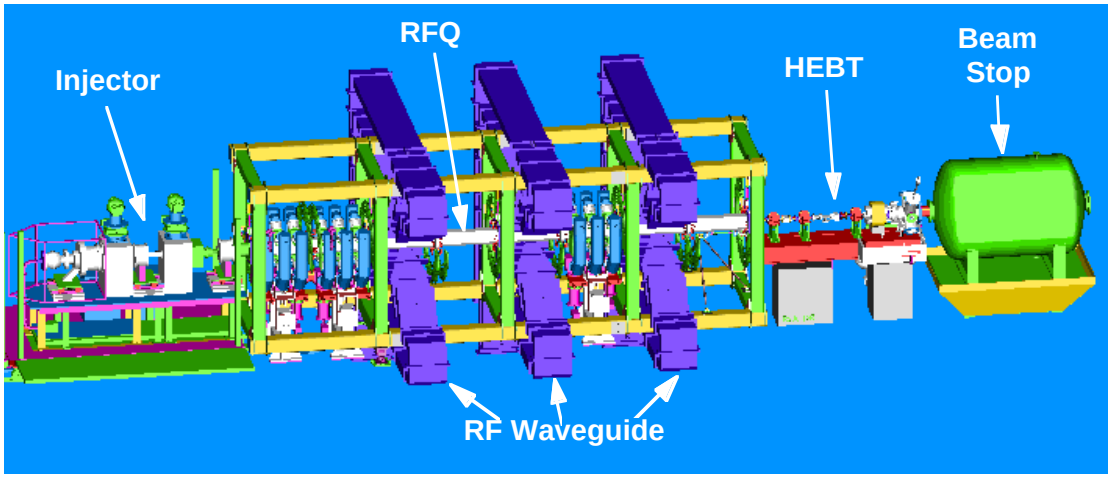

Figure 3-5. Schematic of the injector, RFQ, HEBT, and beamstop installed in LEDA.

3.3.2 Design Description

The design of the normal-conducting linac follows from the APT design and is described in detail in the LE Linac System Design Description (SDD), APT document PPO-A12-G-SYD-X-00002.

The RFQ, shown in Figure 3-6, receives the continuous stream of protons from the injector, forms it into bunches with a high capture efficiency (~95%), and then accelerates these bunches to 6.7 MeV. Operating at a frequency of 350 MHz, the RFQ consists of an 8-meter-long cylindrical resonant cavity inside which four scalloped vanes are mounted in an orthogonal array about the axis, providing the necessary RF focusing and accelerating fields. The cavity is constructed in four resonantly coupled sections. The LEDA RFQ has successfully operated at currents of up to 100 mA continuous-wave at 6.7 MeV. It is anticipated that the LEDA RFQ will require very few modifications for implementation in ADTF.

Figure 3-6. LEDA radio-frequency quadrupole.

The CCDTL accelerates its input beam to about 100 MeV. The CCDTL consists of a sequence of 700-MHz resonantly coupled short drift-tube-linac (DTL) structures embedded within a magnetic focusing lattice. Each DTL cavity contains a drift tube (and consequently two accelerating gaps), and is coupled to its neighbors by side-coupling cells, as in a CCL. The CCL consists of 700-MHz single-gap cavities appropriately coupled together into segments. Coupling the segments to each other by an Inter-Segment Coupling Cavity forms a module. The transverse focusing is provided by a FODO (focus-drift-defocus-drift) arrangement of singlet quadrupole magnets located between cavities in the CCDTL and between the segments of the CCL. Figure 3-7 sketches the transition between CCDTL and CCL accelerating structures.

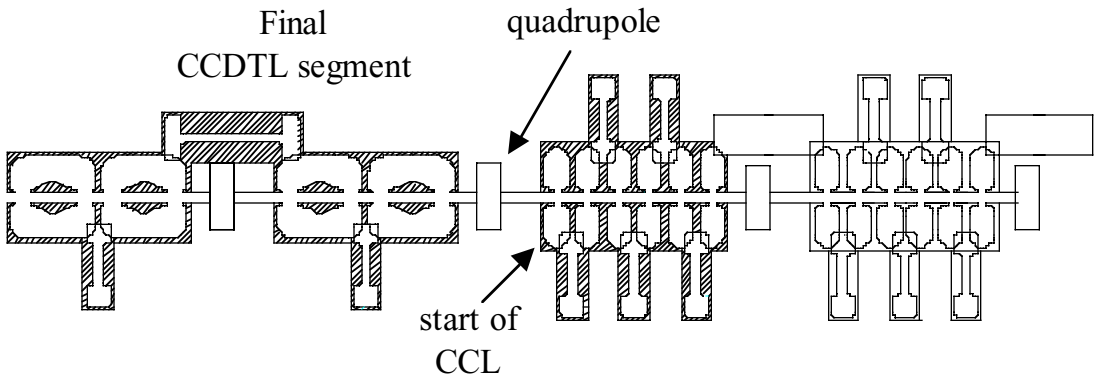

Figure 3-7. Transition from CCDTL structure to CCL at 100 MeV.

A major design challenge of this linac section for the APT Program was to accelerate the 100-mA proton beam while supplying enough transverse focusing to contain the beam (including halo) with negligible losses. Those losses, if significant, would degrade the maintainability of the accelerator by producing activation levels that limit hands-on maintenance. Beam dynamics simulations indicate that the 13.3-mA beam of the ADTF does not place a stringent requirement on the transverse focusing lattice of this part of the linac (or the following superconducting section); however, the requirement to provide for an upgrade to APT-like currents (100-mA continuous-wave) drives the design to provide a tight transverse-focusing channel similar to that in APT, with close spacing of quadrupoles, particularly in the CCDTL. Simulations carried out in the APT accelerator design have shown that an 8-$\beta\lambda$-period focusing-lattice in the LE linac limits beam losses enough to permit hands-on maintenance at currents up to 100 mA. (β is the particle velocity as a fraction of the speed of light, and λ is the free-space wavelength at 700 MHz.)

To take advantage of the design work already done for the APT linac and to accommodate the high-current upgrade path, the design of the APT CCDTL and CCL will be used as the reference basis for ADTF. Some changes in architecture may be necessary as a result of lessons learned in the APT ED&D Program and to minimize costs in the ADTF linac as initially deployed.

The overall availability requirement for the APT plant was another of the design challenges for the low-energy linac. To overcome the downtime from anticipated failures of RF stations, the CCDTL and CCL were arranged into so-called *supermodules*. A supermodule is a long, coupled accelerating structure that shares the power from several klystrons. By including one klystron more than the minimum needed to power each supermodule, the accelerator could remain online following the failure of any one klystron station. The number and size of supermodules was a trade-off among factors such as cost, fabrication practicality, and functionality. In one extreme, an extra klystron station is provided for each needed klystron station (resulting in very short modules). In the other extreme, only one extra klystron station is provided for the entire CCDTL or CCL. The first approach is very

expensive, requiring the purchase of twice as many klystron stations as the base number. The second imposes prohibitively tight tolerances on machining and brazing of the individual cavities that make up the very long, coupled resonator, as well as a large field droop between the RF feeds and the endpoints due to finite coupling. For the 100-mA APT beam, the optimum arrangement was six supermodules in the CCDTL, powered by 21 klystrons, and five supermodules in the CCL, powered by 30 klystrons.

For the 13.3-mA beam of the ADTF linac, optimization will be different. In this situation, the total RF power delivered to the LE linac is only about half of that required in the APT design. An architecture using the same kind of cost calculation used for APT would double the length of the supermodules, which is unworkable for the reasons given above. Of equal importance to availability for ADTF is the need for very high beam reliability, or the reduction of beam interrupts to a level much lower than common in existing accelerators (by factors of 10 to 100). The combination of these requirements drives the LE linac to shorter supermodules than in APT. This approach relaxes machining tolerances for the resonant cavities and has been incorporated into the revised design for the APT linac. During conceptual design for the ADTF, the optimum arrangement of LE linac modules will be determined, with the intent to simultaneously minimize the additional RF power required to support an upgrade to 100 mA for the tritium mission, should it be called for. Figure 3-8 through Figure 3-10 shows a few representative LE linac modules.

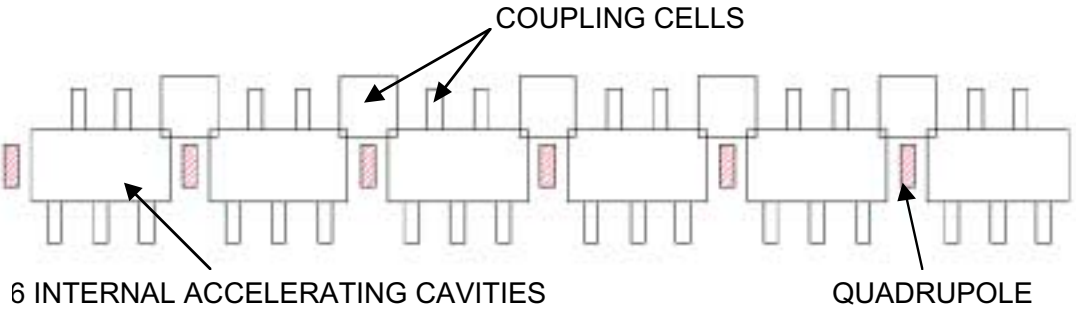

Figure 3-8. Full-length representative CCL module at 150 MeV. One klystron would power this module.

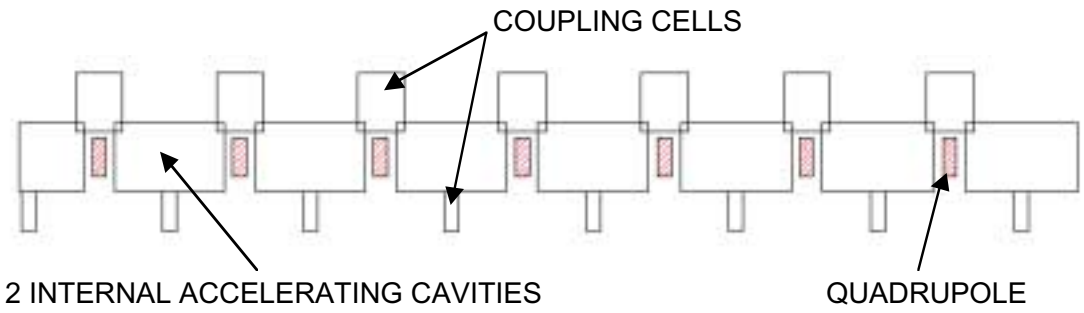

Figure 3-9. Two-thirds of a representative CCDTL module at 80 MeV. Each accelerating cavity has two gaps. One klystron would power a full module.

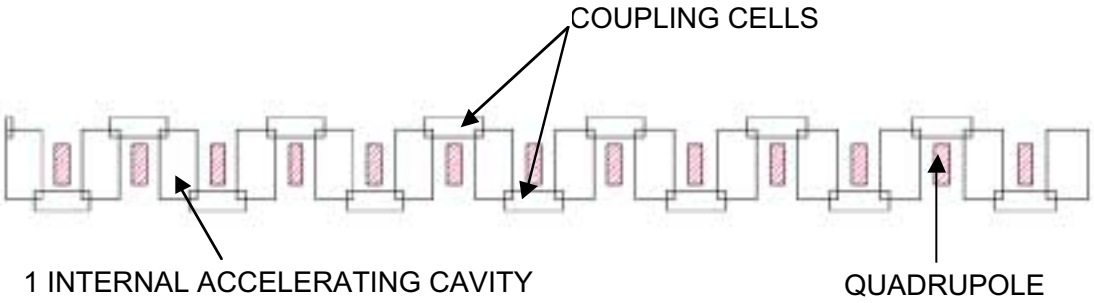

Figure 3-10. One-half of a representative CCDTL module at 30 MeV. Each accelerating cavity has 2 gaps. One klystron would power a single module. The bridge couplers required for this module are not shown.

Components integrated with the RFQ, CCDTL, and CCL needed for high-current continuous-wave proton beam acceleration are:

1. Mechanical supports on which the accelerating structures are mounted, beam-diagnostic equipment, and alignment hardware;
2. Vacuum pumping systems that provide the required vacuum level in the accelerating cavities;
3. Resonance Control Cooling Systems that remove RF heat loads from the copper accelerating structures and precisely control the cavities' temperature, thus maintaining their resonant frequency at 700 MHz;
4. Ceramic RF vacuum windows to transmit RF power from the waveguides into the accelerating cavities; and

5. Quadrupole magnets with associated power supplies for beam focusing and steering magnets for beam centering.

The design of these components has proceeded well into the preliminary design phase for the APT linac. No significant changes are foreseen for the ADTF linac. Discussions of the designs and how they meet the functions and requirements imposed by the linac system can be found in PPO-A12-G-SYD-X-00002, *Low-Energy Linac System Design Description*.

3.4 High-Energy Linac System

3.4.1 Introduction

The HE linac system is the third major section of the ADTF accelerator. The primary functions of the HE linac are to accelerate the ~200-MeV beam produced by the LE linac system to the final energy of 600 MeV and deliver that beam, within specified parameters, to the HEBT and expander system.

3.4.2 Design Description

The design of the HE linac is derived from the APT HE linac design described in PPO-A13-G-SYD-X-00003, *High-Energy Linac System Design Description*. It consists of a series of superconducting accelerating cavities arranged in cryomodules. The cavities operate at a temperature of 2.15 K. Pairs (doublets) of room-temperature quadrupoles located between cryomodules provide transverse focusing. To make a smooth transition from the FODO focusing lattice of the LE linac to the doublet lattice of the HE linac, the first set of cryomodules are shorter than those in the rest of the HE linac. This transition section has two cavities per cryomodule, while the rest of the HE linac has three. In addition to isolating the cold cavities from the ambient room temperature, each cryomodule provides the cryogenics connections and liquid helium flows to keep the cavities cold, contains a mechanical tuner to keep the cavities resonating at 700 MHz, and includes power couplers for coupling the RF power into the cavities. Figure 3-11 shows a simplified sketch of a two-cavity cryomodule, and Figure 3-12 shows an isometric cutaway view that illustrates the main design features.

The superconducting cavities consist of five connected elliptical cells that operate as a single resonator coupled together through the beam iris. The distance between cell centers is 0.64 $\beta\lambda$, the value chosen for the lower-energy portion of the APT superconducting linac. These cavities provide efficient acceleration over the energy range 200 MeV to 600 MeV in the ADTF superconducting linac. An upgrade to the APT energy of 1,030 MeV can be accomplished by adding a second superconducting linac section containing cavities with 0.82 $\beta\lambda$ cell-to-cell spacing. Cavity quality factor Q and accelerating gradient EoT were specified in the APT Program as 5×10^9 and up to 5 MV/m respectively for the $\beta = 0.64$ cavities. As part of the ED&D Program in the APT project, several five-cell cavities were built and tested to levels in excess of both these parameters. During conceptual design of the ATDF linac, we will specify the gradient-Q operating point of the superconducting cav-

ities, in light of APT test results and results from other laboratories that have built similar cavities.

RF power is electrically coupled into the superconducting cavities via coaxial antenna-type power couplers mounted in the adjacent beam tubes. Dual ceramic windows in each power coupler separate the cavities, which are under vacuum, from the atmospheric pressure in the RF distribution system (waveguides). It was planned in the APT linac design that up to 420 kW could be transmitted through each power coupler. The ED&D Program of the APT project developed such a coupler, which was tested up to 800 kW continuous-wave. Since RF cavity wall losses in the HE linac are negligible, reduction of the beam current by a factor of 7.5 (100/13.3) reduces the required RF power by the same factor. To take maximum advantage of the investment in the APT ED&D Program, and to readily provide the upgrade path to APT-like beam currents, the same coupler will be used for ADTF, however.

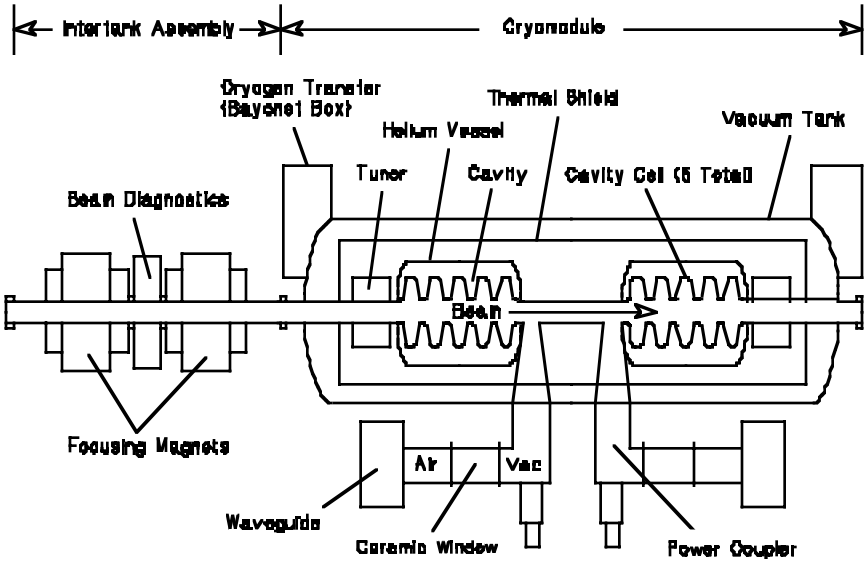

Figure 3-11. Simplified schematic in plan view of two-cavity cryomodule and its adjacent intertank quadrupole doublet assembly.

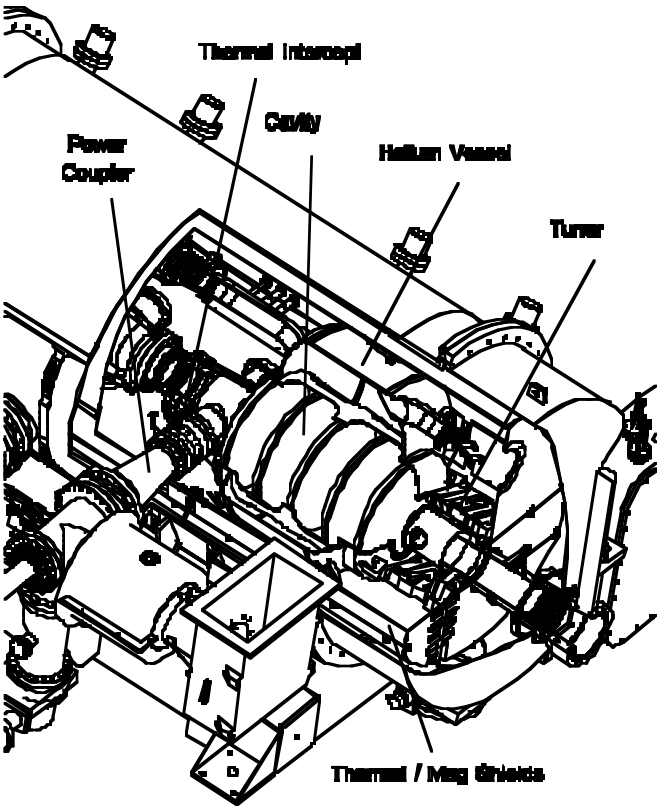

Figure 3-12. Two-cavity cryomodule isometric with shell cutaway showing internal construction.

Electromagnet quadrupole doublets, installed in the warm sections between the cryostats, provide transverse focusing of the proton beam. Prototypes of these magnets were built and successfully tested as part of the APT ED&D Program. All the quadrupoles contain dipole steering windings to correct for small beam misalignments. The intertank assemblies between cryomodules also include space for beam diagnostics and the vacuum pumping interface.

3.5 High-Energy Beam Transport, Expander System, and Beamstop

The ATDF HEBT system will be similar to the APT HEBT, which is described in PPO-A13-G-SYD-X-00003, *High-Energy Linac System Design Description*. The HEBT consists of a periodic magnetic transport line that delivers the beam from the end of the linac to either the ADTF target-multiplier assembly, a high-power tuning beamstop, or a low-power tuning beamstop. The beam expanders located at the end of the periodic lattice provide either

a large-area uniform density footprint at the spallation target or a suitable beam size for the tune-up beamstops.

The periodic HEBT focusing lattice continues the doublet-quadrupole optics in the superconducting linac to a magnet switchyard. In the switchyard the beam is directed through a nominal bend angle of 45° either to a high-power tuning beamstop that can take the full-energy beam power levels, or into the beamline serving the target-multiplier assembly, or if none of the bends are energized, to a low-power tuning beamstop in the zero-degree position. The 45° beamlines terminate in raster beam expanders, which convert the small-diameter Gaussian-like beam distribution into large-area rectangular uniform distributions at the target and beamstop. The beam expander consists of vertical-plane and horizontal-plane sweep magnets that paint the beam uniformly across the spallation target once every 30 to 100 ms. The high-power tuning beamstop will be similar to the 3.4-MW beamstop designed for APT, and is described in PPO-A13-G-SYD-X-00003, *High-Energy Linac System Design Description*.

3.5.1 Beam Expander Design Description

A high-reliability beam-rastering system suitable for expanding the 600-MeV, 13.3-mA continuous-wave proton beam onto an ADTF spallation target was developed and demonstrated for the APT Program and is described in detail in PPO-A13-G-SYD-X-00003, *High-Energy Linac System Design Description*. The APT expander concept is depicted in Figure 3-13 below. Ferrite-core magnets driven with triangular waveforms by IGBT modulators deflect the beam in the horizontal and vertical planes to produce a rectangular pattern. Four sweep magnets are used in each plane. Drive frequencies are near 500 MHz, but slightly different in the horizontal and vertical, so that a uniformly painted distribution is produced. A multiply redundant modulator fault-detector system protects the spallation target from excess beam-power density caused by degradation or interruption of the sweep pattern. These modulators are supplied by uninterruptible power sources. The magnet multiplicity limits the beam-power density increase at the target to about 33% in the event of any single-point failure.

Large-aperture quadrupole magnets focus the rastered beam through a small aperture in a downstream steel-and-concrete block that functions as a collimator (backshine shield) to minimize the flux of back-streaming neutrons from the target-multiplier assembly. After passing through this aperture, the rastered beam expands onto the target with the desired footprint dimensions.

One proposal for the ADTF beam transport requires a vertical entry into the spallation target. This introduces a vertical achromatic bend into the beam expander shown below. The design alternatives involve either introducing the bend before the raster expander or to place the bend between the raster magnets and the expander quadrupoles. Both of these approaches are straightforward and detailed studies will be performed during conceptual design.

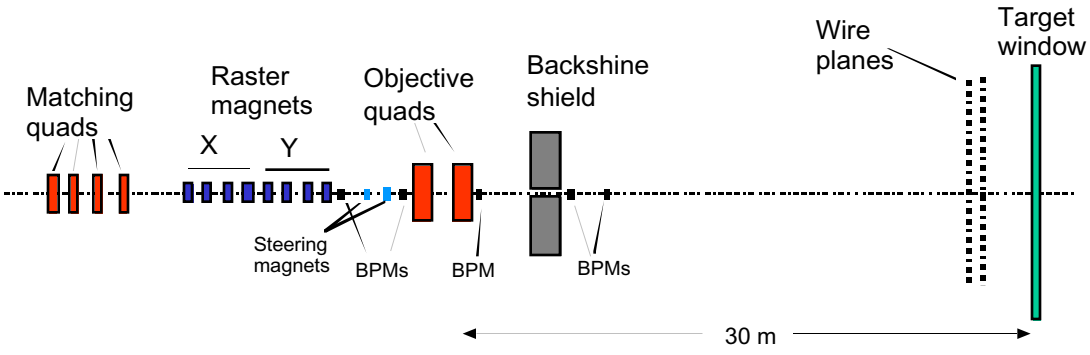

Figure 3-13. Raster beam expander concept.

Collimators with adjustable apertures are placed near the downstream end of the HEBT to intercept any beam halo. Beam losses and the resultant activation are localized in these collimators, which are surrounded by shielding. Remote-handling will be necessary in this area. With the exception of these collimators, remote maintenance is not expected to be necessary in the HEBT.

3.5.2 High-Energy Beam Transport

The ADTF beam-transport configuration, shown conceptually in Figure 3-14, will be similar to that of the APT HEBT. A doublet focusing lattice, with the same period length as in the superconducing linac, transports the beam to a switchyard where it can be directed around an achromatic 45° bend to the high-power beamstop, directed around a similar bend into the channel serving the target-multiplier, or proceed straight ahead to a low-power tuning beamstop. The functions and capabilities of these beamstops are described below in Section 3.5.3. Both bends use the same doublet-focusing period as in the straight sections of the transport system.

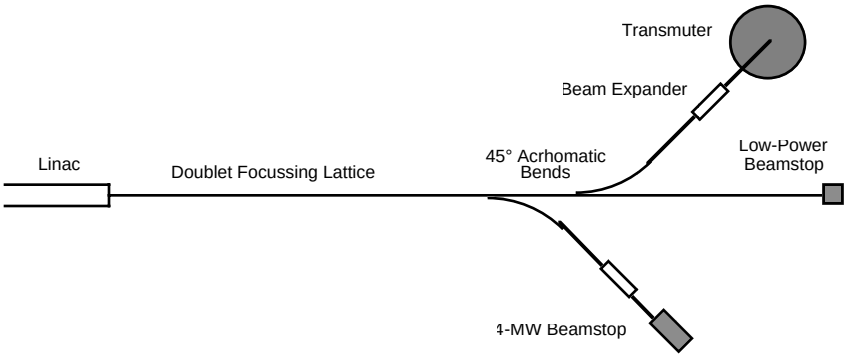

Figure 3-14. Concept of ADTF high-energy beam-transport system.

3.5.3 Beamstops

There will be two beamstops in the ADTF HEBT. A low-average-power beamstop will be installed at 0°downstream from the switchyard. It will have the capability to absorb approximately 1% of the maximum beam power, or about 100 kW, and allow accelerator tuning to be carried out at low duty factors, with short pulses and low repetition rates. For example, it would permit full-peak-power beam tune-up with 1-millisecond-long pulses at rates up to 10 Hz. This beamstop will be used for initial commissioning studies of the linac, and also to support restoration of normal beam operation following a fault.

A high-power beamstop, with a design similar to the beamstop for APT, will be located at the end of the upstream beam-channel that branches from the HEBT switchyard (see Figure 3-1). This beamstop will have the capability of absorbing a large fraction of the maximum linac beam power and will enable accelerator tuning to be carried out under continuous-wave high-power conditions, an essential prerequisite for establishing a reliable beam for the target-multiplier assembly. This beamstop will allow the linac to be fully commissioned well before the target-multiplier installation is completed. It also will provide for continuous-wave accelerator start-up and tuning while maintenance or refueling operations are taking place in the target-multiplier assembly. A raster beam-expander at the end of the channel provides a relatively low-power density for this beamstop.

The high-power beamstop designed for the APT is constructed from graphite modules, as shown in Figure 3-15. The modules are cooled by helium passing through a series of slots running transverse to the beam. The slot widths and spacings were set to maintain a maximum graphite temperature of 930°C. The beamstop modules are mounted inside an aluminum cylindrical vessel 1.8 meters in diameter. Fitted graphite blocks occupy the space between the beamstop modules and the vessel. Commercially available water-cooled panels are attached to the inner surface of the vessel to absorb heat transferred from the beamstop graphite absorber modules through these blocks

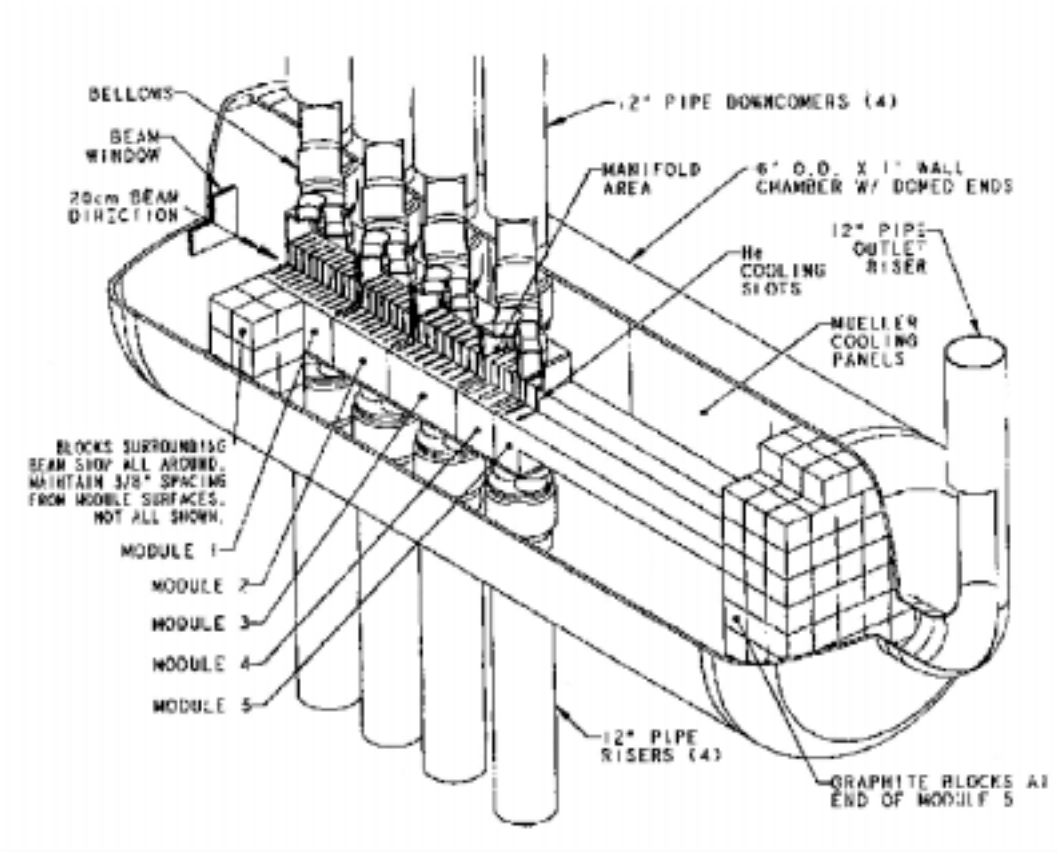

Figure 3-15. High-energy beamstop vessel layout.

The shielding requirements, atmosphere, enclosure method, and shielding cooling requirements for the ADTF high- power full-energy beamstop will be developed during conceptual and preliminary design.

3.6 Beam Simulations and Dynamics

The primary beam-dynamics goal is to achieve very low losses to assure unrestricted hands on maintenance for the linac. This is realized through a design concept that provides a tight focusing lattice to control space-charge-induced emittance growth and halo formation at low energies and apertures that are much larger than the rms beam size at high energies, where the activation threat is greatest. The ADTF beam-dynamics design follows from the APT design, which is described in detail in PPO-P00-N-TRT-X-00163, *APT Beam Dynamics*. This section describes the general beam-dynamics design issues, including beam-halo generation and beam loss, and shows the beam-dynamics simulation results. The linac design successfully addresses the beam-dynamics objectives for APT and ADTF.

3.6.1 Beam Dynamics Design Issues

The primary objective of the beam-dynamics design for the LE linac is to deliver a high-quality (i.e., low-emittance) beam at to the HE linac. This is achieved by providing strong focusing and avoiding abrupt focusing transitions that could produce beam mismatch and beam halo. The primary beam-dynamics objective of the high-energy linac is to accelerate the beam to full energy while controlling losses to low values to permit hands-on maintenance. These objectives are accomplished through smooth changes in transverse and longitudinal focusing, avoidance of mismatches so that beam halo formation is minimized, and use of a large cavity aperture relative to beam size.

The beam-dynamics advantages of the superconducting high-energy linac, compared with a normal-conducting linac, are that the superconducting structures have a much larger bore diameter, higher accelerating gradient, and considerably more flexibility in operation. The large bore diameter minimizes the risk of beam loss (and consequent activation of the accelerator) and relaxes alignment, steering, and focusing requirements. The low beam-loss makes the linac easier to commission and operate with the high-power beam. Limiting the number of cells per cavity to the small number of five, and the number of cavities per RF drive to two or three provides advantages for operational flexibility. Together with the large bore radius, these features allow continued operation in a variety of off-normal or fault conditions. Normal conducting quadrupoles are installed in the warm spaces between the cryomodules to provide a periodic doublet lattice. Steering windings are incorporated in every quadrupole magnet to correct the beam transverse position in the presence of alignment errors. Beam matching is provided between sections where the focusing period changes.

In the 100-mA APT design, beam-induced wakefields associated with excitation of higher-order modes in the superconducting cavities have a perturbing effect on the beam that is ten times smaller than the applied accelerating fields in the cavities. These effects are much smaller than the effects of field errors. The beam power transferred to the wakefields represents additional power dissipation, through ohmic losses in either the structure walls or a load. The wakefields add a small amount to the refrigeration load in a superconducting linac. Based on calculations for APT, wakefields are not a concern for ADTF, given the lower current.

3.6.2 Beam Halo Formation and Beam Losses

The ADTF beam-loss objective is to restrict losses to levels that will allow unconstrained hands-on maintenance throughout the linac. This supports high availability for the facility. The specific goal, based on the 800-MeV LANSCE (Los Alamos Neutron Science Centre) linac operating experience and beam-loss/activation correlations, is a loss rate of less than 0.2 nA/m at 600 MeV; higher losses would be acceptable at lower energies. The very large apertures of the superconducting linac provide high confidence in the ability to achieve this goal.

The principal halo-formation mechanism for ADTF is a resonant interaction between particles in the beam fringes and the space-charge field of the beam core that is oscillating

because of mismatch. Modeling and simulations have shown that these phase-space mismatches (and nonlinear space-charge forces) are the main factors leading to beam-halo growth. The critical region for halo formation is the low-energy portion of the accelerator where the space-charge forces are high and the beam is more sensitive to mismatches. Multi-particle beam-dynamics simulations done for APT and described in the next section show that the beam halo produced by the small mismatches that exist in an *as-built* linac produce no significant beam loss above 20 MeV.

3.6.3 Effects of Random Linac Imperfections

Unavoidable small and random imperfections, each of which contributes a small phase-space mismatch, can cause beam halo growth in a linac. The mismatch is distributed along the machine rather than being concentrated only at a few transitions. A multi-particle beam-dynamics simulation code modeling the linac randomly distributes the machine parameter errors within specified tolerances. Calculations with this code are used to make predictions of the resulting beam transverse density distribution along the machine, including the halo. APT beam-dynamics simulation results at 100 mA are summarized in Figure 3-16.

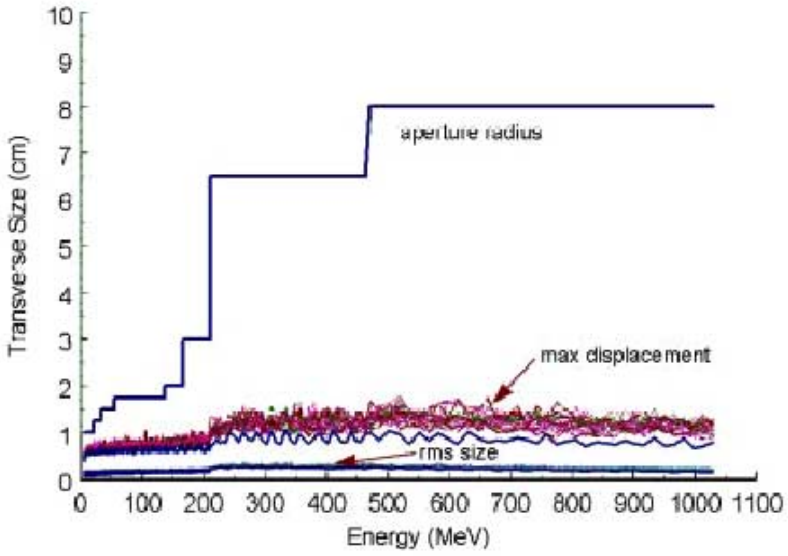

Figure 3-16. Transverse rms beam size, maximum particle displacement, and aperture radius vs. beam energy in APT linac from 30 simulation runs with 100,000 macroparticles per run and different random errors based on using the full error set.

Using 30 simulations with different conservatively chosen random error sets and with 100,000 macroparticles per run, no particle loss was observed above 20 MeV. The result

is a beam-loss upper bound of 0.05 nA/m anywhere in the linac above this energy, which is well below the ADTF design goal. In these simulations, five particles were lost after the RFQ and below 20 MeV. This loss rate is estimated to result in a very low and acceptable dose rate of < 1 mrem/hr along that part of the LE linac, after the beam is turned off. These simulations thus support the conclusion that the APT design meets the requirements for low beam loss and hands-on maintenance. Because of the nearly identical APT and ADTF linac designs, and because the ADTF beam current is only a fraction of the APT beam current, the risk of beam loss for ADTF is much less than that estimated for APT.

3.7 RF Power System

3.7.1 Design Description

The primary function of the RF power system is to provide and regulate the electromagnetic fields in the ADTF linac accelerating cavities. The RF power system receives electric power in the form of alternating current from the main power supply system, rectifies and conditions the power to dc, converts the dc power to RF power, and transmits the RF power to the ADTF accelerating structures at 350 MHz for the RFQ and at 700 MHZ for the rest of the linac. For the high beam current of the APT linac, 1-MW klystrons were the appropriate choice for all 700-MHz power. In the LE linac, RF dissipation in the copper structures is the same as in APT and dominates the power demand, so even with the much lower beam current, the total power requirement per unit length of structure is only reduced to about half of the APT value. So as in APT, 1-MW klystrons appear to be the correct choice for this part of the ADTF linac. In contrast, in the HE linac where cavity losses are negligible, RF power requirements of each cryomodule are reduced in proportion to the lower beam current. This results in a dramatic reduction in the required RF power; a different approach is required for the ADTF HE linac RF configuration, both in terms of numbers of cavities per generator and choice of generator. A possible RF configuration would be to drive all the cavities within one cryomodule using a single medium-power klystron, as shown schematically in Figure 3-17; an alternative would be to provide each cavity with its own RF drive, as sketched in Figure 3-18. Commercially available inductive output tubes (IOTs) used in the television broadcast industry do not quite produce the power required for a single superconducting cavity, but may be technologically within reach. Low-power klystrons are also an option. During conceptual design, trade studies will determine the best configuration of RF generators and distribution for the entire linac.

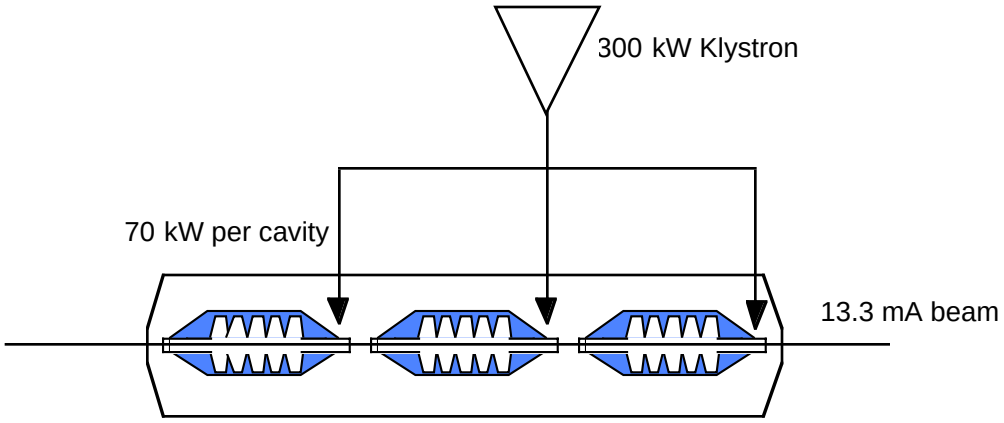

Figure 3-17. RF configuration with single klystron driving all cavities in cryomodule.

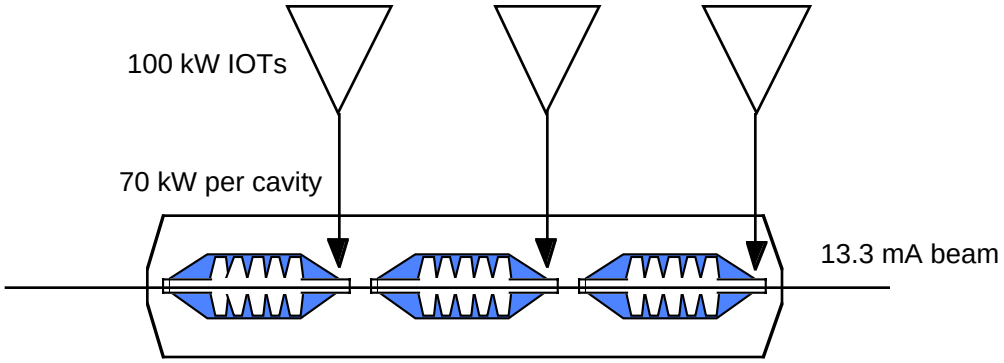

Figure 3-18. RF configuration with each cavity driven by its own IOT.

A simplified schematic of an RF station layout is shown in Figure 3-19. RF system controls have been developed for the LEDA RFQ in the APT Program. Those controls are applicable to the corresponding system in the ADTF. That system controls three 350-MHz klystrons as a single RF power source, so nested control loops are employed. The ADTF will take advantage of the lessons learned at LEDA in the design of the low-level radio-frequency for the RFQ. Depending on the degree of modularity chosen for the LE linac (see Section 3.3), this approach may not be needed in the rest of the linac.

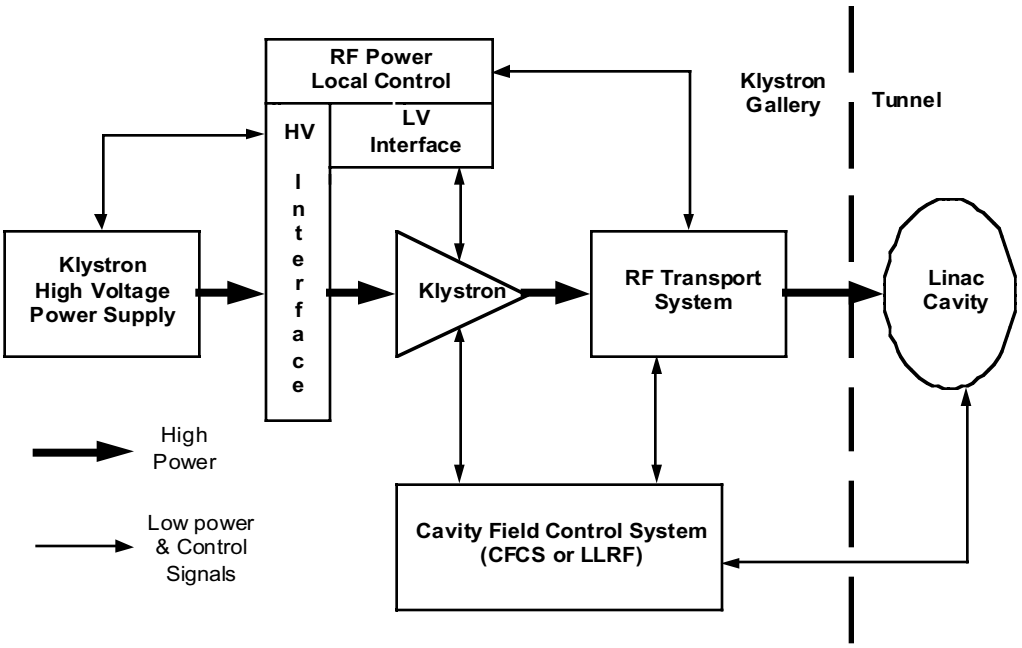

Figure 3-19. Typical RF power station.

3.7.2 RF Architecture for the Linac System

The RF system architecture for the ADTF is based on that developed for the APT accelerator. RF power generators are housed in the Klystron Gallery adjacent to and above the linac tunnel, and a system of resistive loads and circulators isolate and protect the generators from reflected power. The RF supply architecture for the APT $\beta = 0.64$ superconducting cryomodules is shown in Figure 3-20, where one 1-MW klystron feeds three cavities. The figure depicts the relationship between the principal system components: the klystron, circulator, power splitters, switches, resistive loads, and power couplers. In the ADTF linac, only one power coupler per cavity will be needed for a 13.3-mA beam.

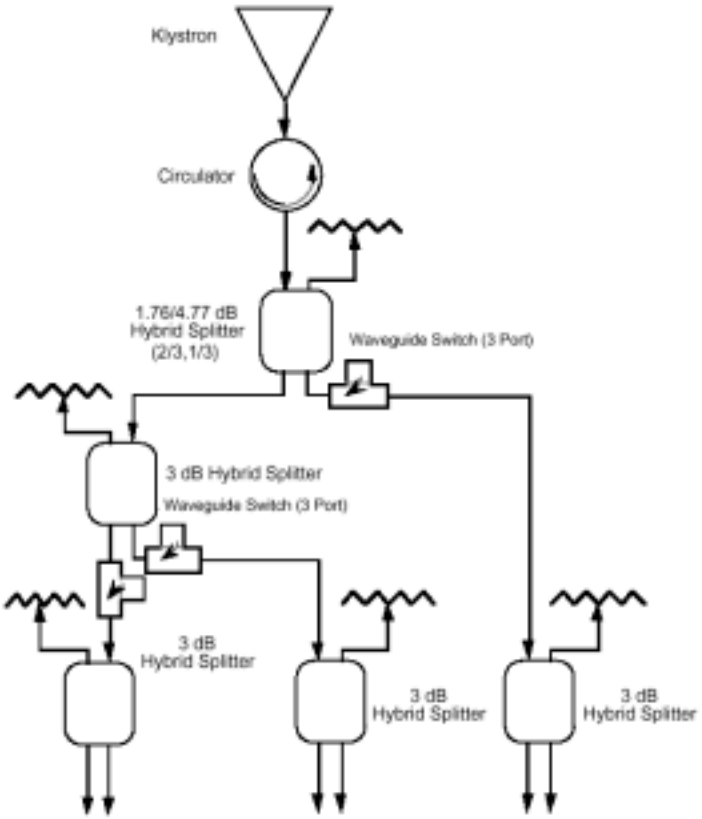

Figure 3-20. RF architecture for APT three-cavity $\beta = 0.64$ cryomodule.

In the APT accelerator design, described in detail in PPO-A21-G-SYD-X-00005, *Radio-Frequency Power*, beam availability requirements led to implementation of the supermodule concept. The normal-conducting modules 2 through 11 of the linac were grouped into modules driven by multiple klystrons. The reduced beam current of the ADTF linac makes this architecture less attractive as a means to achieve the availability required. One option is to install *hot spares* in the Klystron Gallery, which are ready to be switched into service in the event of a failed klystron. This option, as well as others, will be assessed with respect to availability and cost during conceptual design.

The superconducting portion of the linac overcomes potential availability and/or reliability limitations in a different way. Because individual RF generators drive cavities or cryomodules, the phase and amplitude of the power to each one can be independently adjusted to accommodate changing beam conditions; therefore, in the event of a failure of an RF station, cavity, or cryomodule, the power from downstream RF generators can be increased to accommodate the failed cryomodule by adjusting amplitude and phase, thus restoring the specified output beam energy.

3.8 Cryogenic System

3.8.1 Introduction

The ADTF cryogenic system supplies the necessary cryogenic fluids for maintaining the high-energy linac cryomodules at the correct operating temperature. The cryogenic system provides 2.15 K superfluid helium for the superconducting cavities and 4.5 K to 55 K helium in the supercritical state for thermal shielding and power-coupler cooling. Preliminary calculations give an ADTF cryogenic system that has one-third the capacity of the APT cryogenic system. The APT facility is depicted in Figure 3-21.

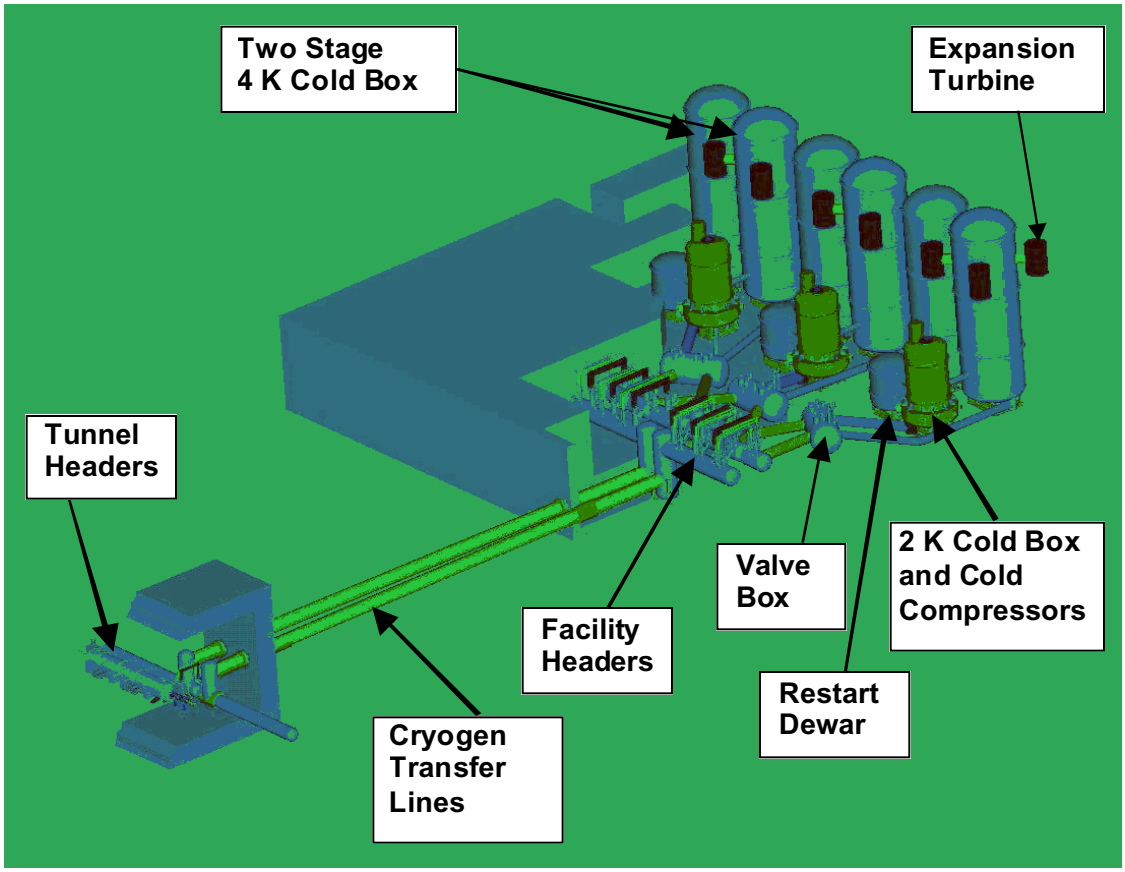

Figure 3-21. APT cryogenic system isometric showing three interconnected cryoplants. Two cryoplants can provide the necessary cold helium for the APT linac. Having a third cryoplant provides redundancy to meet the APT plant availability requirement.

3.8.2 Design Description

The ADTF Cryogenic System will follow the design developed for the APT plant. The general configuration of that system is described in PPO-A22-G-SYD-X-00006, *Cryogenics*, and is presented in detail in PPO-A22-G-TS-X-00011, *APT Cryogenic System Configuration Optimization Trade Study*. The basic configuration of a single APT cryoplant includes a 4.5 K cold box with associated warm helium compressors, a 2-K cold box that contains the subatmospheric cold compressors, a restart dewar to facilitate rapid recovery from a system upset, and associated controls and support systems. While three such plants were envisioned for the APT linac, only one is needed for the lower energy of the ADTF machine. The cryoplant interfaces to the linac through a supply return transfer line system.

Steady-state operation is the common mode for nominal support of the linac when all the HE linac cavities are powered and the beam is on. The performance characteristics associated with this mode are presented in Table 3-1. The table assumes that the cryomodules operate at the APT-specified operating point of $Q = 5 \times 10^9$ and $E_{acc} = 5$ MV/m. These parameters may be modified during conceptual design, affecting the size of the cryoplant.

Table 3-1. ADTF Cryogenic System Performance Requirements: RF ON

Flow Circuit	Temperature (K)	Heat Load (kWatts)	Mass Flow (gram/sec)	Supply Pressure (atm)	Return Pressure (atm)	Imput Power (MWatts)
2K Circuit	2.15	7.3	206	3	0.0465	6
Power Coupler and Shields	4.6	32.7	105	18	(up to 17)	1.9
Note: Input power does not include additional power required for auxiliary systems (I.e. vacuum pumps, recovery compresors, return heaters, cold compressor motors an bearings, etc.)					**Total Power (MW)**	**7.9**

Reduced capacity operation, as is shown in Table 3-2, will occur when the HE linac is not fully powered; for example, when tuning the LE linac or for maintenance of any part of the facility. The performance characteristics of the cryoplant will vary depending on the situation; however, the cold compressors are only capable of 40% maximum turndown. Lower RF loads can be accommodated by using the cryomodule control heaters. The 2-K refrigeration power will be reduced by lowering the mass flow and speed through the cold compressors, while 4.5 K cold box performance is reduced by throttling down the expansion turbines and reducing the discharge pressure on the second-stage warm helium compressors.

Table 3-2. ADTF Cryogenic System Performance Requirements: RF OFF

Flow Circuit	Temperature (K)	Heat Load (kWatts)	Mass Flow (gram/sec)	Supply Pressure (atm)	Return Pressure (atm)	Input Power (MWatts)
2K Circuit	2.15	4.9	124	3	0.0465	3.7
Power Coupler and Shields	4.6	23.4	60	18	(up to 17)	1.2
Note: Input power does not include additional power required for auxiliary systems (I.e. vacuum pumps, recovery compresors, return heaters, cold compressor motors an bearings, etc.)					**Total Power (MW)**	**4.9**

3.9 Accelerator Support Systems

3.9.1 Beam Diagnostics

The ADTF linac beam diagnostics provides information on various beam properties to the I&C system so that the machine may be operated properly over a range of normal and off-normal conditions. The two types of beam diagnostics are (1) characterization diagnostics and (2) operational diagnostics. All beam diagnostics will be designed for high reliability. Also, each kind of beam measurement will incorporate a calibration method that can be accessed from the accelerator control room.

Operational (or permanent) diagnostics provide a subset of beam information using non-interceptive or minimally interceptive techniques. The average continuous-wave beam-power density in the ADTF linac will vary from kilowatts per square centimeter to over a million kilowatts per square centimeter. Operational diagnostics must be designed to operate throughout this range under a variety of continuous-wave and pulsed beam conditions. The bulk of the diagnostic devices in the linac will be of the operational type. These include beam position monitors, capacitive probes to measure bunch phase and energy, and ionization chambers to measure beam loss. A multi-plane harp placed upstream of the spallation target window will also provide beam shape and power-distribution monitoring and feedback to assure the proper behavior of the expanded beam. At low energy there are also video-profile monitors and flying wires for measuring transverse beam positions and profiles. The remaining devices are graphite jaws for measuring beam halos, beam transformers (toroids) for measuring pulsed and dc beam currents, and special capacitive probes for measuring the bunched-beam phase spread.

Characterization diagnostics are used during accelerator commissioning and restarts where significant tuning of the linac is required. Characterization diagnostics more fully measure the six dimensions of beam-phase space, but at the cost of intercepting the beam. Because of the very high power density in the beam at continuous-wave conditions, intercepting diagnostics are designed to function only at low duty factors. In the low-energy part of the linac, characterization diagnostics include Faraday cups, view screens, and segmented collimators. In the high-energy linac wire scanners will measure beam profiles and positions.

3.9.1.1 Transverse Measurements

Beam position measurements are made by four-element stripline Beam Position Monitors (BPMs) inserted in the beamline. The striplines pick up signals from induced image currents. These signals and their ratios are used to determine the transverse offset of the beam centroid. Signal strengths are in proportion to the distance between the beam centroid and each BPM element; equal-strength signals indicate a centered beam, and unequal signals indicate an off-center beam and the amount of offset.

3.9.1.2 Beam Intensity Profiles

Beam intensity profiles are used to calculate the rms emittance and the Courant-Snyder parameters for both the horizontal and vertical axes. Standard wire scanners are used during commissioning and restarts. For normal operations above 100 MeV, a flying-wire measurement will acquire the beam profiles. For energies below 100 MeV, the energy deposited in the flying wire raises its temperature above a practical limit, and, therefore, another beam profile measurement method is required. For the lower energies, video profile monitors observe fluorescence from beam ionization of low-pressure gas that is admitted into the beam vacuum. A third beam-profile method, Residual Gas Ionization Proportional Monitor (RGIPM), is being considered for operational use in the HEBT. The RGIPM collects the electrons that are freed when the passing beam ionizes the residual gas in the beamline vacuum. However, the RGIPM needs development and beam testing in the Accelerator ED&D Program.

3.9.1.3 Beam Loss Measurements

Detection of small beam losses along the ADTF accelerator using beam-loss monitors (BLMs) provides key information that the operators use in achieving and maintaining a correct linac tune. BLMs are typically simple gas-filled ionization chambers placed near the beamline that sense lost beam particles through the ionizing radiation produced by them. The BLMs continuously monitor accelerator loss levels, and provide early warning of changes in parameters that might need readjustment. If a component failure causes a sudden increase in beam loss that could threaten the integrity of downstream structures, nearby BPMs also react within microseconds and feed signals to the Fast Protect system that aborts the beam at the injector before damage can occur.

3.9.1.4 Beam Current Measurements

Both pulsed and direct current measurements are located at the beginning of each ADTF accelerator section (CCDTL, CCL, two-cavity cryomodule sections, and three-cavity cryomodule sections in the high-energy linac and HEBT. Such placement allows the beam transmission through each major section of the accelerator and transport system to be determined.

3.9.1.5 Energy, Phase, and Longitudinal Phase Space Measurements

To properly tune the CCDTL and CCL accelerating cavities, measurements must be made throughout the linac on both the beam energy and phase relative to the 700-MHz RF accelerating field. The energy measurement is accomplished by performing a time-of-flight measurement using signals from two cylindrical capacitive probes separated by an appropriate drift distance.

The beam momentum spread is an important parameter for ascertaining the proper operation of the accelerator and is determined from measurements of the phase spread or bunch length. Phase-spread measurements employ specially designed probes much like the capacitive probes used for the beam-energy measurements, but with bandwidths greater than 10 GHz, to measure the Fourier harmonic content of the wall (image) currents produced by the bunches. This parameter is also determined by measuring the beam width in the bending plane at a high-dispersion region of the HEBT.

3.9.2 Vacuum Systems

Vacuum system designs for the ADTF accelerator will be taken from the design work done for the APT project. The Injector and RFQ vacuum systems have been built for LEDA, and design modifications for the APT plant have been proposed and accepted. Vacuum systems for other parts of the linac are at the preliminary design stage, with extensive modeling and costing completed. The vacuum requirements and design solutions are driven not so much by the beam current as by the required performance (accelerating fields, reliability, maintainability, etc.), so they will be directly applicable to the ADTF accelerator. Descriptions of those designs can be found in the SDDs referenced in the preceding sections. A variety of vacuum pumping systems are used: cryopumps for the RFQ; ion pumps for the CCDTL, CCL, and beamlines; and turbomolecular pumps for the ion source, cryostats, and superconducting cavities. Because of the very low temperature of the superconducting cavity surfaces (2.15 K), the cryomodules themselves provide nearly the entire vacuum pumping in the HE linac during operation.

3.9.3 Water Cooling and Resonance Control

The copper accelerating structures in the LE Linac require removal of substantial heat created by RF power losses in the copper-cavity walls, which is accomplished by high-flow-rate water cooling systems. These cooling systems are also used to control the precise temperature profile of each of the accelerating structures, and therefore their dimensions and resonant frequency. Temperature control and cooling are provided by Resonance Control Cooling Systems (RCCS). These are primary cooling loops that incorporate an ensemble of mixing valves, pumps, and feedback loops that maintain tight regulation of the accelerating structure temperatures. Each module of accelerating section in the LE linac has one RCCS unit. Each RCCS is coupled to the low-level RF feedback system for that accelerating section. The RCCSs have been modeled and designed for the APT linac, and those designs will be directly applicable to the ADTF accelerator.

Resonance control for the superconducting cavities in the HE linac is accomplished by mechanically deforming the cavities. The mechanical tuner developed by the ED&D Program of the APT Project will be used in the ADTF cryomodules.

3.10 Accelerator ED&D Program

A focused ED&D Program will demonstrate and prototype key components and systems that support the ADTF linac design. The program will be described in detail in a Core Technology Plan and will be integrated with the accelerator Preliminary and Final Design through a set of Design Data Needs. The ADTF Accelerator ED&D effort will be built on the achievements of the APT Accelerator ED&D Program, will continue that program to meet the requirements of the ADTF linac design, and will address new issues relevant to the ADTF accelerator.

While the ADTF accelerator concept has benefited greatly from the work accomplished within the APT ED&D Program, several key elements of that program need to reach completion to provide full support for Preliminary and Final Design. Since the APT design was initiated, significant advances have been made in a number of technology areas that could yield important performance and cost benefits. The ADTF linac also has new performance requirements in the areas of beam reliability and beam sharing that call for development and prototyping not addressed in the APT Program. The required beam reliability can be attained through the accelerator design approaches described in Section 3.7.2, which need to be backed up by a strong ED&D Program.

The APT Accelerator ED&D Program base, from which the ADTF ED&D Program will evolve, consists of three main areas: Low Energy Demonstration Accelerator (LEDA), Superconducting RF, and Other Linac ED&D.

3.10.1 Low-Energy Demonstration Accelerator

3.10.1.1 Introduction

The Low-Energy Demonstration Accelerator (LEDA), shown schematically in Figure 3-5, prototypes the front end of a 100-mA continuous-wave proton linac, including the first three accelerating structures (Injector, RFQ, and CCDTL) the high-power RF systems, and all the support systems, including beam diagnostics, instrumentation and controls, resonance-control water cooling, and vacuum systems. The purpose of LEDA is to confirm beam performance parameters, demonstrate integrated operation at full continuous-wave power, assess overall availability, and identify component failure mechanisms.

3.10.1.2 LEDA ED&D Description

The continued operation of the LEDA accelerator will enable confirmation of designs for ADTF components, reduce risks, and minimize program delays. In particular, LEDA can be used to test and refine prototype components and subsystems, and qualify major components before incorporating into the ADTF design. LEDA will be used to define

commissioning approaches and refine operational procedures for the ADTF linac, and also to provide early operator training. Finally and importantly, LEDA will be used to address some of the beam reliability issues for the ADTF accelerator by determining systems that cause beam interrupts, devising improvements to the most troublesome systems, and testing the improved systems to demonstrate reduced beam trip rates and shortened recovery times.

In the APT Program, the LEDA program would have terminated with the addition of a 600-keV section of CCDTL to the RFQ, bringing the final energy to 7.3 MeV. To support the ADTF Low-Energy Linac reference design, additional CCDTL sections may be tested on LEDA. LEDA could also carry out beam tests of low-β superconducting accelerating structures (discussed below) that are seen as potential alternatives to normal-conducting structures in the Low-Energy Linac.

3.10.2 Superconducting Radio-Frequency

The APT SCRF ED&D Program has been aimed at demonstrating and prototyping the superconducting accelerator technology underpinning the linac design. The program has built and tested five-cell, medium-β elliptical superconducting cavities to beyond the APT performance specifications (Gradient = 5 MV/m and Q = 5×10^9), and high-power coupler/window units for transmitting RF power to the superconducting cavities that have been tested to 1 MW continuous-wave. Cavity test program results are shown in Figure 3-22 below. The final stage of the APT SCRF program was to design, build, and test a complete prototype of a two-cavity medium-β cryomodule. The design has been completed, and much of the procurement has been done. Clean room and processing facilities have been installed at Los Alamos in preparation for assembly of the cryomodule.

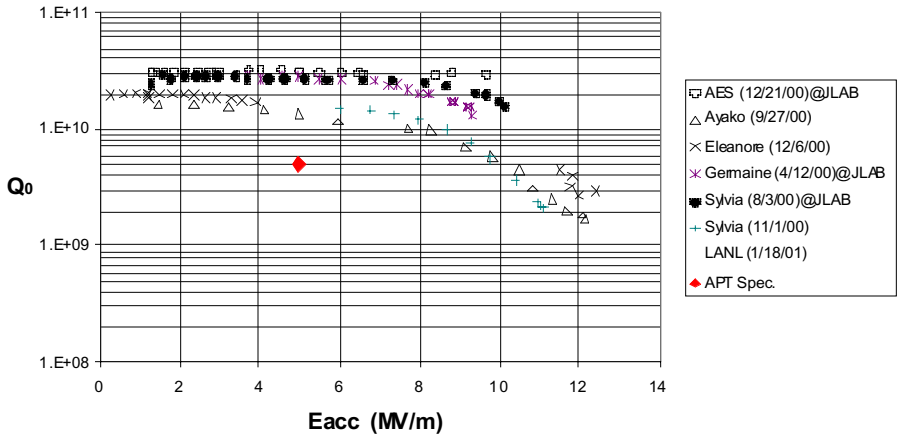

Figure 3-22. Results from recent APT five-cell β = 0.64 cavity tests; red diamond is APT design specification.

3.10.2.1 Superconducting Elliptical Cavities

High-gradient testing of existing five-cell cavities will be continued to confirm the ADTF cavity operating parameters to provide a lower cost and shorter high-energy accelerator. Currently, the target values are E0T = 9.5 MV/m (compared to 5 MV/m for APT) and $Q = 5 \times 10^9$. Cavity cleaning and processing procedures to ensure consistent cavity performance reproducibility may be refined.

Beta = 0.5 elliptical-cavity cryomodules could replace the CCL in the region 100 MeV to 200 MeV. These would be a relatively straightforward extension of elliptical-cavity superconducting technology at higher beta values. To support the design of an alternate superconducting linac section that could replace this linac segment in the reference ADTF Low-Energy Linac, multi-cell $\beta = 0.5$ cavities would be built and tested to confirm performance.

Significant effort has been invested in the two-cavity, $\beta = 0.64$ cryomodule prototype. Completion and testing with RF power would confirm design parameters, thermal loads for the cryogenics system, component integration, and constructability.

3.10.2.2 Superconducting Spoke Resonators

As discussed in Section 3.1, the ADTF linac must satisfy a stringent requirement on beam reliability. The high-energy portion of the ADTF linac, the superconducting section, is designed using very short accelerating structures, driven individually or in small groups. With the failure of a cavity or its RF drive, the phases and RF amplitudes of the nearby cavities can be rapidly adjusted to make up the beam-energy deficit. This design approach addresses reliability and availability requirements for the high-energy linac. As discussed in Section 3.2.2, reliability and availability in the low-energy linac have been addressed through redundancy in the RF drive system.

As is implied in Section 3.10.1.2, the prototype CCDTL cavities have not yet been tested with full continuous-wave RF power, nor have they been integrated with LEDA and operated with beam. While there is high confidence that those tests will be positive, other accelerating structures for the ADTF low-energy linac are being studied. So-called *spoke resonator* cavities (Figure 3-23) are short superconducting RF structures suited to the energy region below 100 MeV that may be applicable to the needs of the ADTF. These structures have been developed in recent years at Argonne National Laboratory for the proposed Rare Isotope Accelerator (RIA) project. Similar structures (¼ wave resonators) integrated into cryomodules have been in use by Argonne for the Atlas accelerator since the early 1980s. Use of these superconducting structures would reduce the total RF power requirement for the ADTF accelerator by more than a factor of two for a 13.3-mA beam, saving on both capital and operating costs. The higher gradient attainable in superconducting structures also allows the use of independently excited cavities, without sacrificing overall linac length. Independent resonators would permit fast recovery from faults by compensation in the rest of the linac in the same fashion as discussed above for the HE linac. Finally, the larger apertures that can be achieved in spoke cavities would reduce the possibility of beam loss in the LE linac and make it more tolerant to imperfections in

assembly or operation. In short, spoke resonators may provide significant advantages over the CCDTL for the ADTF linac design.

An alternative *all-superconducting* accelerator layout for ADTF is shown in Table 3-3. This design differs from the design of Section 3.3 in that the LE normal-conducting linac (CCDTL/CCL) from 6.7 MeV to 211 MeV is replaced by superconducting cavities. Spoke resonators operating at 350 MHz would be used from the RFQ to 104 MeV. In the region from 104 MeV to 211 MeV, low-beta ($\beta = 0.5$) 700-MHz elliptical cavities would be employed; the entire linac (with the exception of the injector and RFQ) would be superconducting.

Table 3-3. Layout of ADTF Alternative Superconducting Linac Design

RFQ	Spoke	Spoke	Spoke	Elliptical	Elliptical
350 MHz	350 MHz	350 MHz	350 MHz	700 MHz	700 MHz
	2-gap	3-gap	3-gap	5-cell	5-cell
	bg=0.175	bg=0.20	bg=0.34	bg=0.50	bg=0.64
6.7 MeV	14 MeV	40 MeV	104 MeV	211 MeV	600 MeV

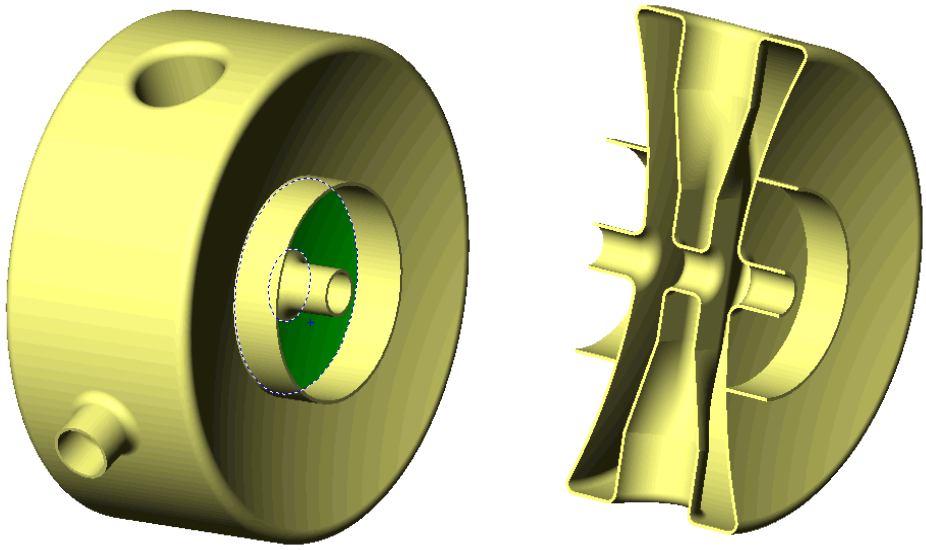

Figure 3-23. Spoke resonator.

Pending the outcome of CCDTL tests at LEDA, and pending more definitive determination of the target-multiplier requirements on beam trips, the ED&D Program could pursue an aggressive development of spoke resonators. Prototype spoke cavities have been excited with RF power, and the basic performance properties (gradient and Q) of this kind of cavity have been confirmed. Further cavity development work is needed, however, including a power coupler for ADTF-level currents. Furthermore, a prototype spoke-resonator cryomodule must be designed and tested before this technology can be considered sufficiently mature for the ADTF accelerator.

3.10.3 Beam Reliability and Testing

It was pointed out in Section 3.1 that the target-multiplier assembly may place challenging requirements on the accelerator performance, in terms of the allowed frequency and duration of beam interrupts. Those requirements and limitations will become clearer as the target-multiplier moves through conceptual design. Some accommodation of the target-multiplier requirements is, of course, possible by designing in redundancy or extra capacity of the linac hardware. In other cases the Accelerator ED&D Program will be able to test concepts and components that will make the accelerator more effectively meet the reliability requirement of the ADTF. Some examples of equipment testing are given here. A fuller listing will be incorporated in the Core Technology Plan, issued during conceptual design.

- **Fast retuning of the accelerator:** The superconducting linac architecture is arranged such that operation can continue in the event of a failure of a single accelerating unit by using neighboring elements to compensate. Recent developments in very fast digital signal processors may make it possible to carry out the retuning process in a few tens of milliseconds. The failed cavity may be physically detuned in a similar time. Tests of the hardware and software required to do this may be done in the ED&D Program.
- **RF power switching:** Several fault scenarios in the accelerator involve the failure of some part of the RF power system, e.g., circulators, klystrons, and power supplies. All the proposals for mitigation of these faults imply the use of a moderately fast RF switch to allow the prompt replacement of the failed component. Development and testing of an RF switch can be done at LEDA.
- **Operating parameters for high reliability:** To minimize the stress on critical components of the linac such as klystrons and superconducting cavities, the range of operating fields that lead to long lifetimes and high reliability may be determined as part of the ED&D Program. Some components can be tested on LEDA.
- **High-fidelity, high-reliability equipment protection:** The ability to predict incipient failures of critical equipment will allow replacement during a planned shut-down period. Beam interrupts caused by spurious *fault* signals also result in unnecessary beam aborts. These problems can be addressed with advanced protection circuits and diagnostics that are capable of predicting equipment failure, while more robustly distinguishing false from real signals. Again, LEDA can be used as a test bed for development and demonstration of these advanced protection circuits.

3.10.4 Other High-Energy Linac ED&D

Several other ED&D Programs undertaken to support the APT high-energy accelerator design will also be important to the ADTF facility. These programs include:

1. lifetime testing of coaxial RF windows at high-power levels to accumulate information on MTBF values;
2. development of waveguide valves to improve system availability;
3. development of an alternative (waveguide-type) RF window that would permit simplification in the RF distribution system;
4. proof testing of 700-MHz RF loads and circulators at high-power levels; and
5. development of beam diagnostics for measuring profiles of the high-energy, high-intensity proton beam and for measuring the expanded beam distribution at the target.

Most of the above activities need to be continued at some level to support ADTF accelerator design. If beam sharing or splitting is required to address multiple missions, prototype hardware for beam sharing, such as high-repetition-rate fast kicker magnets, must also be developed.

4 Balance of Facility Design

Major features of Balance of Facility (BOF) design are driven by the large input electric power required to the accelerator to produce an 8-MW (13-mA at 600 MeV) proton beam. Balance of Facility design is also driven by an estimated 25 MW of energy released in the target-multiplier systems, the distributed nature of the utilities within the plant, shielding requirements dictated by the effects of moderate energy neutrons, temporary storage of nuclear fuel and the need to remotely handle radioactive materials.

Use of liquid metal as the coolant for the fuel assembly and possible selection of lead-bismuth as the target necessitate use of systems and facilities that protect the workers and the public from the chemical reactivity of the liquid metals, especially the radioactive liquid metals, under off-normal and Design Basis Accident conditions. BOF requires containment and confinement of systems containing primary sodium coolant to limit interactions with the surrounding atmosphere and structures resulting in adverse conditions under design basis failures of the sodium pressure boundaries. Design of BOF also requires appropriate systems and structures for secondary sodium coolant, even though not radioactive, to provide protection for the workers and the public against release of large quantities of sodium caused by failure of sodium pressure boundaries.

A primary substation converts the incoming alternating current power from a local utility to a lower ac voltage for distribution to the accelerator, target/ multiplier, and balance of facility systems. Heat exchangers and their attendant cooling towers are placed along the length of the accelerator to remove heat from the power-using equipment. Rejection of the energy from target-multiplier systems to the ultimate heat sink is also accomplished by the BOF systems. Decay-heat-removal capability is provided by multiple and diverse heat-removal systems, with a back-up power supply to facilitate active decay-heat removal.

The ADTF plant structures (Figure 4-1) are designed to provide natural phenomena hazard protection for the systems and components that they house. These structures also provide a barrier, where required, to mitigate the release of radioactive and hazardous materials.

The major BOF structures are as follows:

1. Accelerator Tunnel (including the Injector Building and High-Energy Beam-Transport Tunnel);
2. Klystron Gallery;
3. Target-Multiplier Building;
4. Operations Building/Main Control Room;
5. Cryogenics Building;
6. Accelerator Maintenance Building;
7. Back-up Power Building; and
8. primary substations.

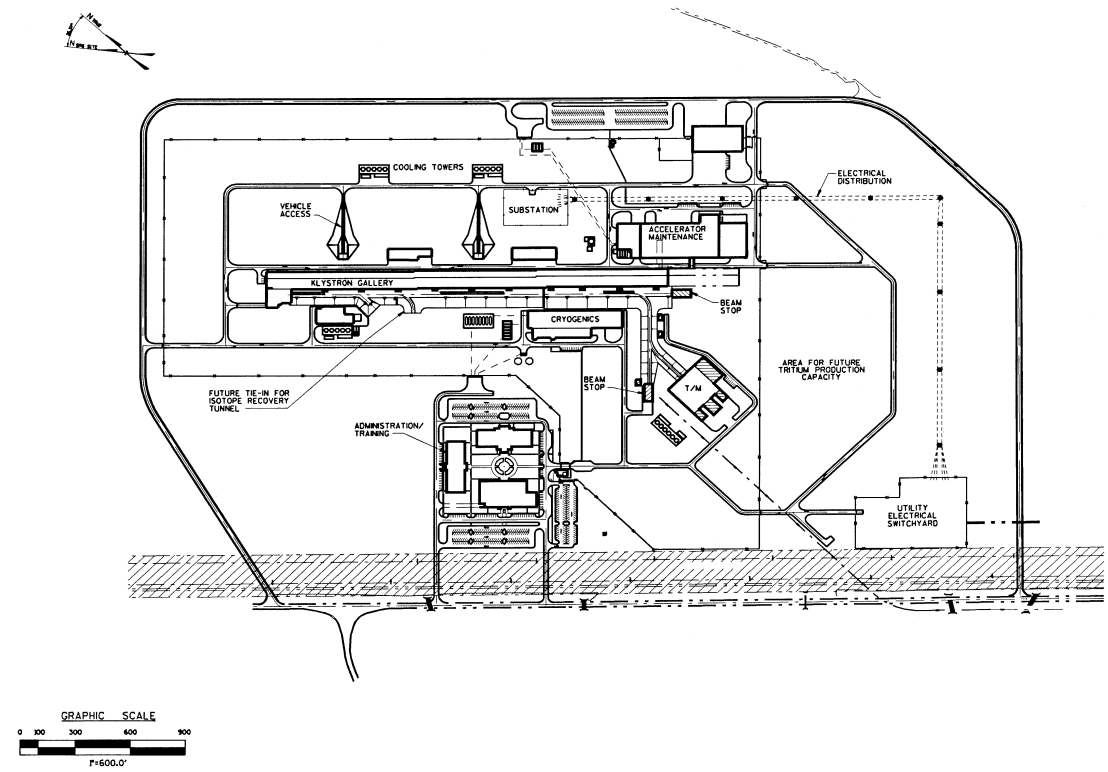

Figure 4-1. ADTF site layout.

Major BOF systems are as follows:

1. Power Distribution System;
2. Heat-Removal System;
3. HVAC Systems;
4. Radioactive Waste Treatment System;
5. Remote-Handling System;
6. Integrated Control System;
7. Radiation Monitoring and Protection System;
8. Non-sodium Fire Protection System;
9. Health Protection and Environmental Monitoring;
10. Safeguards and Security System;
11. Sodium Fire Protection System;
12. Inert Gas System;
13. Inert Gas Cooling Systems;
14. Liquid Metal Piping Heat Tracing System; and
15. Plant Communications System.

There are also infrastructure support services, including tie-ins to site communications, water, and sanitary sewer systems.

4.1 Site Plan

The ADTF is currently configured for the Savannah River Site. Its design, however, is generic and can be applied to almost any Department of energy (DOE) site. Regardless of location, the principal generic site design assumptions are as follows:

1. Stable granular or sandy/clay soil exists down to a depth of 20 meters;
2. Any groundwater is located at least 10 meters below grade;
3. The site is a geologically stable region (no major earthquakes of record);
4. Electric power is available in the quantities required;
5. Ample cooling water is available from either a local aquifer or a nearby river;
6. The security boundary lies well within the site boundary (where the site boundary defines the points beyond which safety requirements regarding radioactive releases are applied); and
7. The site is on a government reservation, with existing rail access, potable water, and sewer systems.

Approximately 1 million square meters (250 acres) of land area are needed to accommodate the ADTF, including future upgrades to the plant, such as that necessary for tritium production (see Figure 4-1). The site will be bounded by a fence (to demarcate owner-controlled and vital areas) with an appropriate access-control facility for entry. Both rail and road access will be provided to the site.

For the ADTF to be extendable in the future to produce tritium, it must accommodate a 100mA 1030 MeV proton beam. As such, the site will include a berm not only over the ADTF accelerator tunnel but also over the proposed extension of the tunnel to induce the same degree of settlement over the two sections.

4.2 Plant Arrangement

The overall ADTF site is divided into five major building groups:

1. Accelerator Tunnel,
2. Klystron Gallery,
3. Target-Multiplier Building,
4. Radwaste Facility, and
5. support facilities.

Each building fulfills the following common functions in addition to plant-specific functions:

1. provide Natural Phenomena Hazard (NPH) protection for structures, systems, and components located within boundaries of the plant;
2. provide barriers to control release of radioactive and hazardous materials from the structure;

3. provide an envelope for environmental controls required for systems and components during all modes of operation; and
4. provide emergency access and egress in accordance with life safety requirements of NFPA and plant operational needs.

The BOF structures, as shown in Figure 4-1, are discussed below:

4.2.1 Accelerator Tunnel

The Accelerator Tunnel is a subterranean, rectangular-shaped, reinforced-concrete structure. The tunnel houses the accelerator components and consists of three major sections: the injector building, main tunnel, HEBT tunnel. The Injector Building is located at the low-energy end of the accelerator. The main tunnel contains the low-energy linac system and the high-energy linac system. The main tunnel terminates at the HEBT tunnel. An earthen berm is provided over the main and high-energy beam-transport tunnel sections for radiation shielding. Vehicle ramps and personnel access portals will be provided along the length of the main Accelerator Tunnel. Access to the HEBT components is through stairwells and access shafts.

4.2.2 Klystron Gallery

The Klystron Gallery extends the length of the injector and main accelerator sections. It is located adjacent to the tunnel berm. The gallery houses the klystrons and associated support components. The gallery accommodates all the controls, cabling, and access required to operate and maintain the RF systems. The Klystron Gallery is divided into several zones by means of firewalls. Personnel access from the Klystron Gallery to the Accelerator Tunnel is provided by means of stairwells leading to the Accelerator Tunnel ramps.

4.2.3 Target-Multiplier Building

The Target-Multiplier Building will house the spallation target, subcritical multiplier assembly, and their associated heat-removal loops. This building will also house the remote-handling equipment needed for refueling and retargeting activities. The primary function of this building will be to contain or confine the accidental releases of radioactive materials. The configuration of this building will be dependent on the selection of the target-multiplier design option. For the sodium-cooled pool concept, it is expected that the building will be a containment structure. For the modular option, if the hot-cell area can be demonstrated to meet the containment requirement, the building itself will act as confinement boundary with ventilation systems designed to prevent unmitigated releases. The hot-cell area will contain the entire primary coolant inventory outside of the target-multiplier. The hot-cell area will be lined and its atmosphere inerted. Lining of the hot-cell area prevents sodium-concrete reactions and minimizes demand for inert gas. Inerting of the hot-cells prevents sodium-air reactions and facilitates early detection of sodium piping crack propagation/ leakage.

The areas of the liquid sodium and modular options containing secondary sodium coolant loops will be provided with catch pans with decks at appropriate locations. The decks limit the amount of air available to react with sodium collected in the catch pans in case of a sodium spill.

4.2.4 Operations Building

The Operations Building provides office space, secure conference rooms, and a plant Main Control Room for the ADTF plant The Operations Building is located adjacent to the Target-Multiplier and Access Control Buildings. The facility has space to accommodate Main Control Room is equipped with computers to monitor vital systems.

4.2.5 Back-up Power Building

The Back-up Power Facility encloses two diesel-powered generators. The facility is used to protect the equipment from natural phenomena hazard events and fire. The diesel generators are in two separate rooms, with a three-hour firewall between. A diesel day-tank is located in each room. Dikes surround the day-tank, fuel line, and engine. The diesel engines and generators are mounted on 12-inch pedestals to keep spills away from the equipment. A separate diesel storage tank is provided for each diesel.

4.2.6 Radioactive Waste Building

The Radioactive Waste Building provides storage for characterized and packaged solid radioactive waste prior to shipment for final disposition. Area monitoring for exterior radiation levels and surface contamination is provided. Space is provided for waste shipment record maintenance.

4.2.7 Administration Building

The Administration Building provides offices, conference rooms, lunchrooms and medical facilities for ADTF management and staff. Access is through a vestibule that opens into the lobby. An information desk is provided. A medical area is located adjacent to the lobby. Space is allocated for a waiting area, medical reception/patient files, nurse reception area, doctor's office, first-aid/minor surgery, vision exam, audio exam, blood work, EKG, supplies, storage and two recovery rooms. Offices are provided for the managers and engineering, licensing, environmental, and procurement personnel.

4.2.8 Access Control Building

The Access Control Building vestibule provides ingress/egress for the plant. A passageway links the Access Control building with the Operations building. A corridor provides controlled entrance into the Target-Multiplier Building. This building houses facilities to support radiation monitoring and worker protection functions. Change room facilities are provided for changing into and out of radiological-area protective clothing.

4.2.9 Accelerator Maintenance Building

This building provides facilities to perform maintenance on klystrons, magnets and cryo-modules; including calibration, and assembly/disassembly activities. This building also provides facilities and equipment for repair of klystrons and maintenance of RF windows. This building is connected to one end of the Klystron Gallery to simplify handling of klystrons requiring maintenance. Layout of the building accommodates klystron support vehicles, which straddle and lift the klystron for transport.

4.2.10 Cooling Tower Structures

The cooling tower structures consist of the cooling tower basin, pads that support associated circulation pumps, and chemical injection system.

4.2.11 Mechanical Services Buildings

These facilities include components for HVAC and process-heat removal. Primary heat exchangers for cooling-water systems associated with components in the Accelerator Tunnel are encircled by concrete walls to provide radiation shielding.

4.2.12 Simulator and Training Facility

This building is located outside the ADTF security perimeter. The simulator control room is an exact replica of the ADTF main control room and provides for operator training and examination. It will be used throughout the plant-life cycle to evaluate and develop new operational procedures. The building also serves as a receiving and training location for new employees.

4.2.13 Fire Pump House

The Fire Pump House contains primary (electric powered) and secondary (diesel powered) pumps to provide water flow to the various plant fire-protection systems. It is a reinforced-concrete structure with three-hour firewalls between each of the fire pumps.

4.2.14 Demineralizer Building

This Demineralizer Building houses systems for treatment and supply of make-up water for use in the demineralized closed-loop cooling water systems and a water chemistry laboratory. The caustic storage tank and acid storage tanks are located outside the building in diked areas. The unloading pump, metering pumps, cation exchangers, degasifiers, anion exchangers, mixed-bed polisher, and after filters are located inside the building.

4.2.15 Security Building

This building houses security personnel and facilities to control access to the ADTF plant.

4.2.16 Cryogenics Facility

The Cryogenics facility houses the cryogenic equipment and a control room. Tanks for helium and liquid nitrogen are located outside the building.

4.3 Power Supply System

The ADTF electric power distribution is comprised of the main power supply system, the onsite back-up ac power system, dc and UPS power systems and various subsystems for plant support. Two standby diesel generators provide back-up ac power to SS classified loads in the Target-Multiplier Building, Beamstop Building, the BOF target-multiplier heat-removal system, and for the radiation exposure protection system. These two standby diesel generators also provide back-up power for the personnel protection and investment protection loads located in the various facilities and structures. Safety-class (SC) and safety-significant (SS) classified batteries, battery chargers, and uninterruptible-power-supply (UPS) systems are provided to support the associated SC/SS loads in the target-multiplier building, and the MCR. General Services (GS) classified battery chargers/inverters are provided to support loads pertaining to the process systems and the support facilities, such as Administration Building, Security Building, electrical equipment areas and primary substations. The ADTF power system design, including the power distribution component selection, is adaptable and upgradeable to support the APT reference plant design.

The ADTF total electric power requirement is estimated to be **TBD MW**, consisting of three major loads:

- the electric power of approximately110 MW necessary to produce a proton beam of 13 mA magnitude at 600MeV,
- the electric power necessary to support BOF facilities and the systems loads of approximately 30 MW, and
- the TBD MW of power necessary to support the Target and Multiplier facility systems

Two separate 100% capacity transmission lines from the local utility assure a very reliable power source for the alternating current plant distribution system. ADTF Plant primary substations are fed from overhead high voltage distribution lines. Loads identified as essential to meet safety requirements are fed from both the normal and back-up power systems. The back-up power system consists of two approximately TBD kW power generators and several UPS. Station batteries power substation control and protective equipment. A brief description of the various electrical sub-systems, necessary for the ADTF project, is provided below:

Refer to Figure 4-2 for the illustration of ADTF Electrical Power Distribution System.

4.3.1 Utility Interface

The ADTF power supply system is connected to the utility company at the load side of utility supplied circuit breakers in the high voltage switchyard. The utility switchyard busses

are fed from two independent transmission lines to improve off-site power source reliability.

The 230-kV_{ac} switchyard, step-down transformers, switching devices (fuses, circuit breakers, etc.), protection and metering equipment are provided, operated and maintained by the utility company. The utility switchyard is located outside the ADTF plant security fence.

4.3.2 Main Power Supply System

The normal power for the ADTF project, to conduct normal operation, start-up, and orderly shut-down of the plant, is provided by the Main Power Supply System (MPSS). The MPSS is designed as a non-safety-class system and does not perform any safety-related function. The MPSS is the preferred power supply source under accident and post accident conditions. The MPSS consists of overhead 230kVac-distribution subsystem, primary substations, medium and low voltage distribution equipment and the power cables for all plant loads.

The 230-kV_{ac} distribution provides the bulk electrical power to the accelerator and balance of facility loads through circuit breakers and disconnect switches. The 230-kV_{ac} plant distribution subsystem includes two overhead lines (Bus A and Bus B) that provide power to the MPSS Primary Substation transformers. The step-down transformers located in the primary substations supply electrical power to medium voltage distribution subsystem to support various plant electrical loads. The ADTF plant electrical loads include klystron high-voltage power supplies and accelerator auxiliary loads, cryogenics loads, klystron control power, the associated BOF heat-removal system loads, target-multiplier primary coolant systems, and other BOF systems.

Electrical loads are divided as equally as possible between the two in-plant high-voltage distribution buses. It is estimated that two 50/66 MVA (Hold) rated transformers will be necessary to provide ac input power of approximately 100 MW (Hold) to the klystrons to produce the desired beam power of 13 mA at 600 MeV. This power estimate may change based on the final selection of power margins for superconducting cavities and the redundancy requirements.

The secondary selective 13.8 kV_{ac} and 4160 V_{ac} *double-ended* switchgear assemblies consisting of two buses with a tie-breaker that connects the two buses are used to further improve the power supply source availability for the low voltage distribution where necessary.

Low-voltage distribution is accomplished via 480-V_{ac} indoor switchgear and 4160/480-V_{ac} or 13800/480-V transformers, as applicable, which are located through out the plant area at the load centers.

4.3.3 Back-Up AC Power System

The back-up ac power system is designed compatible with the requirements of the connected loads. Selection of these loads is based on the consideration of such things as operating personal and public safety, environmental, process, and equipment protection.

The back-up power system is designed in accordance with the IEEE 446 and DOE-STD-3003-94.

It is anticipated that two diesel generators rated at TBD kW (D/G capacity rating estimate depends on the target-multiplier system selection) are adequate to support the critical heat removal and all personnel and equipment protection functions.

4.3.4 Non-Safety DC and UPS System

The safety-significant (SS) classified battery chargers, batteries, and UPS systems are provided to support the SS loads in the target-multiplier building, and the main control room. The normal ac power source for the battery chargers that provide dc power for plant controls and UPS loads is provided from the standby diesel generator backed essential MCCs. The stationary battery provides back-up dc power when the ac power source to the battery chargers is lost.

4.3.5 Safety-Class DC and UPS System

The safety-class dc and UPS system provides uninterruptible power for the safety-class instrumentation, control, monitoring of plant systems and other vital functions that are required to maintain ADTF plant parameters within acceptable limits established for a design base event. In the event of a total loss of ac power to the ADTF facility, including the offsite power and onsite ac power sources (diesel generator), the dc batteries are the source of electrical power for operation of the required dc and ac instrument uninterruptible power supply loads associated with the beam shut-down and radiation monitoring and protection systems.

4.3.6 Other Electrical Support Systems

The ADTF electrical system also includes various subsystems that are necessary for facility support and operation convenience. A brief description of these subsystems is provided below.

The Grounding and Lightning Protection System performs the following principal functions to provide personnel safety and investment protection:

1. Maintain safe voltages across the primary substation, switchyard and unit substation areas during high voltage system transients.
2. Provide a low impedance ground fault current return path.
3. Maintain safe voltages within APT plant structures during electrical transients.
4. Provide instrumentation ground.
5. Minimize the effects of lightning surges on equipment and structures.

The Plant Lighting System provides normal lighting to meet the visual requirements of occupied and unoccupied plant areas when the normal ac power source is available. The system design also includes the emergency lighting should the normal lighting be not available.

The Plant Communication System provides effective and diversified means of communication within the ADTF plant area and external to the plant during all modes of operation. This system consists of four subsystems: Telephone/Page, Private Automatic Branch Exchange (PABX), Wireless Telephone, and Sound Powered Telephones. Each subsystem is designed to be completely independent such that a failure of a subsystem will have no effect on the operability of other subsystems.

The Heat Trace System provides electrical heating to satisfy any system needs where an elevated temperature above ambient is required for system operation, or to provide freeze protection.

The Cathodic Protection System provides means to control external corrosion for the underground and submerged metallic piping and structures as identified by interfacing systems, that could be subject to electrochemical corrosion.

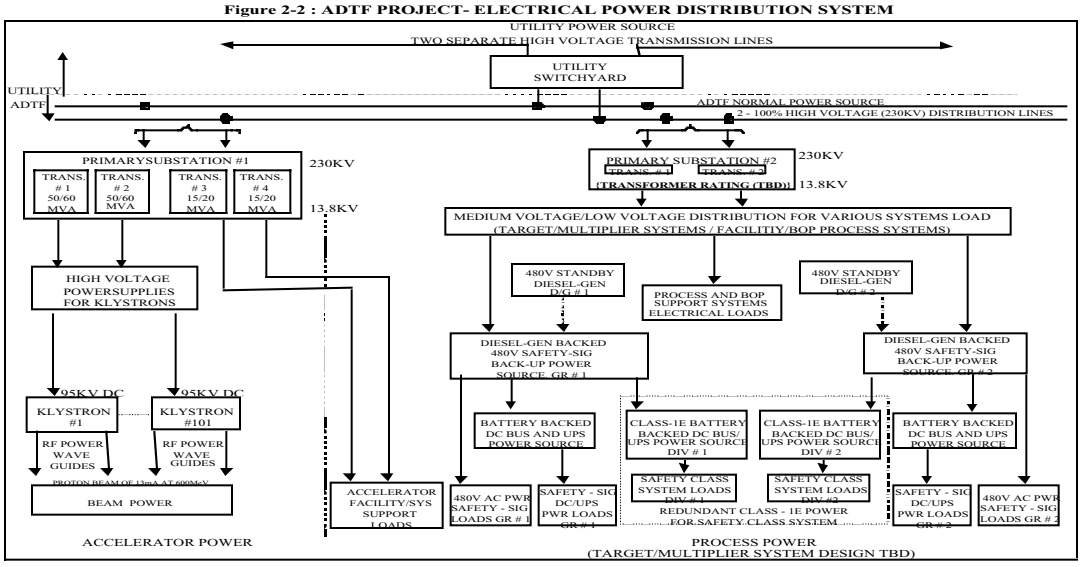

Figure 4-2. ADTF Project electrical power distribution system.

4.4 Heat-Removal System

Generally, the BOF Heat-Removal Systems cover all cooling loops that transfer waste heat directly to the ultimate heat sink. These systems include the open cooling tower circulation loops of the target-multiplier processing area, injector, linac, HEBT, klystron, and maintenance facility.

The Accelerator Secondary Heat-Removal Subsystem provides cooling water to the RF components of the accelerator, including the injector, RFQ, CCDTLs, and CCLs, as well as the magnets, RF circulators, RF switches, RF splitters, RF loads, wave-guides, low-

energy beamstop, and klystron cooling networks. The BOF portion of this system is limited to the secondary side of the primary loop heat exchangers and chillers. In addition to removing waste heat from the primary heat-removal heat exchangers and process chillers, heat is removed from pump bearings and seals, compressors, and various other equipment located along the accelerator tunnel and klystron gallery. The Accelerator Secondary Heat-Removal Subsystem is divided into dedicated cooling tower stations located along the accelerator tunnel. A separate cooling tower station provides the ultimate heat sink for the target-multiplier processing systems and beamstops.

Cryogenics cooling stations are also provided to support the superconducting accelerator cavities. Two separate forced-draft cooling towers provide ultimate cooling for the Cryogenics Facilities.

4.5 Other Plant Support Systems

This section contains discussions of BOF support systems.

4.5.1 Heating, Ventilation, and Air-Conditioning Systems

The various Heating, Ventilation, and Air-Conditioning (HVAC) Systems include systems for providing personnel comfort and for process related ventilation purposes, such as the confinement of airborne radionuclides and equipment cooling. Specific systems include: the Accelerator Tunnel HVAC system, Klystron Gallery HVAC, Injector Building HVAC, target-multiplier Building HVAC and Main Control Room HVAC.

4.5.1.1 Accelerator Tunnel HVAC System

The accelerator tunnel HVAC system operates in three modes: normal, purge, and maintenance. The period during accelerator operation is the normal HVAC mode. During this operation mode, air-handling units (AHU), located on the berm, circulate air from the tunnel, condition it and discharge it back to the tunnel. Exhaust/purge fans (EFAN) and air filter units (AFU), located on the berm, complement the AHUs. During the normal operation mode the exhaust/purge fans discharge tunnel air to the stacks in sufficient quantity to maintain the tunnel at a negative pressure with respect to surrounding spaces and the atmosphere.

During purge mode, the AHUs process 100% outside air and deliver it to the tunnel. The exhaust/purge fans draw the air through the HEPA AFUs and discharge it to the stack. All stack discharge is monitored.

During maintenance mode the AHUs recirculate the conditioned air including sufficient ventilation air to meet personnel occupancy requirements.

4.5.1.2 Injector Building HVAC

The Injector HVAC system operation modes are identical to those described for the accelerator tunnel. Three AHUs, EFAN s, and AFUs support this operation.

4.5.1.3 Klystron Gallery HVAC

Supply/recirculation AHUs, located on the berm, condition the air supply to the Klystron Gallery crane bay, mezzanine and maintenance aisle. Sufficient outdoor air is supplied to the spaces to maintain a slight positive pressure with respect to the atmosphere, and to meet occupancy requirements.

Variable-speed roof fans serve to exhaust air from the crane bay and maintenance aisle during the economizer cycle operation. These fans also serve as smoke purge fans in the event of fire.

One exhaust fan is provided to ventilate each Klystron garage. The exhaust fan draws ambient air from the crane bay area and discharges it to the maintenance aisle.

Variable-speed roof exhaust fans ventilate the high voltage power supply by drawing outdoor air into the space.

4.5.1.4 Target Multiplier HVAC

The HVAC systems for the Target-Multiplier Buildings for the pool and module (loop) target-multiplier concepts are described below:

- For the Liquid Sodium Pool option, the HVAC system circulates air through the building in a once-through mode through the containment building surrounding the pool. Fast closing isolation valves are provided to isolate the containment in case of an accident to prevent uncontrolled releases. An additional cooling system is provided to cool the pool area structure and supporting structures to keep the long term concrete temperatures below the permissible limit of 150°F.
- For the modular concept, the HVAC System serves the areas external to the inerted hot-cells. Areas containing secondary sodium components are also served by this system. This system is also a once-through system. Fast closing isolation valves are provided to isolate the containment in case of an accident.

4.5.2 Radioactive Waste Treatment System

The Radioactive Waste Treatment System (RWTS) accomplishes the required handling, preparation, treatment, storage, and transport of ADTF-generated low-level radioactive and mixed wastes for transport to storage and disposal sites. The radioactive wastes generated by the ADTF plant will be classified as low-level and mixed waste. The ADTF RWTS will include systems to handle solid, liquid, and gaseous radioactive waste streams.

The major sources of ADTF radioactive waste are spent resin from water treatment ion exchangers, personal protective equipment, job control material from routine operation and maintenance activities, and the change-out of target-multiplier modules, window modules, etc. Waste streams from these activities account for roughly three-fourths of all radioactive waste streams generated by the ADTF.

4.5.3 Remote-Handling Systems

Included under the designation of remote-handling (RH) systems are individual systems for accomplishing the required remote- and material-handling functions. RH systems are implemented for applications where ALARA considerations restrict contact maintenance and material-handling systems are implemented when mechanical assistance is required because of the object's weight, size, or physical location.

The primary purpose of these systems is to provide maintenance, inspection, and RH functions required for the unique equipment of the ADTF facilities.

In the Accelerator facility, material-handling systems (cranes, hoists, transport carts, etc.) are provided for beam tube components, vacuum system components, RF system components, electromagnet system components, beam-diagnostic sensors, and klystrons. In the accelerator tunnel, RH equipment is provided to allow maintenance and inspection where ALARA considerations may restrict contact maintenance. RH equipment is also provided for components of the HEBT, including the expander, and the beam expansion system.

In the target-multiplier facility and the HE beamstop facility, material-handling systems (cranes, hoists, etc.) are provided for remote-handling of components.

4.5.4 Integrated Control System

The Integrated Control System (ICS) is comprised of a global portion and a distributed portion. The global portion coordinates and controls ADTF systems and provides operator interface, data acquisition, alarm management, data archiving and retrieval, data distribution, self-checks and diagnostics, and save and restore functions. The distributed portion of the ICS includes control processors and input/output functions, automatic sequencing, closed-loop control and system tuning, and operating mode control within individual systems. It is connected to data highway linking the plant systems within the accelerator, target-multiplier, BOF, and Main Control Room.

Operation of the ADTF facility is accomplished from a centralized location, the Main Control Room. Furthermore, major subsystems and equipment can be operated locally in the field, using locally connected portable consoles similar in function to those in the Main Control Room.

4.5.5 Radiation Monitoring and Protection System

The Radiation Monitoring and Protection system (RMPS) consists of two main systems: the Target Beam Shut-down (TBS) and the Radiation Exposure Protection system (REPS).

TBS provides a functionality to protect the plant from releases associated with the Target design basis accidents (DBAs). TBS is designed to shut down or remove the beam from the Target before damage could occur that would result in a release above applicable

safety evaluation guidance. DBAs will be defined during the development of the ADTF safety evaluation.

The TBS system consists of primary and back-up redundant safety-class instrumentation, logic solvers, beam shut-down mechanisms and displays and controls. The beam shut-down mechanisms interrupt the production of the beam. The MCR displays and controls provide the operators with manual beam shut-down actuation and monitoring.

REPS is a radiation monitoring and entry interlock system designed to keep personnel out of prompt radiation areas (e.g., the accelerator tunnel) when there is a possibility of measurable radiation exposure. REPS prevents beam transport if an excessive beam spill is detected, or if an entryway door/gate is opened into a protected area that could lead to a prompt radiation hazard. A key control system is provided to allow operations to control the access of personnel to the protected areas.

4.5.6 Fire Protection System

The Non-Sodium Fire Protection System (FPS) is comprised of two subsystems, fire detection and alarm, and fire suppression. The Fire Protection System includes active and passive components.

The system uses water as the principal medium for suppressing and extinguishing a fire. The water is supplied by two 100%-capacity fire pump packages from redundant water storage tanks.

The Fire Detection System includes both area and duct detectors. Area detection is used to actuate an automatic suppression subsystem, provide early warning of fire in a critical area, or provide a redundant back-up to an automatic suppression subsystem. Duct detectors shut down HVAC fans and actuate duct actuation dampers when smoke is detected in the air supply ducts.

The Fire Alarm System monitors all other systems comprising the Fire Protection System, except the passive fire protection features. The Fire Alarm System includes local and remote fire alarms and remote trouble and supervisory alarms. The system consists of both plant and master fire alarm panels to initiate appropriate programmed response to the alarms.

4.5.7 Health Protection and Environmental Monitoring System

The Health Protection & Environmental Monitoring System (HP&EMS) covers radiation protection design, radiation monitoring equipment to protect plant personnel, and monitoring equipment to detect airborne and aqueous effluent releases.

4.5.8 Safeguards and Security System

The APT plant will be protected as a Property Protection Area (PPA) per DOE M 5632.1C. The ADTF Safeguards and Security system interfaces with the following safeguards and security systems:

- Materials Control and Accountability
- Information Security and the Security Badging system
- Physical Protection, Detection and Alarm systems
- Security and Emergency Communications
- Property Management and Emergency Management
- Personnel Security and Computer Security
- The Site protective force

4.5.9 Sodium Fire Protection System

The sodium fire protection system serves to detect sodium leaks in areas containing primary and secondary sodium. The fire protection system relies on inerting of the module plant hot-cell area and other areas that contain primary sodium. Areas of both the pool and the modular plant that contain secondary sodium are provided with catch pans with decks. The catch pans are located to collect spilled sodium, which is then drained to collection tanks. The decks located on the top of the catch pans limit the access of air to the sodium surface while allowing the spilled sodium to drain through them. The sodium fire protection system also provides operator-controlled inerting capabilities in selected areas of the plant where the normal atmosphere is air. Hazard to the plant personnel caused by the release of inert gas can be minimized by actuation of alarms before release of the inert gas.

4.5.10 Inert Gas System for the Modular Plant Hot-Cell Area

Hot-cell area of the modular plant is lined and inerted. Inerting of the hot area prevents sodium-air reactions and facilitates early detection of sodium piping crack propagation/ leakage.

The inert gas system in the modular plant monitors the oxygen and water vapor present in the inert atmosphere of the hot-cell and other areas of the plant. The system utilizes periodic feed-and-bleed of the inert gas atmosphere in the inerted areas to maintain oxygen and water vapor concentrations within the permissible limits and to also maintain a slightly negative pressure with respect to the areas located adjacent to the inerted areas.

4.5.11 Inert Gas Cooling Systems

The inert gas cooling systems serves the hot-cell and other inerted areas of the modular plant. The inert gas cooling system keeps the inerted areas of the plant within permissible temperatures. The coolant medium for the cooling systems will not react with the liquid sodium.

4.5.12 Liquid Metal Piping Heat Trace System

All primary and secondary sodium piping in the plant is provided with heat trace to maintain the sodium in liquid state under plant start-up and plant cold shut-down conditions. This system provides trace heaters strapped to the sodium piping in an annular space between the piping external surface and the inner face of the insulation. This inner annular space is also utilized for locating sensors to monitor sodium leakage.